PRODUCTION OF BIOCOMPOSITE MATERIALS FROM ACTIVATED SLUDGE: POLYHYDROXYALKANOATES REINFORCED WITH FILAMENTOUS BACTERIA

by

Xiangmin Liang

A dissertation submitted to the Faculty of the University of Delaware in partial fulfillment of the requirements for the degree of Doctor of Philosophy in Civil Engineering

Spring 2023

PRODUCTION OF BIOCOMPOSITE MATERIALS FROM ACTIVATED SLUDGE: POLYHYDROXYALKANOATES REINFORCED WITH FILAMENTOUS BACTERIA

by

Xiangmin Liang

Approved: _____
Jack A. Puleo, Ph.D.
Chair of the Department of Civil and Environmental Engineering

Approved: _____
Levi T. Thompson, Ph.D.
Dean of the College of Engineering

Approved: _____
Louis F. Rossi, Ph.D.
Vice Provost for Graduate and Professional Education and
Dean of the Graduate College

I certify that I have read this dissertation and that in my opinion it meets the academic and professional standard required by the University as a dissertation for the degree of Doctor of Philosophy.

Signed: _____

Daniel K. Cha, Ph.D.
Professor in charge of dissertation

I certify that I have read this dissertation and that in my opinion it meets the academic and professional standard required by the University as a dissertation for the degree of Doctor of Philosophy.

Signed: _____

Harry W. Shenton III, Ph.D.
Member of dissertation committee

I certify that I have read this dissertation and that in my opinion it meets the academic and professional standard required by the University as a dissertation for the degree of Doctor of Philosophy.

Signed: _____

Chaoying Ni, Ph.D.
Member of dissertation committee

I certify that I have read this dissertation and that in my opinion it meets the academic and professional standard required by the University as a dissertation for the degree of Doctor of Philosophy.

Signed: _____

Jennie P. Saxe, Ph.D.
Member of dissertation committee

ACKNOWLEDGMENTS

I would never be able to complete my degree without the help from my committee members and unconditional supports from my family and friends.

My appreciation to my advisor, Professor Daniel K. Cha, can never be fully expressed by words. He is always professional, caring, amiable and supportive. It is a wonderful experience to conduct research under his guidance. I would also like to express my appreciation to Professor Harry W. Shenton III, Professor Chaoying Ni, and Professor Jennie P. Saxe for their constructive and unique opinions from material and environmental aspects. Their professional suggestions strengthened my abilities in finishing my research.

I would also like to thank all my lab mates for their help and encouragements. It was an enjoyable experience working with Rachel Burch and Savannah Sipes. Their optimism and enthusiasm to both research and life always inspire me. I will never feel upset when they were beside me. Many thanks to Dr. Inyoung Kim for her help throughout my study. Her excellent management makes our office and lab always in perfect order. My thanks also go to Michael Davidson, Dr. Yu-Han Yu and Xuerui Song for helping me construct and operate my bioreactors, collect samples and analyze data.

I will always be grateful to Delaware Environmental Institute and Hagerty Environmental, LLC for their generous funding to support my research.

I will never forget supports from my wife, Dr. Jiayi Tang, my parents, and parents in law. They always stand with me and cheer me up. Their unconditional supports and encouragements are my solid backing when I pursue my degree.

TABLE OF CONTENTS

LIST OF TABLES

LIST OF FIGURES

ABSTRACT

Polyhydroxyalkanoates (PHAs) are intracellular microbial polyesters that serve as bacterial carbon and energy storage substances. They share similar properties with many petroleum-based polymers, thus attracted significant interest due to their potential biodegradability and environmental benefits. In order to improve the mechanical properties of PHAs, many types of natural plant-based fibers have been successfully used as reinforcement agents of PHA-based composites. The overall goal of this research is to obtain both the matrix (PHA copolymer) and the reinforcement agents (filamentous bacteria) for biorenewable composites from adapted wastewater treatment systems, thus, develop biocomposite materials that are derived entirely from microorganisms growing naturally in wastewater treatment processes.

Biocomposite materials with commercially available poly(3-hydroxybutyrate-co-3-hydroxyvalerate) (PHBV) as matrix and filamentous bacteria as reinforcement were fabricated by melt extrusion and 3D printing. Filamentous bacteria were cultivated and enriched in a laboratory membrane bioreactor. Low dissolved oxygen, and nitrogen and phosphorus limited conditions were provided in the MBR, resulting in proliferation of filamentous bacteria with the sludge volume index as high as 703 mL/g. *Sphaerotilus* spp. were identified as the dominant filamentous bacteria by 16S rRNA gene sequencing. A relative abundance of these filamentous bacteria was 19% in the mixed cultures. The morphology of filamentous bacteria was observed using optical microscopy and atomic force microscopy (AFM). The aspect ratio (length to width ratio) of the filamentous bacteria was 346.

The thermal properties of PHBV and filamentous bacteria were evaluated by differential scanning calorimetry and thermogravimetric analysis. The results suggested that the processing temperature of these composite materials should be around 185 °C to minimize thermal degradation of both commercial PHBV and filamentous bacteria. Tensile properties (e.g., tensile strength, elongation at break, and tensile modulus) and notched impact strength of composites with different fiber contents were also evaluated. The results showed that tensile modulus and notched impact strength of the composite with 20% fiber content (mass basis) increased 12% and 95%, respectively.

AFM-based nanoindentation method was used to examine the mechanical properties of filamentous bacteria. The measured Young's modulus of *Sphaerotilus* spp. was 91.4% higher than that of non-filamentous bacteria. The Halpin-Tsai and Tsai-Pagano equations were used to determine the theoretical Young's modulus of filamentous bacteria-reinforced poly(3-hydroxybutyrate-co-3-hydroxyvalerate) (PHBV). The predicted values closely matched the experimental values, indicating that filamentous bacteria were randomly oriented and uniformly distributed in PHBV.

A sequencing batch reactor was operated to enrich for PHA-accumulating bacteria, and the production of PHBV by the enriched cultures was maximized by a fed-batch reactor. The highest PHA content of 59% dry cell weight was obtained with 68% PHB and 32% PHV. PHBV extracted from the bacterial cells in the fed-batch reactor had a purity of 99.3%. A membrane bioreactor was used to cultivate filamentous bacteria-dominating cultures (19% relative abundance of *Sphaerotilus* spp.). Differential scanning calorimetry and thermogravimetric analysis of microbial PHBV suggested that the melt extrusion and 3D printing temperatures to be 170 °C

and 180 °C, respectively, to minimize the thermal degradation of PHBV. Mechanical tests showed that the tensile modulus and notched impact strength of microbial PHBV improved by 57% and 45%, respectively, following the addition of 20% membrane bioreactor sludge.

The research presented in this dissertation demonstrated that both biopolymer matrix and the natural fiber reinforcement for the composite materials can be recovered from microorganisms present in wastewater treatment systems. This development of biocomposite materials that are derived entirely from microorganisms growing naturally in wastewater treatment processes will help reduce the quantity of waste sludge from wastewater treatment plants and produce a green alternative to petroleum-based composite that are environmentally friendly, biodegradable, and sustainable.

Chapter 1

INTRODUCTION

Wastewater treatment plants (WWTPs) use a combination of physical, chemical, and biological processes to remove suspended and soluble organic contaminants in municipal and industrial wastewater (Demirbas et al., 2017; Wei et al., 2003). Biosolids, also called waste sludge, are semi-solid by-products of wastewater treatment process. They are generated because the principle of biological wastewater treatment is that bacteria convert contaminants into their own biomass. The United States Environmental Protection Agency (USEPA) reported that about 4.75 million tons of dry biosolids were generated by large public WWTPs in the U.S. in 2019 (United States Environmental Protection Agency, 2021). In China and the European Union, annual dry biosolids productions were 11.2 million tons and 10 million tons, respectively (Yang et al., 2019). The global biosolids generation was predicted to increase rapidly due to increases in population, economy scale, urbanization, and municipal wastewater treatment system coverage (Bharathiraja et al., 2014; Wang et al., 2018). Thus, biosolids generation and management have become one of the most serious concerns in the WWTPs industry (Lu et al., 2021; Wang et al., 2021).

Biosolids need to be properly treated and disposed because of their offensive odor and potential negative impacts on the environment and public health (Guo et al., 2013; Wei et al., 2020; Zheng et al., 2020). Current major biosolids disposal methods include landfill, incineration, land application, and anaerobic digestion.

Landfill and incineration are the most common conventional biosolids treatments. Landfill is widely used since it is the cheapest way to dispose biosolids, however, no energy or materials are recovered in landfill (Campbell, 2000; Yang et al., 2015). Overall, 38 percent of biosolids were disposed by landfill in the U.S. (Fericelli, 2011). However, landfill sites are limited due to high land demands from agriculture, urbanization, and industrialization (Mulchandani & Westerhoff, 2016). The landfill sites used for biosolids disposal exacerbate the scarcity of land resources. Biosolids dewatering is usually required to meet regulations of water content limits in some countries (Xiao et al., 2020), which will also increase the cost of landfill disposal. Another factor that makes landfilling unsustainable is that it may cause secondary pollution (Tang et al., 2018; Zhang et al., 2017), such as potential groundwater contamination from leachate leakage (Giusti, 2009). Other issues, such as greenhouse gas emission, landfill odor, and increasing costs of transporting biosolids from WWTPs to landfill sites, make landfill environmentally and economically unfriendly (Mulchandani & Westerhoff, 2016).

Due to multiple issues associated with landfilling, focus has shifted to recover energy and reusable materials from biosolids during disposal. Although the heat generated during biosolids incineration could be further used for heating and electricity generation, operation cost is normally high due to high moisture content in biosolids (Fericelli, 2011; Zhong et al., 2020). Incineration could reduce 90 percent of biosolids volume, but the ash left after biosolids incineration still needs to be disposed by landfill (Raheem et al., 2018; Wu et al., 2016). Moreover, incineration has detrimental impacts on the environment and public health by emitting greenhouse gases, volatile organic compounds (VOCs), heavy metal dust, and particulate matter

(Hong et al., 2009). The cost of air pollution controls may be higher than the value of recovered energy from incineration (Fericelli, 2011). Thus, the overall process is not economical, ecofriendly, and sustainable.

For repurposing biosolids, land application was initially considered environmentally friendly, because organic matters and nutrients in biosolids can support plant growth during this process (Wang et al., 2008). However, newly emerging concerns about heavy metal contamination, persistent organic toxins, and pathogen-borne diseases highly limit the widespread usage of land application (Arthurson, 2008; Chu & He, 2021).

Anaerobic digestion is a mature technology that treats biosolids while carbon is recovered as methane or organic acids (Jain et al., 2015; Wang et al., 2021). However, the disadvantages of anaerobic digestion technology include the requirement of large reactors due to long sludge residence time (SRT) (Ruffino et al., 2016; Tiehm et al., 2001), low digestion rate and low methane yield (Zhang et al., 2017; Zhen et al., 2017), and high operation costs (Budzianowski, 2016).

As discussed above, a new method to reduce biosolids volume and recover reusable materials at the same time needs to be developed. In the recent decade, the concept of converting WWTPs from bioreactors to biorefineries has become popular. This requires WWTPs to turn their biosolids into some valuable materials.

Recovering polyhydroxyalkanoates (PHAs) from microorganisms in biosolids may be an attractive way to retrieve valuable materials from WWTPs. PHAs are bacteria-produced polyesters that are synthesized from their metabolic transformation of various sugars and volatile fatty acids (VFAs) (Albuquerque et al., 2007, 2010, 2011; Fradinho et al., 2014). Producing PHA discharges less carbon dioxide than

producing some other polymers. For example, producing 1 kg of PHAs from bacteria using corn starch as feedstock reduced 2.9 kg carbon dioxide discharge than that from producing the same amount of high-density polyethylene (Dietrich et al., 2017). This makes PHAs more renewable materials compared to the petroleum-based polymers. Another advantage of PHAs is that they are easily biodegradable. While petroleum-based polymers usually need hundreds to thousands of years for complete natural degradation, PHAs take much shorter time for this. Woolnough et al. (2013) reported that polyhydroxybutyrate (PHB) film can be 60% degraded (weight basis) in soil in 112 days. 90% degradation of PHB film in marine condition in 100 days was also reported by Thellen et al. (2008). Therefore, PHAs can be suitable alternatives to many petroleum-based plastics. However, limitations in mechanical properties, such as brittleness, restrict wide applications of PHAs in single-use plastic productions, medical supplies, and many other industries.

One approach to deal with this problem is reinforcing PHAs with fibers. Synthetic fibers, such as carbon fiber and fiber glass, possess high strength and lightweight. However, producing these synthetic fibers contributes to greenhouse gas emission, and their disposal is usually not renewable and sustainable. Some natural fibers, such as plant-based fibers, are not compatible with PHAs, and required further treatments to achieve better interface affinity. Therefore, interest has shifted to a novel natural fiber existing in activated sludge, which is filamentous bacteria. Filamentous bacteria are microorganisms with large length-to-width ratio. As backbones of activated sludge flocs, filamentous bacteria are potential substitutes for synthetic and plant-based fibers in reinforcing PHAs.

A schematic diagram of fabricating the all-natural biocomposite material from a modified wastewater treatment plant is proposed in Figure 1.1. The overall objective of this study is to investigate the possibility of fabricating a composite material with all the components (PHAs and filamentous bacteria) derived from activated sludge and to evaluate the mechanical properties of this composite material. The specific objectives are:

1) to investigate the possibility of filamentous bacteria serving as a reinforcement agent of PHAs. The thermal properties of a commercially available PHA and filamentous bacteria cultivated from a laboratory membrane bioreactor (MBR) will be assessed and will be used to determine the processing conditions of fabrication. The tensile and impact properties of composite specimens with different fiber ratios will be evaluated to determine the reinforcing effects of filamentous bacteria.

2) to identify the filamentous bacteria cultivated from a laboratory membrane bioreactor and assess their properties. Filamentous bacteria cultivated from an MBR will be identified by 16s rRNA gene sequencing. The morphology and Young's modulus of filamentous bacteria will be assessed to deepen the understanding of these microorganisms. A model will also be applied to predict the reinforcement effects of filamentous bacteria on PHAs.

3) to demonstrate a method of fabricating an all-natural biocomposite material from activated sludge with PHAs as the matrix and filamentous bacteria as the reinforcement. PHA-accumulating bacteria will be selected from activated sludge in a laboratory sequencing batch reactor and subsequently used to produce PHA in a fed-batch reactor. Thermal properties of this microbial PHA will be evaluated and used to

determine the processing conditions of composite fabrication. Mechanical properties of these biocomposite materials with different fiber ratios will be assessed.

The research presented in this dissertation demonstrates production of all-natural biocomposite materials from activated sludge using PHA as the matrix and filamentous bacteria as the reinforcement agent. Chapter 2 presents an overview of the background information of PHA, including PHA production, extraction, purification, and modification. Chapter 3 describes an approach to fabricate a composite material using commercial PHA as the matrix and filamentous bacteria cultivated from a membrane bioreactor as the reinforcement agent. Tensile and impact properties are determined to evaluate the reinforcing effects of filamentous bacteria. The research presented in chapter 4 demonstrates the characteristics of filamentous bacteria cultivated from the membrane bioreactor. Filamentous bacteria are identified by 16s rRNA gene sequencing. The morphology and Young's modulus of filamentous bacteria are also assessed in this chapter. The research presented in chapter 5 demonstrates fabrication of biocomposite materials using microbial PHA produced from laboratory bioreactors as the matrix and filamentous bacteria cultivated from a membrane bioreactor as the reinforcement agent. Tensile and impact properties of this composite material are determined and compared with those of composite materials fabricated with commercial PHAs. The summary of results of this dissertation is presented in chapter 6. Chapter 7 presents a design of fabricating the biocomposite material from a modified wastewater treatment plant and the potential applications of this biocomposite material.

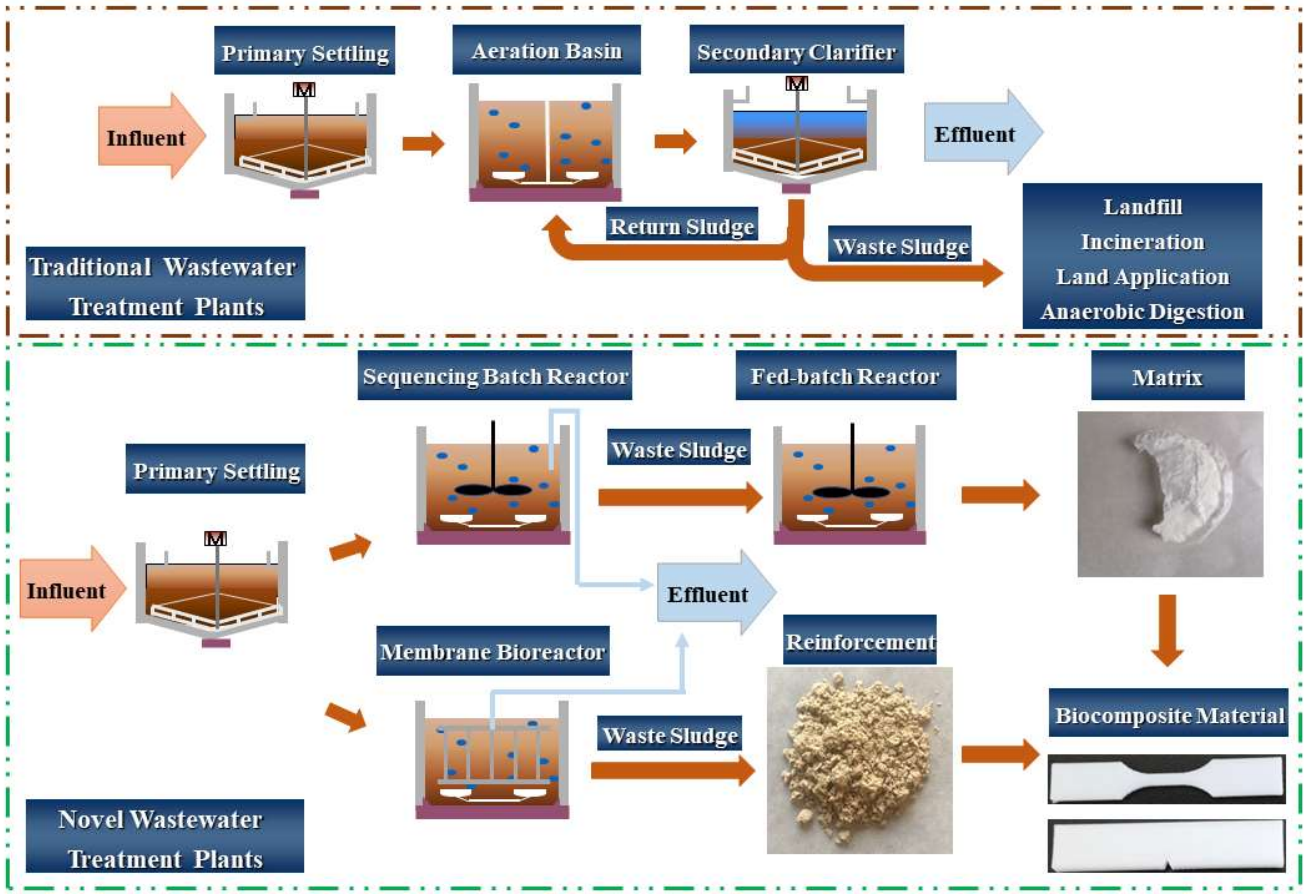

Figure 1.1. Schematic diagram of fabricating an all-natural biocomposite material with all components derived from activated sludge.

Chapter 2

LITERATURE REVIEW

This chapter provides an overview of the fundamental knowledge of PHAs and filamentous bacteria. The classification, biosynthesis, extraction and purification methods, mechanical property modifications, and applications of PHAs are summarized in this chapter. This chapter also includes the classification and growth conditions of filamentous bacteria. This chapter will help better understand the method demonstrated in this dissertation.

2.1 Classification and properties of PHAs

The general chemical formula of PHAs is shown in Figure 2.1.a (Shah & Vasava, 2019). The monomers of PHAs are connected by ester bonds, thus PHAs can be divided into three groups based on the carbon chain length of their monomers. Monomers with 3-5 carbon atoms are classified as short chain length PHAs (scl-PHAs), while monomers with 6 to 14 carbons atoms are medium chain length PHAs (mcl-PHAs) (Madison & Huisman, 1999). Monomers with more than 14 carbon atoms are classified as long chain length PHAs (lcl-PHAs) (Sharma et al., 2021; Zinn et al., 2001). Poly (3-hydroxybutyrate) or in short P(3HB) and poly(3-hydroxyvalerate) or in short P(3HV) are the most common scl-PHAs, while poly(3-hydroxyhexanoate) or in short P(3HH) is an example of the mcl-PHAs group (Asrar et al., 2002; Joyyi et al., 2017). The number 3 in P(3HB) means the hydroxyl of the monomer connects with the third carbon atom of the chain. The difference of n value results in different

number in the polymer name. Some common PHAs are summarized in Table 2.1 (Anjum et al., 2016).

PHAs exist as homopolymers or copolymers. P(3HB) and P(3HV) are PHA homopolymers. PHA copolymers contain two or more kinds of monomers within their carbon chains, and are commonly bipolymers and terpolymers (general chemical formulas are shown in Figure 2.1.b and 2.1.c, respectively). P(3HB-co-4HB) and P(3HB-co-3HV-co-3HH) are common bipolymer and terpolymer of PHAs, respectively (Bhubalan et al., 2010; Jung et al., 2019; Mannina et al., 2020).

Generally, polymers in PHA family are thermoplastic, and they share some common properties such as low gas permeability, water insolubility and UV ray resistance (Keskin et al., 2017; Laycock et al., 2014; Li et al., 2016; Scarfato et al., 2015). However, various monomer components result in PHAs with different mechanical properties. For example, although P(3HB) and P(4HB) are both PHA homopolymers, P(3HB) is brittle and thermally unstable during processing due to its high crystallinity, while P(4HB) is strong and elastic (Chodák & Blackburn, 2009; Li et al., 2016; Williams et al., 2013). PHA copolymers, such as P(3HB-co-3HV) and P(3HB-co-3HV-co-3HH), generally have better elasticity and flexibility than scl-PHA homopolymers (Tsuge et al., 2004). This is because the incorporation of different monomers decreases the crystallinity of polymers (Du et al., 2001). Also, the longer chain length results in higher flexibility of molecular structure, which makes PHAs softer and higher in elongation at break(Laycock et al., 2014; Tanadchangsaeng et al., 2009).

Some physical and mechanical properties of PHAs are similar to some common petroleum-based polymers, such as polypropylene (PP), low-density

polyethylene (LDPE), rigid polyvinyl chloride (PVC), and polyethylene terephthalate (PET). The comparison of their physical and mechanical properties is summarized in Table 2.2. The melting temperature and crystallinity of all polymers in Table 2.2 are basically in the same range. The differences in glass transition temperature indicate that PHB, PHBV, PP, and LDPE are in the rubbery state, while rigid PVC and PET are in the glassy state at room temperature. PHA has good properties in hardness. Its Young's modulus and tensile strength have no clear difference from other polymers in the table. The major weakness of PHA is its extensibility. The elongation at break of PHA is generally one order of magnitude lower than the other polymers. That means neat PHA is unfavorable as a material that needs to bear tension. Improving the extensibility of PHA is the key area of modification of PHA.

2.2 PHA production

2.2.1 PHA biosynthesis pathways

PHA plays a vital role in microbial competition and survival in an environment. Since nutrients are not always sufficient in the environment, bacteria with PHA-accumulating abilities can utilize intracellular PHA to obtain energy under famine conditions (Figure 2.2). This allows PHA-accumulating bacteria to survive longer than bacteria without these abilities (Tan et al., 2014). Besides, research has discovered that intracellular PHA protects bacteria from harmful environments, such as ultraviolet irradiation, heat, and osmotic shock (Kadouri et al., 2005). Therefore, many bacteria have adapted to adverse conditions and developed their enzyme systems to use various carbon sources to synthesize PHA. Thus far, eight PHA biosynthesis pathways have

been identified (Chen, 2010). The major three pathways are summarized in Figure 2.3, and the major enzymes involved are summarized in Table 2.3.

In pathway I (green arrows), sugars are the carbon sources. Firstly, sugars are converted to pyruvate through glycolysis and then converted to acetyl-CoA. Two molecules of acetyl-CoA are combined by an enzyme (PhaA) to form one molecule of acetoacetyl-CoA. Reductase (PhaB) then converts acetoacetyl-CoA to (R)-3-Hydroxybutyryl-CoA using NADPH as the proton and electron sources. Finally, (R)-3-Hydroxybutyryl-CoA is polymerized to generate PHAs (Anjum et al., 2016; Serafim et al., 2008; Sudesh et al., 2000; Verlinden et al., 2007; Yogesh et al., 2012).

When nutrients in the environment are sufficient, high concentration of coenzyme A from the tricarboxylic acid (TCA) cycle inhibits PhaA. Under this condition, the transformation from acetyl-CoA to acetoacetyl-CoA is inhibited. Acetyl-CoA is then channeled to the TCA cycle for energy production and cell growth (Ratledge & Kristiansen, 2006). Under nutrient deficient condition, which means carbon sources are in excess while nitrogen or phosphorus is insufficient, the concentration of coenzyme A is not high enough to inhibit PhaA, thus, PHA production will be promoted (Jung & Lee, 2000). This negative feedback process is summarized in the dotted box in Figure 2.3. Therefore, nutrient deficiency triggers the enzyme systems of PHA production and leads to intracellular PHA accumulation. This metabolic mode allows the selection and enrichment of PHA-accumulating bacteria under famine condition, which will be discussed in the section 2.2.2.

In pathway II (red arrows), fatty acids are the carbon sources. In this process, the intermediates of fatty acids degradation (β-oxidation) are used to synthesize PHA. Fatty acids need to be converted to fatty acyl-CoA initially for β-oxidation reaction

(Lopaschuk et al., 2010). During β-oxidation reaction, four key intermediates regulate the PHA formation process, in which enoyl-CoA and 3-ketoacyl-CoA can be catalyzed to form (R)-3-Hydroxybutyryl-CoA. The last step of pathway II is also polymerization of (R)-3-Hydroxybutyryl-CoA into PHAs (Anjum et al., 2016; Schulz, 2008; Sudesh et al., 2000; Yogesh et al., 2012). In pathway I and II, the structures of synthesized PHAs are related to the original carbon sources. For example, n-alkanoates with even carbon number are required for P(3HB) production, while odd carbon number n-alkanoates are required as the starting materials for P(3HB-co-3HV) and P(3HB-co-3HV-co-3HH) generation (Akiyama et al., 1992; Anjum et al., 2016; Fukui et al., 1997). This is because PHA synthase in pathway I and II can only uptake n-alkanoates with certain carbon number (Kumar et al., 2020).

Pathway III (blue arrows), also called fatty acid biosynthesis, uses sugars as carbon sources as well. Acetyl-CoA, as the intermediate of glycolysis, is converted to malonyl-CoA by acetyl-CoA carboxylase (ACC). Malonyl-CoA is then transferred to its acyl carrier protein (ACP) form as malonyl-ACP by ACP transacylase. After that, this intermediate is utilized in fatty acid synthesis. Then, another intermediate, (R)-3-hydroxyacyl-ACP, is formed and converted to its coenzyme A (CoA) form by CoA transacylase (PhaG). Finally, (R)-3-hydroxyacyl-CoA is polymerized to PHAs (Castilho et al., 2009; Chen et al., 2015a; Tsuge, 2002; Wang et al., 2009). The major difference between this pathway and the previous two is that PHA monomers generated from pathway III can have a different structure from their carbon source, not dictated by carbon numbers. This is because bacteria can disassemble and reassemble carbon sources during fatty acid biosynthesis. This allows the potential utilization of

low-cost feedstocks, such as glucose and acetic acid, to generate PHAs containing multiple monomers (Kumar et al., 2020; Sharma et al., 2021).

2.2.2 PHA production via mixed culture biosynthesis

By making use of the metabolic process of PHA biosynthesis, scientists and engineers have successfully achieved high productivity of PHA in pure culture fermentation. The most common strains in pure culture fermentation are *Bacillus* (Pan et al., 2016; Rodríguez-Contreras et al., 2016) and *C. necator* (Ribeiro et al., 2016; Schmidt et al., 2016). The maximum PHA accumulation observed in pure culture fermentation is 89% (dry cell weight basis) by *Bacillus subtilis JCM 1465* (Vijay & Tarika, 2019). Genetic engineering has also been applied in pure culture fermentation as microorganisms, such as recombinant *E. coli*, has been successfully used in PHA production (Leong et al., 2014; Zhang et al., 2020). However, high operation cost of pure culture fermentation limits its widespread commercialization. Thus, interest has shifted to utilize mixed culture fermentation for PHA production.

As discussed above, P(3HB-co-3HV) has better tensile properties, such as elongation at break, than pure P(3HB). P(3HB) can be obtained individually in pure culture fermentation, but produced naturally combined with P(3HV) in mixed culture processes. The mixed culture fermentation also allows the utilization of open microbial reactors, which eliminates the need for reactors and substrates sterilization, therefore, decreasing the fermentation cost. In addition, mixed cultures are more robust than pure cultures, thus are less susceptible to operational and environmental fluctuations in large-scale processes. Moreover, mixed culture fermentation can adapt to various complex feedstocks from many high-volume industries, such as food waste and waste activated sludge (Bengtsson et al., 2008; Lee et al., 2020). This allows

significantly decrease the cost of PHA production, because feedstocks account for 45% of the total PHA production cost (Lee et al., 2020).

Mixed culture fermentation includes three stages. The first stage is pretreatment of feedstocks, in which various raw organic substrates are converted to volatile fatty acids (VFAs) commonly by anaerobic fermentation. VFAs are more preferred substrates than sugars or glycerol because bacteria tend to accumulate glycogen when sugars or glycerol are used as substrates (Kourmentza et al., 2017). Various industrial and agricultural organic wastes can be utilized as fermentation feedstocks to lower the cost of PHA production, meanwhile, the release of organic pollutants to the environment will be reduced. By using organic wastes from food industry, PHA can be produced together with hydrogen gas, which further improved the economic efficiency of PHA production (Lee et al., 2020). The second stage is to select and enrich mixed cultures in which PHA-accumulating bacteria are dominating. One strategy to select PHA-accumulating bacteria dominant cultures is aerobic dynamic feeding (ADF), also known as feast-famine cycle (Johnson et al., 2009). The simultaneous feeding of sufficient carbon sources and other nutrients in the initial feast phase results in short feast phase and followed by a longer famine phase when external substrates are exhausted. During the famine phase, bacteria with PHA-accumulating abilities continue to grow by using their stored PHAs, while bacteria without these abilities stop growing and gradually out-competed during the starvation phase. Another strategy to select suitable mixed cultures is anaerobic-aerobic cycle. This strategy promotes polyphosphate-accumulating bacteria and the glycogen-accumulating bacteria to accumulate PHAs. However, the PHA storing capacity of enriched mixed cultures from anaerobic-aerobic cycle is lower than that from the ADF

strategy (Mannina et al., 2020). Following culture selection and enrichment, intracellular PHA storage can be maximized by unbalanced growth conditions, such as pulsed feeding or fed-batch mode (Mannina et al., 2020). Table 2.4 summarizes the PHA production research using mixed culture fermentation.

Many parameters are involved in the PHA production, and some of them have major effects on the overall production performance. The composition of produced PHA (such as 3HB to 3HV ratio) is directly controlled by VFA composition of feedstocks, which is mainly affected by pH during the anaerobic fermentation process of raw feedstocks. Acetic acid and butyric acid are precursors of P3HB, while propionic acid and valeric acid are precursors of P3HV (Albuquerque et al., 2007; Burniol-Figols et al., 2018; Colombo et al., 2016; Fang et al., 2019; Kourmentza et al., 2015; Perez-Zabaleta et al., 2020; Tamang et al., 2019; Zhang et al., 2014). Colombo et al. (2019) reported that major organic acids in cheese whey fermentation products were acetate, butyrate, and lactate, which resulted in neat PHB production. Colombo et al. (2019) also revealed that PHA yield were 10-20% higher on organic acids consumption than that on total chemical oxygen demand (COD) consumption. This result confirmed that organics acids were preferred feedstocks for PHA production. Albuquerque et al. (2007) compared VFA composition of anaerobic fermented sugar cane molasses under different pH. When pH decreased from 7 to 6, the concentration of acetic acid and butyric acid increased 26% and 27%, respectively, while the percentage of propionic acid decreased 35%. Colombo et al. (2016) reported a similar result during cheese whey anaerobic fermentation. The percentage of butyric acid increased from 13% to 26% when pH changed from 6 to 5.2, which decreased the 3HV content in the final PHA product. pH also has influence on PHA yield and

accumulation. Chen et al. (2015b) studied the PHA production under different pH. When pH changed from 5 to 10, the final PHA yield and accumulation decreased gradually from 0.8 Cmol PHA/ Cmol Substrate and 70 wt.% to 0.63 Cmol PHA/ Cmol Substrate and 65 wt.%, respectively. Similar phenomenon was observed from research of Albuquerque et al. (2007). When applying the same feedstocks but increasing pH from 5 to 7, PHA yield decreased 26%. These results indicate that acidic condition is favorable for 3HB precursor production during feedstocks pretreatment and PHA production. The effects of feedstock composition on overall PHA performance are also related to some toxic chemicals. Kourmentza et al. (2015) compared PHA yield with fermented olive mill wastewater and synthetic feedstock with same composition of major VFAs. The PHA yield decreased by 90% with fermented olive mill wastewater. This could be attributed to inhibitory effect of toxic chemicals, such as polyphenols, on PHA-accumulation bacteria.

The microbial community after selection correlates with selection strategy, organic loading rate (OLR), and feast to famine (F/F) ratio. Multiple studies in Table 2.4 reported that the dominant PHA-accumulating bacteria in their reactors were *Proteobacteria*, such as *Thauera* (Burniol-Figols et al., 2018; Fauzi et al., 2019; Perez-Zabaleta et al., 2020; Wijeyekoon et al., 2018). Morgan-Sagastume (2016) also found that the predominance of this bacteria phylum was highly related to ADF selection. Different OLR and F/F ratio during selection and PHA production also alter the percentage of PHA-accumulating bacteria in the whole microbial community and the overall PHA production. High OLR usually leads to large F/F ratio, which means famine phase is not long enough. In this case, PHA-accumulating bacteria are unlikely to be dominant in the reactor. Ultra-low OLR will provide insufficient nutrients for

PHA-accumulating bacteria proliferation, which leads to high nitrifying bacteria population and low PHA-accumulating bacteria population in the reactor (Sepehri & Sarrafzadeh, 2018). Fauzi et al. (2019) studied the effect of organic loading rate (OLR) and feast to famine (F/F) ratio on PHA yield and accumulation. The F/F ratio increased from 0.4 to 2.0 when OLR changed from 1000 mgC/(L*d) to 1250 mgC/(L*d). This high F/F ratio leaded to a failure of ADF strategy, and therefore, significantly decreased the PHA yield and accumulation from 0.7 mgC PHA/ mgC substrate and 80 wt.% to 0.3 mgC PHA/ mgC and 27 wt.%, respectively. Other research also reported that F/F ratio should be kept low, such as below 0.55, to have better PHA yield and accumulation capacity (Freches & Lemos, 2017; Wijeyekoon et al., 2018).

During the PHA production stage, pulsed feeding and batch feeding had no obvious effects on the final PHA accumulation (Tamang et al., 2019). However, continuous feeding resulted in average 10% higher in PHA accumulation and doubled PHA yield compared to pulsed feeding (Chen et al., 2015a). The reported OLR during PHA production stage in Table 2.4 fell in a range from 1000 to 3600 mgC/(L*d). Generally, high carbon to nitrogen ratio (C/N) and low phosphate concentration could lead to high PHA yield and accumulation (Wijeyekoon et al., 2018). But ultra-high C/N (74.9) was reported to cause bulking and leaded to low PHA accumulation (2.59%) (Fang et al., 2019). Wijeyekoon et al. (2018) also discussed the effect of dissolved oxygen (DO) on PHA yield and accumulation. Their study revealed that the limited DO slowed down PHA accumulation speed, but the overall PHA yield and accumulation were not affected.

2.2.3 PHA production via chemical synthesis

PHA can also be synthesized by anionic, coordination, and cationic polymerization using proper raw materials, initiators, and conditions (Tian et al., 2012). Some common raw materials used in PHA chemical synthesis are β-Butyrolactone for P3HB, γ-Butyrolactone for P4HB, and β-Valerolactone for P3HV (Moore et al., 2005; Rieth et al., 2002). Different kinds of polymerization require different catalysts for PHA chemical synthesis. Thus far, some alkali metal organics, guanidine, phosphazene and amidine have been applied as catalysts in anionic polymerization of PHA (Domiński et al., 2019; Jaffredo et al., 2012). Jaffredo et al. (2012) demonstrated the feasibility of guanidine, phosphazene, and amidine as catalysts in P3HB anionic polymerization under mild conditions. The generated P3HB had average molar mass of 21000 with narrow distribution. Domiński et al. (2019) compared P3HB polymerized from β-Butyrolactone with multiple sodium phenoxides. P3HB with various molar mass was synthesized due to differences in nucleophilicity and basicity of different used catalysts. Metal based catalysts with aluminum, tin, yttrium, zinc, or lanthanide were usually reported in coordination polymerization of PHA production (Domiński et al., 2019). Fang et al. (2013) converted 92% β-Butyrolactone to P3HB within 2 hours at 20 ℃ by using yttrium based catalyst in coordination polymerization. 99% conversion rate from β-Butyrolactone to P3HB within 4 hours was reported by Liu et al. (2010). They used zinc based catalyst at 55 ℃ in coordination polymerization of P3HB. Trifluoromethanesulfonic acid has also been reported as initiators in cationic polymerization of raw materials to PHA. Basko et al. (2013) reported a general procedure for cationic polymerization of β-Butyrolactone to P3HB. This method used trifluoromethanesulfonic acid as catalyst in presence of isopropanol and reached 99% of conversion rate at room temperature. Chemical

synthesis was able to generate atactic, syndiotactic and isotactic PHA (Domiński et al., 2019). However, heavy metal catalysts, toxic organics and strong acids were needed during the synthesis, which would cause pollution. PHA obtained from chemical polymerization usually has low molecular weight, which is another problem needed to be overcome.

2.3 Extraction of intracellular PHA

Since microbially produced PHA is stored inside cells, it needs to be extracted from biomass and then purified. This step is one of the major obstacles for the broad application and commercialization of PHA because extraction and purification require solvents and energy input. Using large amount of solvents not only increase the cost of recovering PHA from biomass, but also cause PHA degradation during the dissolution and precipitation processes. Moreover, the used solvents need to be treated and disposed of properly since most of the solvents are toxic and detrimental to the environment. The high energy input in this step also increases the cost of producing PHA (Rodriguez-Perez et al., 2018). It was reported that more than 50% of PHA production cost was attributed to the extraction and purification steps (López-Abelairas et al., 2015). This section summarizes the most common extraction techniques currently applied in PHA recovery.

Intracellular PHA is extracted from bacteria cells by two different approaches: 1) solubilizing PHA by selective solvents; 2) solubilizing cellular materials surrounding PHA by chemicals. In practical applications, the two approaches are usually used together to achieve high recovery rate and high purity of PHA. Approach 1 is usually carried out by organic solvent extraction. The selected organic solvents dissolve PHA, but not the other intracellular materials. Chlorinated solvents, such as

chloroform, dichloromethane, trichloroethane and methyl chloride, are excellent solvents for PHA dissolution (Mannina et al., 2020). Other organic solvents, such as propylene carbonate, acetone, tetrahydrofuran and ethylene carbonate, are also frequently used solvents for PHA extraction (Kumar et al., 2020). After PHAs are dissolved in solvents, an alcohol (usually chilled methanol or ethanol) is subsequently applied to precipitate the dissolved PHAs. This organic solvent extraction method usually achieves high PHA recovery rate and high purity. Colombo et al. (2020) reported a recovery rate of 63.5% using chloroform as the solvent. Samorì et al. (2015) used dimethyl carbonate as solvent and recovered 63% PHA from mixed culture with a purity of 98% without pretreatment. However, using organic solvents is harmful to the environment and inefficient. The quantity of required solvent is usually over ten times higher than that of recovered PHA (Koller et al., 2013).

Approach 2 involves using chemical or biological methods to digest cellular materials without solubilizing PHA. Various chemicals, such as acids, alkalis, oxidants, surfactants, and enzymes can degrade cellular materials. All these chemicals react with polypeptides or lipids on the cell surface to lyse bacterial cells for PHA release. This process solubilizes most of the cellular materials, while PHA remain in solid granules. Solid PHA granules can be separated from the liquid phase and purified. López-Abelairas et al. (2015) compared three common chemicals: sulfuric acid, sodium hydroxide and sodium hypochlorite and found that sulfuric acid yielded the highest recovery rate and purity of PHA at 79% and 98%, respectively. Sodium hydroxide provided comparable recovery rate but lower purity. Sodium hypochlorite digestion recovered 57% of PHA with 98% purity, but this process had the greatest negative environment impact in terms of greenhouse gas emission. Among the three

digestion chemicals, the least PHA degradation was observed under acidic condition. Overall, acid, alkali, and oxidant digestions are considered as green extraction methods compared to organic solvent extraction, but operational conditions, such as temperature and chemical concentration, need to be strictly controlled for optimum performance.

Enzyme digestion is another option for cell lysis during PHA extraction because of its high efficiency. Lakshman and Shamala (2006) used enzymes from *Microbispora sp.* followed by chloroform extraction to recover PHA produced by *Sinorhizobium meliloti*. The maximum recovery rate and purity were 49% and 94%, respectively. Similarly, Israni et al. (2018) applied a co-culture of *Streptomyces albus* and *Bacillus megaterium* to extract PHA. The lytic enzymes produced by *Streptomyces albus* facilitated the efficient recovery of PHA produced by *Bacillus megaterium*. The final yield rate was 0.55g PHA/g dry cell mass. Although enzyme digestion is highly efficient, the digestion conditions, such as temperature and pH, need to be properly controlled to prevent denaturation of enzymes. In addition, enzyme digestion is expensive in large-scaled applications, which limits its widespread adoption (Mannina et al., 2020). Surfactants, such as sodium dodecyl sulphate (SDS), are frequently used in PHA extraction. Jiang et al. (2015) used SDS treatment along with sodium hydroxide digestion and achieved a 91% PHA recovery rate and 99.1% purity. A combination of SDS treatment and sodium hypochlorite digestion also resulted in 78.7% recovery rate and purity no less than 83.29% (Marudkla et al., 2018). However, a large usage of surfactants for the PHA recovery process leads to secondary problems due to the difficulties in recovering used surfactants (Kunasundari & Sudesh, 2011). A biological method using *Tenebrio*

molitor to digest cellular materials was also reported in the literature (Murugan et al., 2016; Ong et al., 2018). *Tenebrio molitor* is a type of insect that can digest biomass but not PHA. By feeding PHA-containing biomass to *Tenebrio molitor*, undigested PHA granules can be recovered from the excreta of the insect. Additional purification resulted in 100% pure PHA (Murugan et al., 2016). Ong et al. (2018) also reported a recovery of PHA with purity greater than 90% using the same insect digestion method.

2.4 Common filamentous bacteria in activated sludge

Bulking is a common occurrence and a serious problem in the WWTPs. Once bulking happens, gravity separation failure in the secondary clarifier will occur, which results in activated sludge directly discharging into the natural water system. It was reported that more than 50% of WWTPs around the world had periodic bulking (Noutsopoulos et al., 2007). Bulking is caused by a sudden and excessive growth of filamentous bacteria. Therefore, this group of microorganisms are usually treated as unwelcomed bacteria in the WWTPs. Research in the recent several decades of filamentous bacteria mainly focused on their morphology and metabolism for the purpose of identification and controlling growth, without realizing the potential good mechanical properties of them.

The formation of large activated sludge flocs required two steps: 1) filamentous bacteria interacted with each other and formed backbones of sludge flocs; 2) other floc-forming bacteria attached on the filamentous backbones by their extracellular polymeric substances (EPSs) and grew (Cenens et al., 2000; Sezgin et al., 1978). Filamentous bacteria are the essential reinforcements of a stable and robust large sludge floc, which indicated better mechanical properties than those of floc-forming bacteria. As many as 30 kinds of filamentous bacteria were reported existing

in WWTPs (Nielsen et al., 2009). According to a survey, some common filamentous bacteria in the U.S. WWTPs were *Sphaerotilus natans* (*S. natans*), type 021N, *Thiothrix* spp., and *Beggiatoa* spp. (Jenkins et al., 1993).

S. natans plays an important role in biofilm development (Galván et al., 2002). It is a Gram negative bacteria with diameter from 1-2 μm and 100-1000 μm in length (Jenkins et al., 2003). Gridneva et al. (2011) reported that the optimal temperature and pH for *S. natans* growth were 25-32℃ and 6.5-7.5, respectively. Multiple studies have shown that low dissolved oxygen (DO) is a main inducement of *S. natans* growth (Gaval & Pernelle, 2003; Seder-Colomina et al., 2015). *S. natans* is a kind of heterotrophic bacteria, which uses a great variety of simple organics as its energy source (Gridneva et al., 2011; Pellegrin et al., 1999). It was also capable to oxidize iron and deposit iron oxides in its sheath, which helped maintain a firm structure of filaments and protect itself from predation and UV radiation (Glasauer et al., 2022; Seder-Colomina et al., 2014).

Type 021N, *Thiothrix* spp. and *Beggiatoa* spp. are a group of colorless sulphur-oxidizing filamentous bacteria (Nielsen et al., 2000). Their Gram and Neisser staining results are all negative. Type 021N is the longest bacteria in this group with length range from 100-1000 μm, while length of *Thiothrix* spp. and *Beggiatoa* spp. fall in 50-500 μm range (Jenkins et al., 2003). The diameter of three bacteria are from 0.7-3 μm (Jenkins et al., 2003).

There are many specific factors influencing the growth of filamentous bacteria, including DO, nutrient concentration, pH, and nature of organic substrates. Based on the growth conditions of filamentous bacteria, they were divided into four groups in Table 2.5 (Jenkins et al., 2003; Wanner & Grau, 1989).

2.5 Modification of PHA

Properties of a single polymer do not meet all the application requirements. Thus, modifying properties of polymers, using physical, chemical, or biological methods, are necessary to expand polymer applications. In this section, the methods to modify mechanical properties of PHA will be summarized.

2.5.1 Physical modification of PHA

Physical modification is the most common method of improving mechanical properties of PHA due to its effectivity and low cost (Sharma et al., 2021). In this method, selected materials are blended with PHAs to modify their mechanical properties.

2.5.1.1 Blending with other polymers

Blending PHA with other natural or synthetic polymers is a commonly technique to improve mechanical properties of PHA. Although some materials require chemical treatment during blending processes, blending is still classified as physical modification because the structure of PHA is not modified. The advantage of blending is that the added materials, such as polylactic acid, are inexpensive and readily available. Moreover, blending does not require aggressive chemicals, and properties of final products can be predicted from the parents materials (Raza et al., 2020). Table 2.6 summarizes the improved properties of different PHA blends.

In addition, PHA can be blended with many other natural polymers (chitosan, chitin, starch, and lignin) and synthetic polymers (polyvinyl acetate, polyvinyl phenol, polyethylene oxide, and polypropylene carbonate). Most of these combinations reported in the literature focused on the miscibility between two polymers, as well as biocompatibility, biodegradability, water and gas permeability, and UV resistivity of

the final products. Changes in melting temperature, glass transition temperature, and crystallinity are also commonly discussed factors (Sharma et al., 2021). However, changes in mechanical properties after blending are not commonly studied. Generally, PHA blending got improvements in tensile and impact properties compared to pure PHA. Good miscibility between two polymers was concluded as prerequisite of better adhesion and better mechanical properties of blending products. However, Ivorra-Martinez et al. (2020) found that 40 wt.% polycaprolactone addition into poly(hydroxybutyrate-co-hydroxyhexanoate) (PHBH) resulted in 200% increase in impact resistance and 33 times increase in elongation at break, although polycaprolactone and PHBH were immiscible. This indicated that the improvements in mechanical properties should be attributed to change in degree of crystallinity during blending. Research from Aldam et al. (2020) also supported this conclusion.

2.5.1.2 Fiber-reinforced composite material

Mechanical properties of PHA can be enhanced by mixing with fibers to create composite materials. A composite material is made from two or more constituents, one being the matrix and another being the reinforcement, which together provide properties that are superior to either of the individual component material. While PHA serves as the matrix, it needs reinforcement to improve its mechanical properties. Generally, some mechanical properties of polymer, such as elastic modulus and tensile strength, will be improved after fiber reinforcement (Erhard, 2006).

Fiber-reinforced polymer (FRP) composite materials were initially developed as very strong, lightweight materials for the aerospace and defense industries. Conventional FRP composite materials mostly use synthetic fibers, such as glass and carbon fibers, as reinforcement agents, while the recent trend is moving from synthetic

fibers to natural fibers, such as wood and flax fibers. Compared to synthetic fibers, natural fibers are environmentally friendly and inexpensive without compromising mechanical properties to synthetic fibers (Pickering et al., 2016; Sanjay et al., 2018). A drawback of fiber reinforcements is that they usually have low affinity with PHA at their interface, resulting in poor mechanical properties of final products. Therefore, natural fibers usually need to be treated with coupling agents to achieve better adhesion with PHA. Table 2.7 summarizes recent research on composites with PHA as the matrix and natural fibers as reinforcements. Currently, animal-based fiber reinforcement is not reported in the literature to the best of our knowledge.

2.5.1.3 PHA blends with nano materials

Applying PHA with nanoparticle is another method to alter PHA properties. In this method, PHA is either blended with nano-sized materials or reinforced with nanofibers to get improved properties.

The most common inorganic nanomaterials in PHA blending are graphene or carbon nanotubes and clay or silica nanoparticle. Lemes et al. (2019) reported that PHBV/multi-walled carbon nanotube composite fabricated by solvent casting increased tensile modulus and tensile strength by 150% with 1.5 wt.% of multi-walled carbon nanotube addition. Ajmal et al. (2018) fabricated a nanocomposite combining PHBV, polyethylene glycol (PEG) and sepiolite by solvent casting. Tensile strength and elastic modulus of this nanocomposite increased approximately 5.6 and 15 times, respectively, with 18 wt.% PEG and 3 wt.% sepiolite addition. García-Quiles et al. (2019) also studied a PHA/sepiolite nanocomposite manufactured by extrusion moulding. Mechanical test results showed much improved mechanical properties with this combination. A biodegradable nanocomposite combining PHBV and nano silicon

dioxide was fabricated by solvent casting (Ojha & Das, 2020). Compared to the original PHBV, the nanocomposite with 1.5 wt.% of nano silicon dioxide had 3.4 times higher Young's modulus and 12 times higher tensile strength. Besides, the improvement in impact strength of this nanocomposite was also observed. PHA has also been blended with organic nanocrystals, such as nanocellulose (Panaitescu et al., 2018, 2020). Panaitescu et al. (2018) reported 21% higher tensile strength and 19% higher storage modulus from PHB/nanocellulose blending. By blending PHBV and nanocellulose using melt mixing, Panaitescu et al. (2020) observed a 1.7-3 times higher deformation capacity of the final product.

Nanofibers can also reinforce PHA. Valentini et al. (2019) used 0.5 wt.% of fibrillated nanocellulose to reinforce PHBH. The composite fabricated by melt extrusion showed an increase in elastic modulus of 1.4 times. Rivera-Briso et al. (2020) increased the compression modulus of the PHBV composite by 125% using 1 wt.% of nanocarbon fiber as the reinforcing agent. Overall, fiber loading of nanofibers is less than that of macro-sized fibers. This is because nanofibers have larger specific surface area and better dispersion in the polymer matrix.

Physical modification of PHA usually requires high temperature processing, such as PHA melting during injection moulding and melt mixing. However, random chain scission and *cis*-elimination under high temperature is unavoidable and will cause molecular weight loss, which weakens the toughness of PHA (Montano-Herrera et al., 2014; Wang et al., 2016). Therefore, temperature during PHA melting should be carefully controlled. Xiang et al. (2016) studied the relationship between PHBV molecular weight loss and temperature. Their results revealed that the molecular weight of neat PHBV decreased 80% when rising temperature from 180 ℃ to 230 ℃.

Kaygusuz and Özerinç (2019) also reported an extremely low elongation at break when 3D printing temperature over 260 ℃ due to PHA degradation starting from 240 ℃. This suggested that PHA melting process should be short and temperature should be controlled as low as possible.

2.5.2 Chemical modification of PHA

The properties of PHA can be modified by changing its molecular structure. This is usually achieved by adding functional groups or other polymers onto the PHA chain. Carboxyl, hydroxyl, halogen atoms, and epoxy groups are the most common functional groups added to modify PHA. Ashby et al. (2000) converted 37% side-chain olefinic groups on linseed oil based PHA to epoxy groups. This change in molecular structure increased tensile strength and Young's modulus 330% and 3858%, respectively. Attaching other polymers, such as ethyl cellulose, onto a PHA chain, which is called grafting, can also alter thermal and mechanical properties of the original PHA. Iqbal et al. (2014) grafted ethyl cellulose onto PHB by using laccase. The tensile strength and elongation at break increased to 68.3MPa and 13.2%, respectively, due to hydrogen-bonding between PHB and ethyl cellulose. Most studies on chemical modifications focused on change of hydrophilicity, thermal stability, and crystallinity of PHAs (Raza et al., 2018). Few of them reported changes in mechanical properties. Although PHA chemical modification is widely used to expand applications of PHA, a drawback of this method is that it usually requires strict reaction conditions such as temperature and concentrated chemicals (Sharma et al., 2021).

2.5.3 Biological modification of PHA

Different PHA homopolymers exhibit diverse mechanical properties. The elastic modulus of different PHA homopolymers ranges from 2 MPa (mcl-PHA) to 3.5 GPa (scl-PHA). Elongation at break of PHA homopolymers falls into the range of 0.4% (P3HB) to 1000% (P4HB). Similarly, the tensile strength of PHA varies from 0.9 MPa to 190 MPa (M. Singh et al., 2015). Therefore, copolymers of PHA with multiple monomer contents will have different mechanical properties. Both mixed culture and pure culture can spontaneously produce PHA copolymers by using appropriate bacteria stains and feedstocks (Ray & Kalia, 2017b). Rebocho et al. (2020) used a co-culture of *Cupriavidus necator* DSM 428 and *Pseudomonas citronellolis* NRRL B-2504 to produce PHA that consisted of 48 wt.% of PHB and 52 wt.% of mcl-PHAs. The mechanical tests showed that this copolymer exhibited greater deformation capacity than homopolymers. Munir and Jamil (2018) observed a high production rate of PHBV from the co-culture of ST2 (*Pseudomonas sp.*) and CS8 (*Bacillus sp.*) that were fed with propionic acid and glucose. Similarly, a mixture of acetic acid and propionic acid as the feedstock also resulted in high amount of PHBV by using mixed culture fermentation (Munir & Jamil, 2020). Their research revealed that the usage of propionic acid is directly associated with the production of PHV. Other research which studied producing PHA copolymers by different feedstocks in mixed culture fermentation were also summarized in Table 2.4.

Pure culture fermentation can also produce copolymers of PHA by varying feeding compositions. Ray and Kalia (2017a) recovered multiple copolymers of PHA, such as poly(hydroxyoctanoate-co-dodecanoate) (PHOD) and poly(hydroxyhexanoate-co-hydroxydodecanoate) (PHHD), from pure culture of *Bacillus thuringiensis* EGU45 by feeding different combinations of glycerol, glucose, and propionic acid. *Bacillus*

spp. was able to produce PHBV by uptake glucose and propionic acid (Reddy et al., 2009; Reddy et al., 2009), glucose and valerate (Tajima et al., 2003), glucose and pea shell slurry (Kumar et al., 2014). Xu et al. (2021) reported PHA copolymers production from *Pseudomonas putida* KT2440 by feeding a combination of lignin derivatives and glycerol. *Cupriavidus necator* family was widely reported to produce PHBV by feeding fatty acid methyl ester and valeric acid (Bhubalan et al., 2008), glycerol, sunflower meal and levulinic acid (Kachrimanidou et al., 2014), crude glycerol and rapeseed meal (García et al., 2013). Bhubalan et al. (2008) also reported terpolymer poly(hydroxybutyrate-co-hydroxyvalerate-co-hydroxyhexanoate) (PHBVH) as fermentation product by *Cupriavidus necator* H16 using palm kernel oil and valeric acid as the feedstock (Bhubalan et al., 2008). The advantage of biological modification is that PHA copolymers with better mechanical properties are naturally produced in biomass without downstream processing, such as blending.

2.6 Applications of PHA

PHA has been found as suitable material for various industrial applications because of its biodegradation, biocompatibility, and mechanical properties. It has been applied in medicine, agriculture, and packaging industries.

Because PHA has no cytotoxicity and can be biodegraded, it is a suitable material for antimicrobials, drug carriers, tissue engineering, and nontoxic implants. The presence of PHB restricting growth of pathogenic bacteria is an attractive phenomenon. PHB was reported to inhibit the growth of *Vibrio campbellii* LMG21363 (Defoirdt et al., 2007), *Escherichia coli* and *Salmonella* spp. (Defoirdt et al., 2009). Thus, PHB could be used to lower infection risk. The controlled release of medicine against cancer and pathogenic bacteria can be achieved by using PHA as medicine

carrier for its slow biodegradation (Kalia et al., 2019). Kehail and Brigham (2018) reported that PHBH could decrease the growth rate of *Rhodococcus opacus* PD630 by 9% when binding with lysozyme. The biocide treated PHBV nanofibers was used as biocontrol agent and proved to be 98.9% effective in inhibiting *P. aeruginosa* PA01 growth (Li et al., 2020). It was also reported that PHA based medicine delivery carriers were effective in treating multiple diseases including melanoma (Jiang et al., 2019), colon cancer (Kwon et al., 2014), ovarian cancer (Vilos et al., 2013) and diabetes (Chaturvedi et al., 2015). PHA can also regulate cell proliferation, differentiation, and apoptosis by interacting with integrins (Wang et al., 2013). Therefore, PHA has been widely used in tissue engineering, such as helping regenerate intestinal, cardiac, vascular, osseous, and neural tissues (Kalia et al., 2021; Ray et al., 2019). Rai (2017) has successfully used PHBV, PHBH and PHBVH to help *HaCaT* human keratinocytes proliferation. The promotion of mesenchymal stem cell differentiation by hydroxylated PHBV and PHBH was helpful in osteogenesis and memory improvement (Krishnan et al., 2021; Surmenev et al., 2019; Zhang et al., 2013). PHA-based materials were favorable as human implants, because they could reduce inflammatory response by reducing proinflammatory cytokine secretion (Kalia et al., 2021). PHA-based scaffolds were reported as excellent human implants in accelerating wounds healing while resisting infection (Lim et al., 2017; Mukheem et al., 2018; Ray et al., 2019).

Similarly, PHA is also applied in agriculture as the carrier of agrochemicals. Fertilizers or pesticides are bound with PHA to achieve steady and slow release. Murugan et al. (2020) observed higher oil palm growth with a PHA controlled-release fertilizer than that with an immediate-release fertilizer. This result indicated that PHA

controlled-release fertilizer was better for promoting plant growth. Volova et al. (2020) examined controlled-release formulations of herbicides and fungicides embedded in PHA. Their results showed that binding herbicides and fungicides with PHA prolonged herbicidal effects and antifungal activities of the parent compounds. PHA is also successfully used for long-term preservation of cells and seeds. González et al. (2020) investigated the possibility of preserving *Pseudomonas putida* KT2440 by PHA encapsulation. Bacteria remained viable under various hostile conditions, such as alkaline solution and hydrogen peroxide exposure, suggesting that PHA encapsulation may provide good protection against harsh conditions.

Biodegradation of PHA makes them suitable for many single-use products, such as packaging film, plant pots, and plastic tableware (Meereboer et al., 2020). PHA-coated cellulose nanopaper was reported to have lower oxygen permeability and higher hydrophobicity than that of cellulose nanopaper without PHA coating (Urbina et al., 2019). Keskin et al. (2017) reported that biodegradable PHA composites exhibited sufficient gas barrier properties to be potential substitutes for petroleum-based polymers, thus making them a promising material in the packaging industry.

Other than using whole PHA, PHA depolymerization products and their derivatives can be valuable materials as well. Producing *n*-Butanol, which is liquid fuel, from P3HB thermolysis products was studied by Schweitzer et al. (2015). Gene modified switchgrass containing P3HB was pyrolyzed to get crotonic acid. This acid was converted to *n*-Butanol via esterification and hydrogenation under 400 psi and 200 ℃ with cupric oxide based catalyst. Similarly, crotonic acid, as the P3HB pyrolysis product, can be converted to propylene and maleic anhydride via decarboxylation (Peterson & Fischer, 2010) and oxygenation (Somleva et al., 2013),

respectively. The variety of PHA monomers and derivatives allows further expansion of PHA applications. For example, medium chain length 3HAs were reported to have good antibacterial ability against *Salmonella typhimurium*, *Listeria monocytogenes*, and *E. coli* O157:H7 (Kalia et al., 2021). 3HB was reported to activate and help proliferation L929 murine fibroblasts and *HaCaT* human keratinocytes (Pramanik et al., 2016). One derivative of 3-hydroxybutyrate, which named 3-hydroxybutyrate methyl ester, was used as substitution for glucose in treating hypoglycemia (Kalia et al., 2021). Both 3-hydroxybutyrate and 3-hydroxybutyrate methyl ester were reported to inhibit the development of mice osteoporosis (Cao et al., 2014). This derivative was also found to treat Alzheimer's disease by inhibiting cell apoptosis (Zhang et al., 2013).

Table 2.1. Summarization of common PHAs

N value	R group	Name	Abbreviation
1	Methyl	Poly(3-hydroxybutyrate)	P(3HB)
	Ethyl	Poly(3-hydroxyvalerate)	P(3HV)
	Propyl	Poly(3-hydroxyhexanoate)	P(3HH)
	Pentyl	Poly(3-hydroxyoctanoate)	P(3HO)
	Nonyl	Poly(3-hydroxydodecanoate)	P(3HD)
2	Hydrogen	Poly(4-hydroxybutyrate)	P(4HB)
	Methyl	Poly(4-hydroxyvalerate)	P(4HV)
3	Hydrogen	Poly(5-hydroxyvalerate)	P(5HV)
	Methyl	Poly(5-hydroxyhexanoate)	P(5HH)
4	Hexyl	Poly(6-hydroxydodecanoate)	P(6HD)

Table 2.2. Properties comparison of PHAs and other common polymers

Polymer	Melting temperature (°C)	Glass transition temperature (°C)	Crystallinity (%)	Young's modulus (GPa)	Tensile strength (MPa)	Elongation at break (%)	Reference
PHB	175	4	60	3.5	40	5	(Chodák & Blackburn, 2009)
PHBV (20% HV)	145	-1	40-60	1.9	26	27	(Keskin et al., 2017)
PP	170	-10	50	1.5	38	400	(Chodák & Blackburn, 2009; Keskin et al., 2017)
LDPE	110	-30	50	0.2	10	600	(Chodák & Blackburn, 2009)
Rigid PVC	100-260	82	10	3.4	16.5	270	(Gilbert, 1994; Titow, 1984; Wilkes et al., 2005; Zampino et al., 2021)
PET	260	67-81	30-40	2.8-3.1	55-75	50-150	(Ehrenstein, 2001; Lu et al., 2011)

Table 2.3. Major enzymes involved in PHAs biosynthesis

Pathway	Enzyme	Abbreviation	Reference
I	Glyceraldehyde-3-phosphate dehydrogenase	Enzyme 1	(Raberg et al., 2011)
	Pyruvate dehydrogenase complex	Enzyme 2	(Raberg et al., 2011)
	3-Ketothiolase	PhaA	(Peoples & Sinskey, 1989)
	NADPH-dependent acetoacetyl-CoA reductase	PhaB	(Peoples & Sinskey, 1989)
	NADPH-dependent 3-Ketoacyl reductase	FabG	(Kadouri et al., 2005; Peoples & Sinskey, 1989)
	PHA synthase	PhaC	(Ren et al., 2000)
II	(R)-Enoyl-CoA hydratase	PhaJ	(Sato et al., 2011)
III	Acetyl-CoA carboxylase	ACC	(Somleva et al., 2013)
	Malonyl-CoA:ACP transacylase	FabD	(Lee et al., 2011)
	3-Hydroxyacyl-ACP:CoA transacylase	PhaG	(Leo et al., 2005)

Table 2.4. PHA production research using mixed culture fermentation

Raw organic substrate	Inoculum/ Selection strategy	Dominant PHA-accumulation strains (population%)	Feed mode	PHA yield	PHA accumulation (PHA wt./ dry cell wt.)	PHA composition (mol%)	Reference
Crude glycerol	Activated sludge/ ADF	Alphaproteobacteria (42.1%); Gammaproteobacteria (35.5%); Betaproteobacteria (7.2%)	Batch feeding mode with 1000 mgC/(L·d) of OLR and average 0.4 F/F ratio Supernatant from cheese whey anaerobic fermentation was added by batch fed mode. OLR and F/F ratio was maintained at 1500 mgC/(L·d) and 0.07, respectively.	0.7 mgC PHA/ mgC Substrate	80%	3HB: 3HV= 60: 40	(Fauzi et al., 2019)
Deproteinized cheese whey	Activated sludge/ ADF	-		0.76 mgC PHA/ mgC Substrate	62%	3HB: 3HV= 100: 0	(Colombo et al., 2019)

Table 2.4. continued.

Acidified brewery wastewater	Activated sludge/ ADF	-	Pulsed feeding based on DO change using substrate with 2100 mgC/(L·d) of OLR	0.76 Cmol PHA/ Cmol Substrate	44.8%	3HB: 3HV= 59: 41	(Tamang et al., 2019)
Crude glycerol	Anaerobic and aerobic sludge mixture/ ADF	*Thauera (*class *Betaproteobacteria)* (25.2%); *Amaricoccu (*class *Alphaproteobacteria)* (47.2%)	Batch feed using fermented crude glycerol with no nitrogen condition	0.84 gC PHA/ gC Substrate	76%	3HB: 3HV= 84: 16	(Burniol-Figols et al., 2018)

Table 2.4. continued.

Wastewater activated sludge	Activated sludge/ ADF	*Thauera* (61%)	Wastewater activated sludge was fermented followed by wet oxidation. Ammonia was removed from the mixture and DO was maintained at 25% saturation. This mixture was fed hourly.	0.5 Cmol PHA/ Cmol Substrate	37.2%	3HB: 3HV= 76: 24	(Wijeyekoon et al., 2018)
Sugar cane molasses	Activated sludge/ ADF	-	Molasses was anaerobic fermented and batch-fed under low nitrogen condition.	0.62 Cmol PHA/ Cmol Substrate	10%	3HB: 3HV= 62: 38	(Albuquerque et al., 2007)

Table 2.4. continued.

Synthetic mixture (acetate, propionate, butyrate and valerate)	Activated sludge/ ADF	-	Continuous feeding mode	0.81 Cmol PHA/ Cmol Substrate	70.36%	-	(Chen et al., 2015b)
30% food waste with 70% wastewater sludge	Activated sludge/ ADF	*Moraxellaceae* (*Proteobacteria* phylum) (18%); *Rhodobacteraceae* (*Proteobacteria* phylum) (15.4%); unclassified *Alphaproteobacteria* (8.8%)	Nitrogen-limitation fed-batch	-	43.5%	3HB: 3HV= 95: 5	(Perez-Zabaleta et al., 2020)
Paper mill wastewater	Activated sludge/ ADF	*P. acidivorans* (56%)	Fed-batch using fermented acidified paper mill wastewater	0.8 gC PHA/ gC Substrate	76.8%	-	(Jiang et al., 2012)

Table 2.4. continued.

Wastewater sludge and food waste	Activated sludge/ ADF	-	Fed-batch mode using fermented mixture as substrate (organic loading of 3600 mgC/L and 0.3 F/F ratio)	0.54 mgC PHA/ mgC Substrate	About 47%	3HB: 3HV= 74: 26	(Zhang et al., 2014)
Cheese whey	Activated sludge/ ADF	-	Pulsed feeding based on DO change	0.8 Cmol PHA/ Cmol Substrate	81.4%	3HB: 3HV= 60: 40	(Colombo et al., 2016)
Rice winery wastewater	Activated sludge/ ADF	*Zoogloea* (7%); *Rhodobacter* (3.2%)	Fed-batch mode using raw wastewater as substrate (OLR of 2400 mgC/(L·d))	0.23 gC PHA/ gC Substrate	2.59%	3HB: 3HV= 8: 92 (Day 40)	(Fang et al., 2019)

Table 2.4. continued.

Olive mill wastewater	Activated sludge/ Carbon and nitrogen li mitation cycle	-	Fed-batch mode using fermented olive mill wastewater under low nitrogen condition	0.07 gC PHA/ gC Substrate	8.8%	3HB: 3HV= 78: 22	(Kourment za et al., 2015)
Municipal solid waste leachate	Activated sludge/ ADF	*Xanthobacter* (-)*; Azorhizobium* (-)	Pulsed feeding based on pH change	0.2 gC PHA/ gC Substrate	29.0%	-	(Korkakaki et al., 2016)

-: Not reported in the literature

Table 2.5. Common filamentous bacteria and their features

	Microorganisms	Features
Group 1 Low DO aerobic zone growers	*Sphaerotilus natans*	Readily metabolizable substrates
	type 1701	Low DO
	Haliscomenobacter hydrossis	Wide MCRT range
Group 2 Mixotrophic aerobic zone growers	type 021N	Readily metabolizable substrates
	Thiothrix spp.	Moderate to high MCRT Sulfide oxidizing microorganisms Grow under nutrient deficiency
Group 3 Other aerobic zone growers	type 1851	Readily metabolizable substrates
	Nostocoida limicola spp.	Moderate to high MCRT
Group 4 Aerobic, anoxic, anaerobic zone growers	type 0041	Grow in aerobic, anoxic, and anaerobic systems
	type 0675	High MCRT
	type 0092	Possible growth on hydrolysis products of particulates
	Microthrix parvicella	

MCRT: mean cell residence time

Table 2.6. Different PHA blending combinations and their improved properties

Blended material	Blending techniques	Improved properties	Reference
PHA/ polylactic acid	3D printing and injection moulding	Impact strength and notched impact strength	(Ecker et al., 2019)
PHA/ polylactic acid	Melt-mixing	Elongation at break	(Kaygusuz & Özerinç, 2019)
PHA/ polylactic acid	Injection moulding	Impact strength	(Burzic et al., 2019)
PHA/ cellulose acetate	Solvent casting	Tensile strength	(Aldam et al., 2020)
PHA/ hydroxypropyl distarch phosphate	Solvent casting	Tensile strength	(Sun et al., 2017)
PHBV/ natural rubber	Reactive extrusion	Notched impact strength and elongation at break	(Zhao et al., 2019b)
PHBV/ polylactic acid	-	Tensile strength	(Zhao et al., 2019a)
PHB/ polyethylene glycol	Solvent casting	Elongation at break	(Ansari & Fatma, 2018)
PHAs/ polybutylene succinate/ polycaprolactone	Melt mixing	Tensile strength and elongation at break	(Nishida et al., 2019)
PHBH/ polycaprolactone	Extrusion followed by injection moulding	Impact strength and elongation at break	(Ivorra-Martinez et al., 2020)

Table 2.7. Composite material with PHAs as matrix and natural fibers as reinforcements

Matrix	Reinforcement	Fabrication techniques	Improved properties	Reference
PHA	Borneo acacia wood fiber	Compression moulding	Tensile modulus and flexural modulus	(Bakri et al., 2018)
PHA	Wood flour	Micro-screw extrusion	Tensile modulus and flexural modulus	(Tian et al., 2021)
PHB/PHBV	Agave fiber	Compression moulding	Storage modulus, Tensile modulus, flexural modulus, and impact strength	(Torres-Tello et al., 2017)
PHBV	Ceiba pentandra bark fiber	Solvent casting	Tensile strength	(Varghese et al., 2020)
PHBH	Alkaline/organo-silanes treated Aloe Vera fibers	Melt compounding	Storage modulus and loss modulus	(Dehouche et al., 2020)
PHAs	Flax fiber	Film stacking	Tensile strength	(Pantaloni et al., 2021)
PHB	Flax fiber	Film stacking	Stiffness and tensile strength	(Ventura et al., 2017)
PHBV	Lignocellulosic fiber from park and garden waste	Melt extrusion	Young's modulus	(Viretto et al., 2021)
PHBV	Wood fiber	Melt extrusion	Tensile modulus	(Vandi et al., 2019)
PHBV	Luffa Fiber	Compression moulding	Flexural strength	(Guo et al., 2019)

Table 2.7. continued.

PHA	Cellulosic fibers	Dip-coating	Tensile strength	(Zhao et al., 2017)
PHA	Cellulose microfibers	Melt extrusion	Tensile strength and Young's modulus	(Mármol et al., 2020)
PHBV	Sisal fiber	Compression moulding	Tensile strength, tensile modulus and storage modulus	(Kittikorn et al., 2018)
PHBV	Wood fiber	Injection moulding	Young's modulus	(Mazur & Kuciel, 2019)
PHB	Rice husk	Melt mixing	Tensile strength, elastic modulus, elongation at break and impact strength	(Moura et al., 2018)

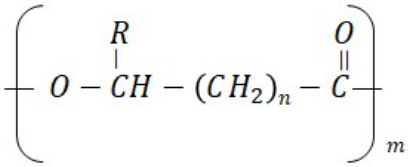

(a)

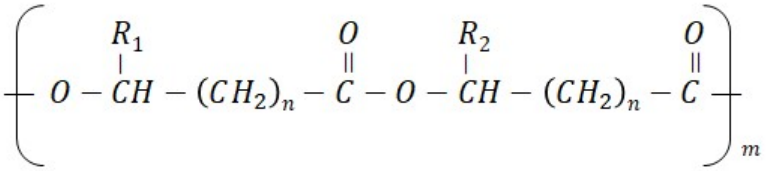

(b)

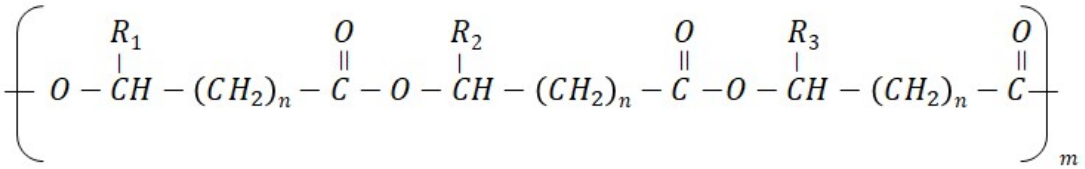

(c)

Figure 2.1. General PHAs formula, where m is degree of polymerization. (a) General chemical formula of PHAs, (b) General chemical formula of PHA bipolymers, (c) General chemical formula of PHA terpolymers.

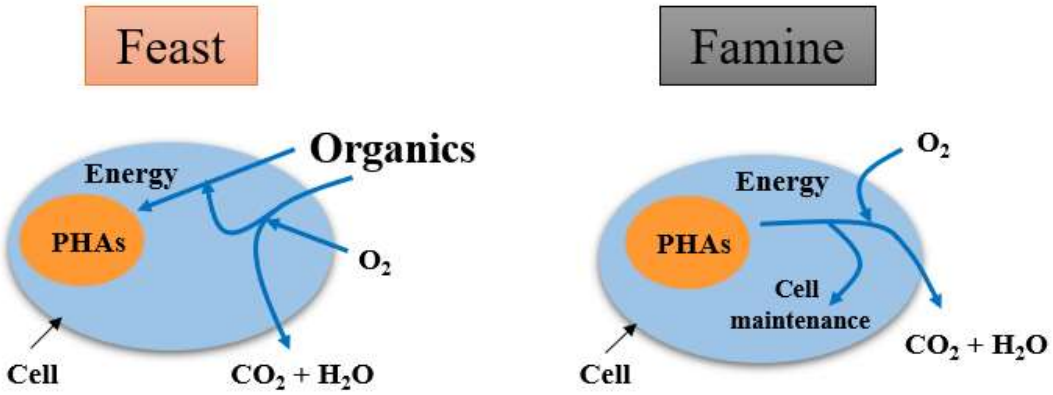

Figure 2.2. Accumulation and consumption of intracellular PHA during feast and famine conditions.

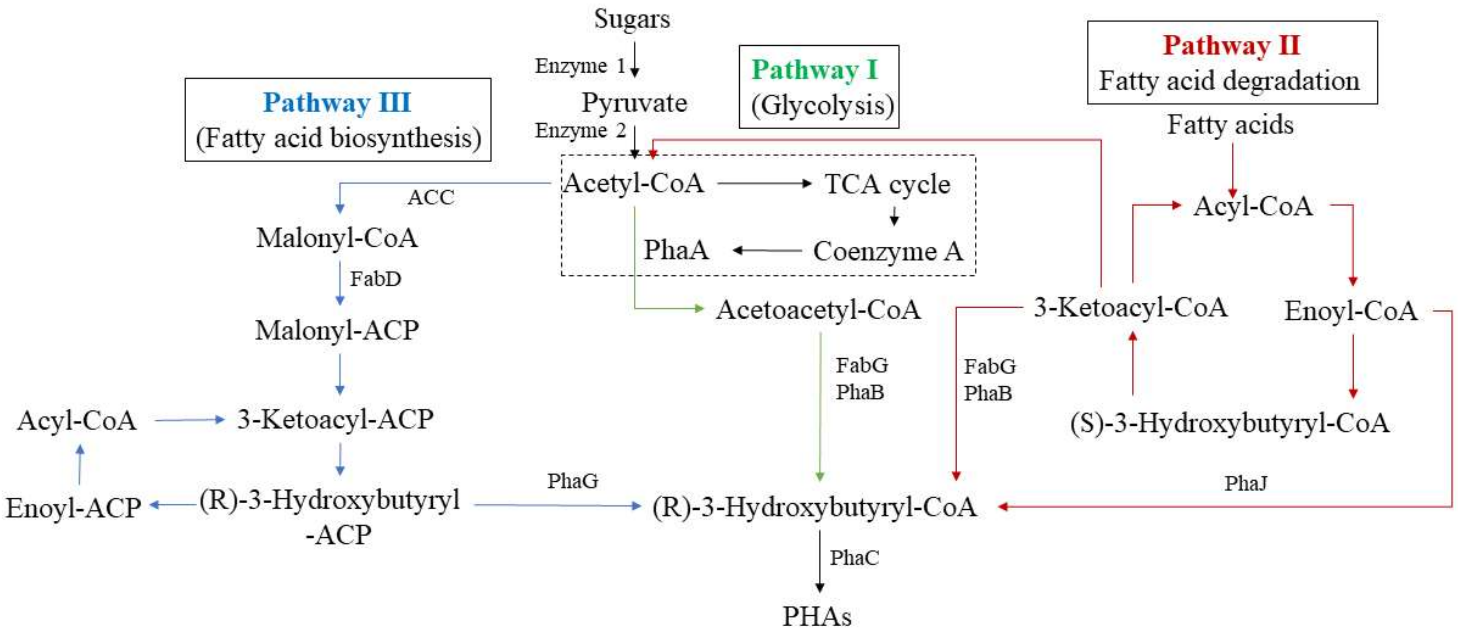

Figure 2.3. PHAs Biosynthesis pathways. Green arrows are pathway I; red arrows are pathway II; blue arrows are pathway III.

Chapter 3

FABRICATION OF BIOCOMPOSITE MATERIALS FROM ACTIVATED SLUDGE: FILAMENTOUS BACTERIA REINFORCED POLYHYDROXYALKANOATES

Abstract

Biocomposite materials with a commercial Poly(3-hydroxybutyrate-co-3-hydroxyvalerate) (PHBV) as matrix and filamentous bacteria as reinforcement were fabricated by melt extrusion and 3D printing in this chapter. Filamentous bacteria were cultivated and enriched in a laboratory membrane bioreactor. The thermal properties of PHBV and filamentous bacteria were evaluated by differential scanning calorimetry and thermogravimetric analysis. The results suggested that the processing temperature of these composite materials should be around 185 ℃ to minimize thermal degradation of both PHBV and filamentous bacteria. Tensile properties (e.g., tensile strength, elongation at break, and tensile modulus) and notched impact strength of composites with different fiber contents were also evaluated. The results showed that tensile modulus and notched impact strength of the composite with 20 wt.% fiber content (mass basis) increased 12 % and 95 %, respectively. Tensile strength and elongation at break of the same 20 % composite deteriorated less than those of plant-based fiber reinforced PHBV at similar fiber content. This chapter demonstrated that filamentous bacteria growing in wastewater treatment systems may be used as reinforcement agents for biocomposite materials.

3.1 Introduction

Due to increasing interest for sustainable materials based on biorenewable resources, polyhydroxyalkanoates (PHAs)-based composite materials have attracted significant interest due to their potential biodegradability and environmental benefits. PHAs are bio-synthesized polyesters, which share similar properties with many petroleum-based plastics such as polyethylene (PE) and polypropylene (PP) (McAdam et al., 2020). Properties of PHAs also include nontoxicity, biocompatibility, water insolubility, and oxygen impenetrability (Vu et al., 2020). Moreover, PHAs have various production sources as more than 300 species of bacteria and several transgenic plants have been reported to produce PHAs (Dobrogojski et al., 2018; Kosseva and Rusbandi, 2018). PHAs have been widely used in pharmaceutical, agriculture, and packaging industries (Anjum et al., 2016) due to their biodegradable properties.

Poly(3-hydroxybutyrate-co-3-hydroxyvalerate) (PHBV) is a PHA copolymer, and is stiff, brittle, and thermally unstable during processing, which limits its commercial use (Chen & Wang, 2002; Pilla, 2011). Thus, improving mechanical properties of PHBV is required for its application in many high volume industries (Sharma et al., 2021). Many studies over the last several decades revealed that the addition of fibers could improve the mechanical properties of PHBV (BanLaanen, 1995; Singh et al., 2008; Srubar et al., 2012; Zhao et al., 2021). Thus far, many types of natural plant-based fibers, such as agave fiber (Torres-Tello et al., 2017), flax fiber (Barkoula et al., 2010), bamboo fiber (S. Singh et al., 2008), and wood fiber (Singh and Mohanty, 2007; Vandi et al., 2019), have been successfully used as reinforcement agents of PHBV.

Torres-Tello et al. (2017) reported that the tensile modulus and impact strength of PHBV were increased by 50% and 66%, respectively, with an addition of 30 wt.%

agave fiber. Barkoula et al. (2010) observed that both tensile modulus and impact strength of flax fiber reinforced biocomposite (40% flax fiber) increased by greater than 300% over that of neat PHBV. Vandi et al. (2019) compared the performance of wood fiber reinforced PHBV to neat PHBV. The results showed a 57% increase in the tensile modulus with the wood fiber reinforcement. Singh et al. (2008) reported on the mechanical properties of biocomposites manufactured using PHBV and bamboo fiber. The tensile modulus of the PHBV composite increased with bamboo fiber loading. Bledzki and Jaskiewicz (2010) compared the performance of PHBV composites reinforced with jute and abaca fibers. Their results showed a significant increase in the tensile modulus and tensile strength with the addition of the fiber reinforcement. Miller et al. (2013) reported on a life-cycle assessment of the production of PHBV and natural fiber composites to study the environmental impacts and potential improvements to the production process. They concluded that the greatest improvements in manufacturing the composites would come from the reduction of steam energy use in the polymer production, and the replacement of highly refined fiber with a reinforcement that requires less processing. The work reported in this chapter addresses both of these issues.

In activated sludge treatment plants, a sudden and excessive growth of filamentous microorganisms is a common occurrence, and this phenomenon is known to cause a solids separation problem called “bulking”. It was reported that more than 50% of wastewater treatment plants around the world experienced periodic bulking problems (Noutsopoulos et al., 2007). As many as 30 different filamentous strains have been reported from various activated sludge treatment plants (Nielsen et al.,

2009). Some of common filamentous bacteria in the U.S. include *Sphaerotilus natans* (*S. natans*), type 021N, *Thiothrix* spp., and *Beggiatoa* spp. (Jenkins et al., 2003).

Diameters of these filamentous bacteria range from 0.5 μm to 3 μm and some of them can grow to a length of 1000 μm. These dimensions are comparable to some of the nanofibers (Khalil et al., 2012) and wood flours being used as reinforcing agents in the fabrication of biocomposites. Facca et al. (2006) pointed out that fiber reinforcement with longer length and smaller diameter fibers were predicted to give composite materials better elastic and tensile performance. The large length-to-diameter ratio of filamentous bacteria makes them promising fiber reinforcements and will potentially give PHBV more favorable mechanical properties. Thus, the filamentous bacteria strains present in the activated sludge may be suitable as a reinforcement for the composite material.

This chapter aims to fabricate all-natural composite material with PHBV as matrix and filamentous bacteria as fiber reinforcement. A membrane bioreactor was constructed to select and enrich a filamentous bacteria predominant culture. The thermal, and mechanical properties of neat PHBV and the biocomposite were evaluated in this chapter.

3.2 Materials and Methods

3.2.1 Materials

3.2.1.1 PHBV as matrix

The PHBV pellets (0.9% polyhydroxyvalerate) were purchased from Tianan Biologic Materials (Ningbo, China). The pellets contain 1% boron nitride, 0.5% antioxidant 1010 (CAS No.: 6683-19-8), and 0.1% maleic anhydride as additives.

3.2.1.2 Microorganisms

Activated sludge cultures used to enrich filamentous bacteria were established in a bench-scale membrane bioreactor (MBR) on a synthetic wastewater. The 3-L MBR was constructed with a cylindrical acrylic tube, and initially seeded with the recycle sludge from a local municipal wastewater treatment plant.

An initial total suspended solid (TSS) concentration of 2000 mg/L was used. The reactor content was continuously stirred with a paddle mixer at 400 rpm. The dissolved oxygen (DO) concentration in the MBR was maintained at 1.5 ± 0.2 mg/L with porous stone diffusers connected to an air pump. The pH of the reactor content was maintained at 7.0 ± 0.5 using 0.1 M sulfuric acid or 0.1 M sodium hydroxide solutions. The synthetic influent wastewater contained of 100 mg/L of glucose, 30mg/L of glycine, 150 mg/L of sodium acetate trihydrate, 20 mg/L yeast exact, 2 mg/L of ammonium chloride, 2 mg/L of potassium phosphate monobasic, 40 mg/L of sodium thiosulfate, 10 mg/L of sodium sulfhydrate, 50 mg/L of sodium lactate, 10 mg/L of calcium chloride dihydrate, 0.2 mg/L of ferric chloride hexahydrate, 1 mg/L of magnesium sulfate heptahydrate, 0.385 mg/L of manganese chloride and 0.01 mg/L of sodium molybdate dihydrate. The hydraulic retention time (HRT) and mean cell residence time (MCRT) were maintained at 12 hours and 25 days, respectively. A constant MCRT was maintained by daily batch wasting of mixed liquor from the MBR. The sludge volume index (SVI) of the mixed liquor was measured weekly to monitor the proliferation of filamentous bacteria. Mixed liquor samples from the MBR were periodically examined under optical microscope to check for the presence of filamentous bacteria growth.

Operation of the MBR was monitored by measuring soluble chemical oxygen demand (COD) values of the influent and effluent, mixed liquor suspended solids

(MLSS), mixed liquor volatile suspended solids (MLVSS), pH, and dissolved oxygen (DO) in the MBR. Soluble COD were determined using a spectrophotometer (DR 5000, Hach Company, Loveland, CO. USA) measuring COD of filtrate through a glass fiber filter (GF-A Glass Microfiber Filters, Whatman). MLSS and MLVSS were determined according to Standard Methods (Vinet & Zhedanov, 2011). Dissolved oxygen (DO) concentration was measured using a DO probe and a YSI DO meter (Yellow Springs, OH, USA). pH was measured using an electrode and Cole-Palmer pH meter (East Bunker Court Vernon Hills, IL, USA) (Maeng & Cha, 2017).

The MBR was operated for 27 months. The sludge containing filamentous bacteria was collected daily from the MBR. The collected sludge was centrifuged, and the supernatant was decanted. The sludge pellet was then freeze dried for 72 hours. A ball mill (JC-QM-2, Jvchuang Group Co., Ltd) with 3 mm Zirconia balls was used to grinded activated sludge into fine power for composite fabrication (Kumar et al., 2018). The freeze-dried pellet was ground in the ball mill for 10 minutes, and the dry sludge power was collected for subsequent thermal assessment and composite fabrication.

3.2.2 Material thermal properties

3.2.2.1 Differential scanning calorimetry

The thermal properties of the PHBV samples were examined using a differential scanning calorimeter (Q2000, TA Instruments, New Castle, DE, USA) under a constant nitrogen flow rate of 50 mL/min. The differential scanning calorimetry (DSC) test was conducted by using a heat-cool-heat method. A 10-mg polymer sample was first heated from -60 ℃ to 200 ℃ at 10 ℃/min and kept

isothermal for 3 minutes. The sample was then cooled back to -60 ℃ and held isothermal for 3 minutes before reheating. The crystallization temperature (T_c) and entropy of crystallization were determined during the cooling cycle. The sample was heated to 200 ℃ again in the reheating cycle to determine the melting temperature (T_m) and entropy of melting.

3.2.2.2 Thermogravimetric analysis

Thermogravimetric analysis (TGA) was performed using a Hitachi STA 7200 thermogravimetric analyzer (Hitachi High-Tech Science Corp., Tokyo, Japan). The TGA tests were conducted with PHBV (10 mg) and a sludge sample containing filamentous bacteria (5 mg). Both samples were heated from room temperature to 800 ℃ at a heating rate of 10 ℃/min under an argon atmosphere.

3.2.3 Composite material fabrication

Specimens of composite materials were fabricated by an extrusion-3D printing technique. The PHBV and freeze-dried sludge pellets were dried in an oven at 60 °C for 6 hours before processing. The polymer matrix and filament-rich sludge were mixed in a bench-top grinder according to the sludge contents listed in Table 3.1. The polymer-sludge mixtures were fed into the Wellzoom filament extrusion system (Wellzoom 2021 models Desktop Extruder Line II, Shenzhen Mistar Technology Co. Ltd., Shenzhen, China). This system consists of a screw extruder equipped with a customized nozzle, a water bath, and a tractor (Figure 3.1). The temperatures of the two heating chambers were 185 °C and 175 °C, respectively, to melt the matrix and to minimize thermal degradation. The extruder screw speed and tractor wheel speed were varied to obtain composite filaments with a diameter of 1.75 ± 0.05 mm for 3D printer

application. The composite filaments from the extruder were cooled in the water bath. The filaments were then collected and dried in an oven at 60 °C for 4 hours before 3D printing. The maximum sludge content was 20% because higher sludge content made it difficult to maintain the required filament diameter for 3D printing.

Specimens for mechanical studies were fabricated by a fused deposition modeling (FDM) 3D printer (Chiron, Anycubic Technology Co., Shenzhen, China). The models of specimens were designed by Ultimaker Cura (V3.2.1) software, and then sent to the 3D printer. Filaments from the extruder were placed layer by layer to achieve required dimensions for mechanical testing. The height of the first layer was set as 0.3 mm. All the following layers were 0.1 mm in height. The temperature of the printing nozzle and the bed were set at 200 ℃ and 60 ℃, respectively. The printing speed was 100 mm/s.

3.2.4 Material mechanical properties

Tensile strength of specimens was determined by a universal material testing machine (AG-X plus Series, Shimadzu, Kyoto, Japan). All tensile tests were conducted according to ASTM International D638-14 (Type V specimens). The specimen thickness was 3 mm and tested at a strain rate of 1 mm/min. A schematic diagram and a picture of the tensile testing specimen are shown in Figure 3.2.

Five specimens were tested for each polymer-sludge composite. The stress-strain curve of each test was recorded, and the linear portion of the curve was used to calculate Young's modulus (E) of each specimen by Equation 3.1 below:

$$E=\frac{\Delta\sigma}{\Delta\varepsilon} \tag{3.1}$$

where $\Delta\sigma$ was the change in tensile strength of the material, and $\Delta\varepsilon$ was the change in strain of the material.

The notched impact tests were conducted using an impact tester (HIT5.5P, Zwick, Ulm, Germany) with a 2.75 J pendulum impactor. The specimen was 3 mm thick, while other dimensions were the same as defined by ASTM International D256-10. Other procedures in impact tests all followed ASTM International D256-10. Five replicates were tested for each polymer-sludge composite.

3.3 Results and Discussion

3.3.1 Cultivation of filamentous bacteria

The activated sludge established in MBR settled well (SVI＜60 mL/g) for the first 20 weeks of MBR operation (Figure 3.3). The MBR system was operated with conditions that lead to the excessive growth of filamentous bacteria to obtain bulking sludge. These include low dissolved oxygen (DO) concentrations, long MCRT, high sulfide concentrations, and nutrient deficiencies. Specifically, the DO concentration in the MBR system was maintained at less than 1.5 mg/L. The synthetic influent contained high organic acid concentrations and low nutrient concentrations to promote the growth of filamentous bacteria.

Mixed liquor volatile suspended solids (MLVSS) values of MBR were 1492 ± 217 mg/L during the first 52 weeks of the MBR operation. The effluent VSS was 0 mg/L, indicating good membrane filtration. The average chemical oxygen demand (COD) of MBR influent and effluent were 213 ± 17 mg/L and 8 ± 2 mg/L, respectively. The average pH and DO were maintained at 6.8 ± 0.3 and 1.3 ± 0.2 mg/L, respectively. SVI values of the MBR sludge increased gradually after 20 weeks, and

the bulking (SVI > 600 mL/g) persisted throughout the experimental period. Microscopic examination of the mixed liquors revealed large amounts of filamentous bacteria in the MBR system (Figure 3.4). These filaments were identified as *Sphaerotilus* spp. and *Leptothrix* spp. by 16S rRNA gene sequencing, which is described in chapter 4.

3.3.2 Thermal Properties of PHBV and bulking sludge

Figure 3.5 shows the DSC thermogram of the cooling and second heating scans of the PHBV sample. The narrow temperature range of melting and crystallization, and the single sharp peak in the cooling and heating scans, indicate fast crystallization and relatively homogeneous distribution of polymer microstructures. The similarities in the melting and crystallization enthalpies also indicate a perfect arrangement of the polymer crystal structures. The degree of crystallization (X_c (%)) was calculated using Equation 3.2:

$$X_c = \frac{\Delta H_m}{\Delta H_m^0} \times 100\% \quad (3.2)$$

where ΔH_m is the enthalpy of the second melting, and ΔH^0_m is the melting enthalpy of 100 % crystalline PHB. Given that ΔH^0_m = 146 J/g (Debuissy et al., 2017), the degree of crystallization was calculated to be 64.9%, which is in agreement with previous research (Chan et al., 2019). Glass transition was not observed during the test probably due to the following reasons: 1) the glass transition temperature is outside the test temperature range; 2) heat flux differences are below the lower detection limit of the instrument; and 3) the rapid temperature change rate causes negligible phase transition.

The TGA thermogram shows the remaining weight percentage with increasing temperatures of PHBV and bulking sludge (Figure 3.6). The remaining weight

percentage of bulking sludge at 100 °C was approximately 95 % because of water evaporation before it reached 100 °C. The onset temperatures of thermal degradation (T_d) of PHBV and bulking sludge were 276.1 °C and 240.2 °C, respectively. At T_d, the masses of PHBV and bulking sludge decreased below 95 % of their initial dry weight. The thermal degradation of PHBV may be attributed to chain scission and hydrolysis at temperatures above 250 °C (S. Singh & Mohanty, 2007; Vahabi et al., 2019). Similarly, the loss of sludge mass during the TGA testing may be due to the decomposition of cellular components. Weiss et al. (2018) reported the T_d values of eight standard amino acids, the essential components of cell structures, ranged between 225 °C and 250 °C, which was comparable to the T_d value of bulking sludge (240.2 °C). The DSC and TGA tests provided the processing temperature for the designed specimens of PHBV-sludge composite, which was between the melting temperature of PHBV (173.1 °C) and decomposition temperatures of bulking sludge (240.2 °C). Since glutamine was reported to have the lowest T_d (185 °C), the processing temperature for bulking sludge was selected to be less than 185 °C.

Therefore, to achieve complete melting of PHBV and minimize decomposition of the matrix and reinforcement, heating zones 1 and 2 of the extruder were set at 185 and 175 °C, respectively. The temperature of the 3D printer nozzle was set at 200 °C due to the fast printing speed (100 mm/s).

3.3.3 Mechanical properties of composite materials

The tensile strength and elongation at break of the composite specimens are shown in Figure 3.7. The average tensile strength of the neat PHBV specimen was 27.2 ± 2.3 MPa, which was comparable to the values reported in the literature for PHBV copolymers (Chan et al., 2019; Singh et al., 2008; Tomano et al., 2022). The

average tensile strength values were slightly lower with filamentous bacterial reinforcement, which is consistent with the general observations reported in the literature (Seggiani et al., 2017; Vandi et al., 2019; C. S. Wu et al., 2017). However, the tensile strength did not decrease further when the bacterial filament content increased from 5 to 20% (Figure 3.7). This could be attributed to the composition of the bacterial cell wall. The bacterial cell wall mainly consists of peptidoglycan (Schaefer et al., 2017). The hydrogen bonding between peptidoglycan and PHBV helped improve interfacial adhesion and fiber wetting (Long Jiang et al., 2008; S. Singh et al., 2008), which prevented further deterioration of tensile strength. The addition of filamentous bacteria decreased the elongation at break when compared to that of the neat PHBV specimen (Figure 3.7). The elongation at break value decreased from 2.72 ± 0.39 % to 2.23 ± 0.25 % with 20 % filamentous bacteria content.

The tensile moduli of specimens with different fiber contents are shown in Figure 3.8. The use of bacterial filaments in the PHBV composite improved the stiffness of the neat PHBV. The tensile modulus of neat PHBV increased from 1.36 ± 0.14 GPa to 1.52 ± 0.09 GPa when bacterial filaments were used as reinforcing agents (Figure 3.8). Generally, the addition of fiber increased the tensile modulus of composites (Bhardwaj et al., 2006; S. Singh et al., 2008; S. Singh & Mohanty, 2007; Srubar et al., 2012), and our results agreed with the findings of the literature. This was due to the added fiber serving as nucleating agents and increasing the X_c of the matrix (Wong et al., 2002). The Young's modulus increased with increasing X_c (Dong et al., 2020; Nielsen & Stockton, 1963). However, maleic anhydride was added to the PHBV as a nucleating agent according to the manufacturer, which limited the nucleating effect of bulking sludge. This could explain why an 11.76% increase in Young's

modulus of PHBV was observed after being reinforced by 20% bulking sludge. A Student's t-test assuming equal variance was performed to check the statistical difference of Young's modulus between the neat PHBV and PHBV composite with 20% bulking sludge. The two-tailed t-test with a degree of freedom of 8 showed a t-value of 2.32 and a p-value of 0.049, which meant a significant statistical difference in Young's modulus between commercial PHBV without and with 20% bulking sludge reinforcement.

The notched impact strength of composite materials improved with increasing fiber ratio (Figure 3.9). The impact strength of neat PHBV was 1.70 ± 0.10 kJ/m^2. It increased to 3.32 ± 0.11 kJ/m^2 when the composite matrix contained 20% fibers. Thus, adding fibers significantly increased the energy needed to break the composite, suggesting good interfacial adhesion between the PHBV and bulking sludge. The notched impact strength of composite materials is also affected by the toughness of the matrix and fiber (Kamdem et al., 2004). Introducing bulking sludge increased the overall impact strength, indicating that the bulking sludge has a higher toughness than the neat PHBV.

Table 3.1. Formulations of composite materials with different sludge contents

Specimen	PHBV (%)	Bulking sludge (%)
PHBV0BS	100	0
PHBV5BS	95	5
PHBV10BS	90	10
PHBV15BS	85	15
PHBV20BS	80	20

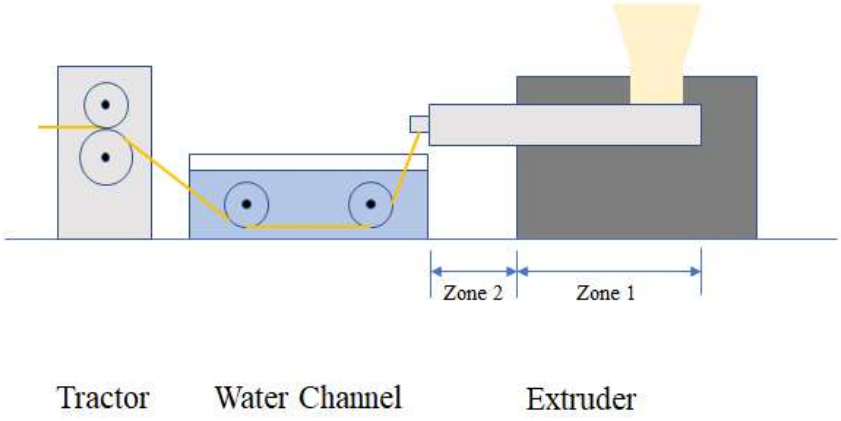

Figure 3.1. Schematic diagram of the melt extrusion system.

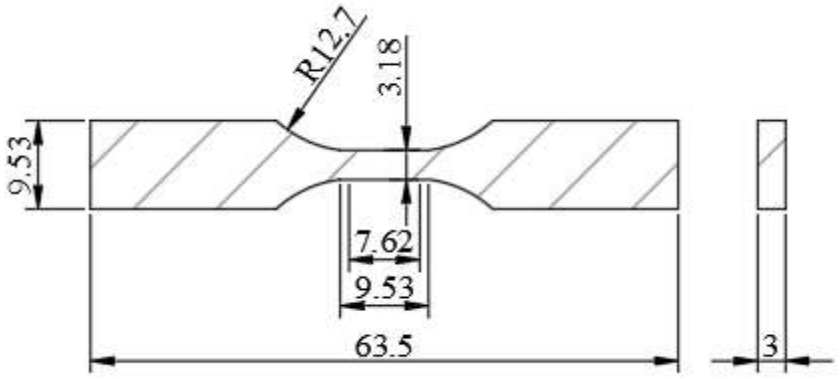

(a)

(b)

Figure 3.2. (a) Schematic diagram of the tensile testing specimen. The unit of the specimen dimensions is millimeter. (b) Actual picture of the tensile testing specimen from 3D printing.

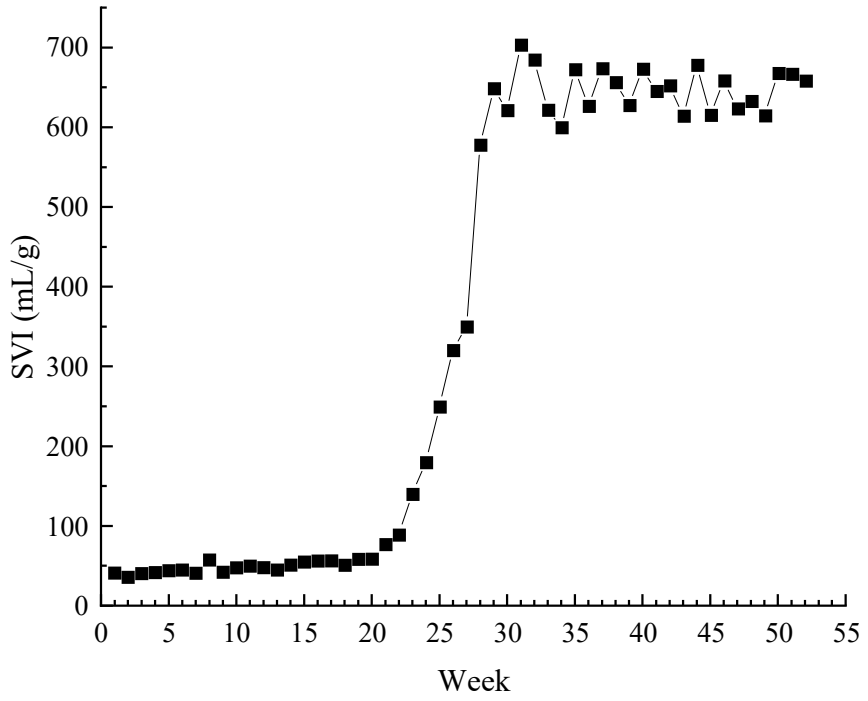

Figure 3.3 SVI of the MBR changed with operation time.

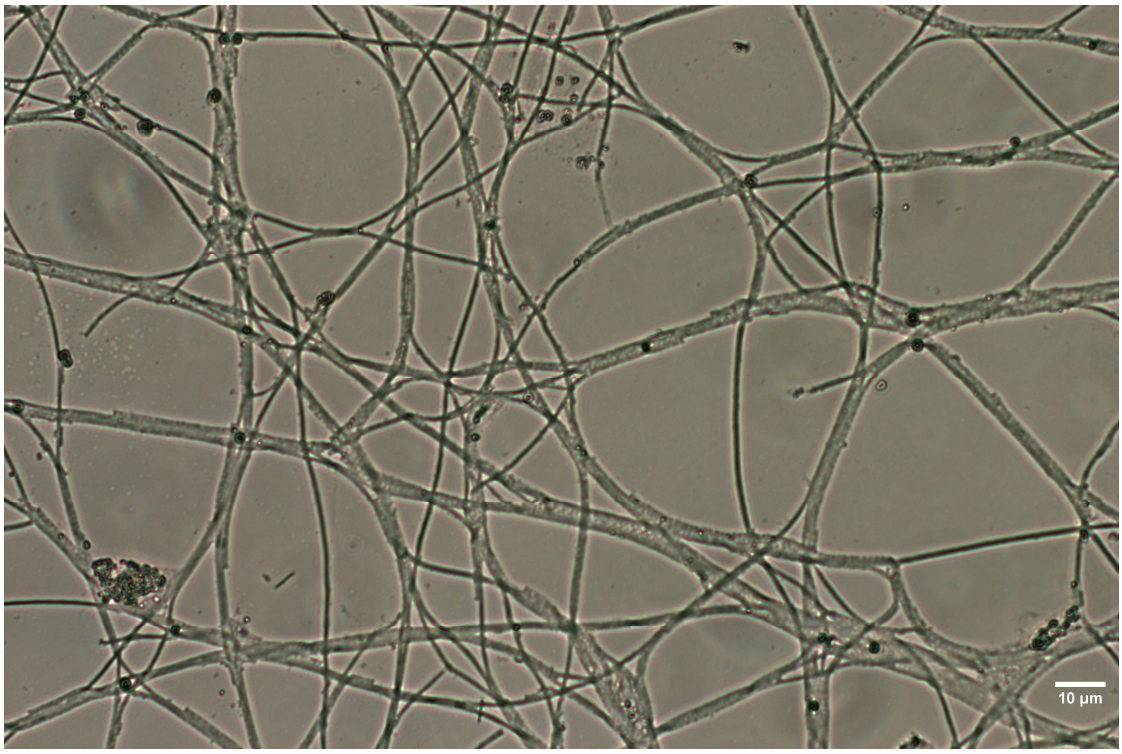

Figure 3.4. Filamentous bacteria-dominant sludge under an optical microscope (630x).

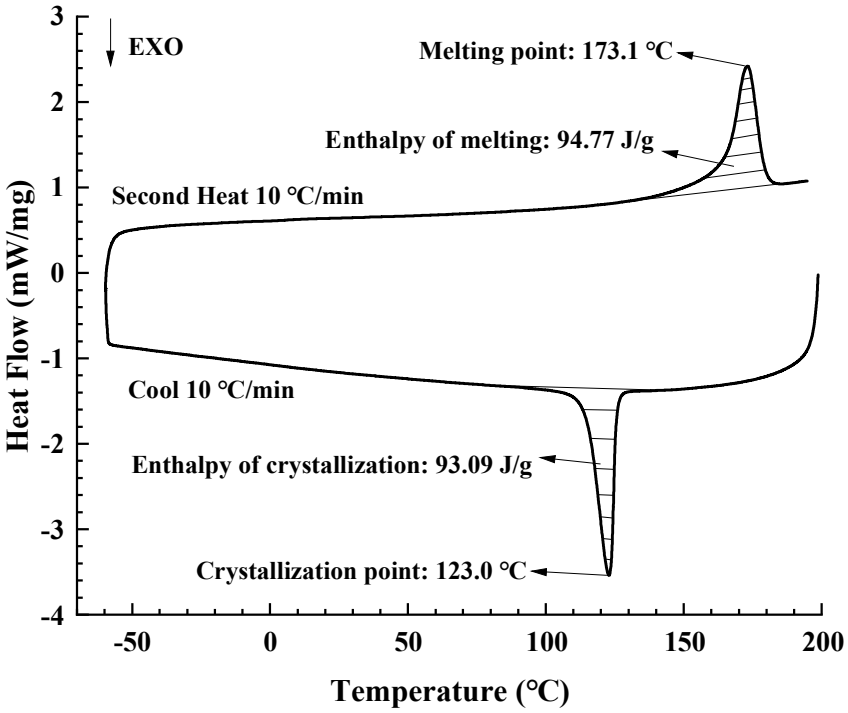

Figure 3.5. DSC thermogram of neat PHBV.

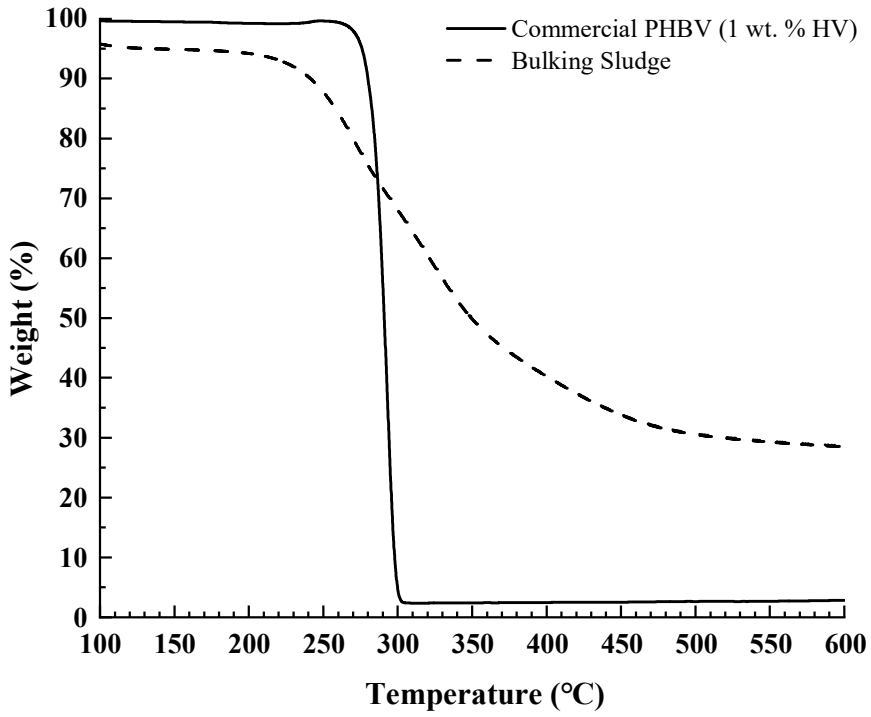

Figure 3.6. TGA thermogram of neat PHBV and bulking sludge.

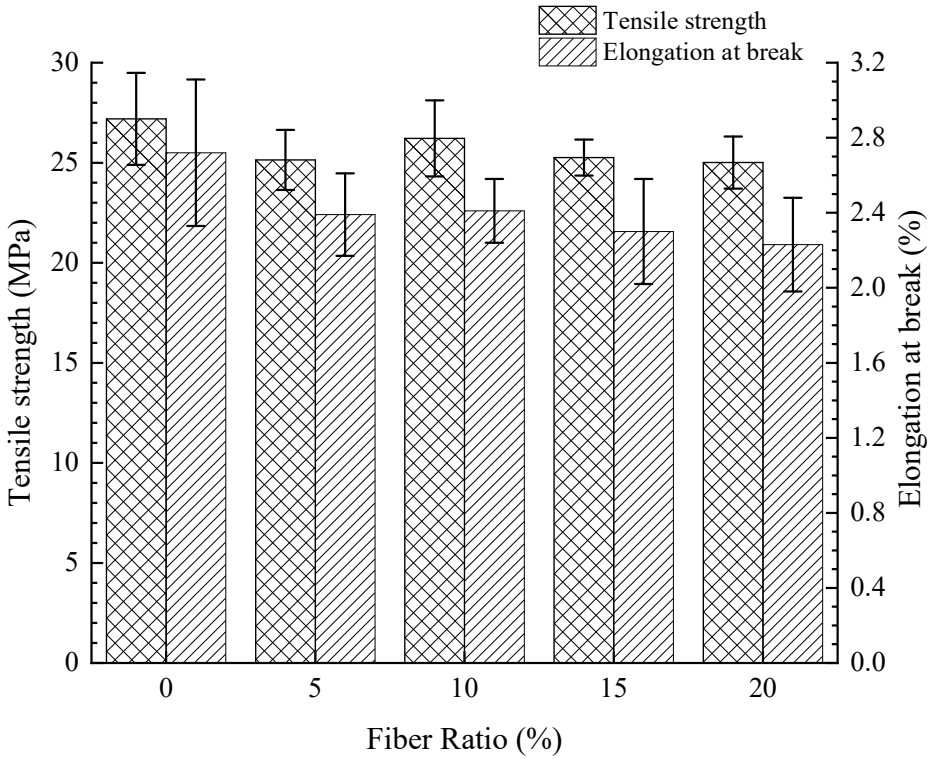

Figure 3.7. Tensile strength and elongation at break of composite materials at different fiber ratios.

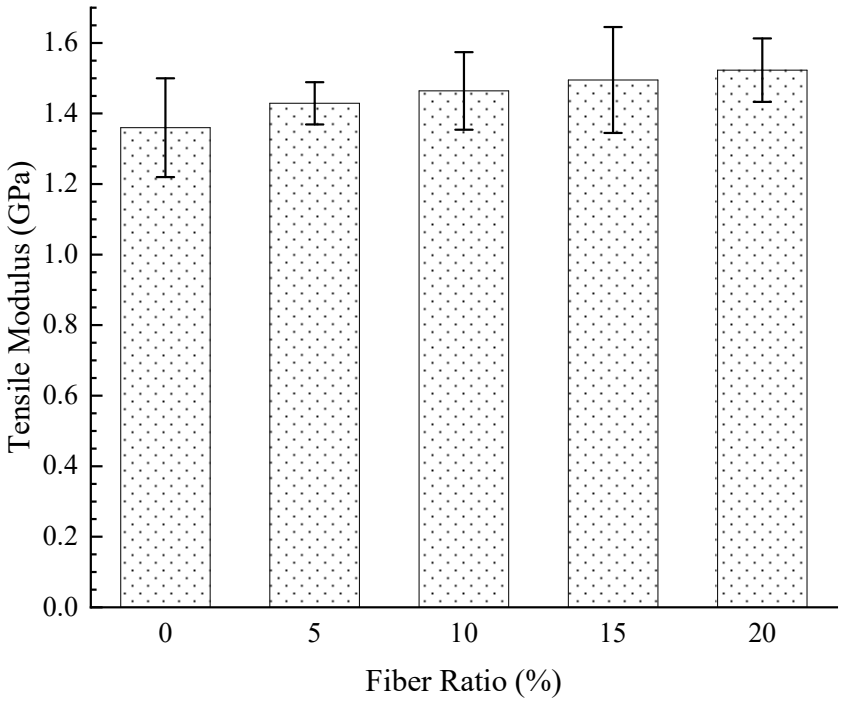

Figure 3.8. Tensile moduli of composite materials at different fiber ratios.

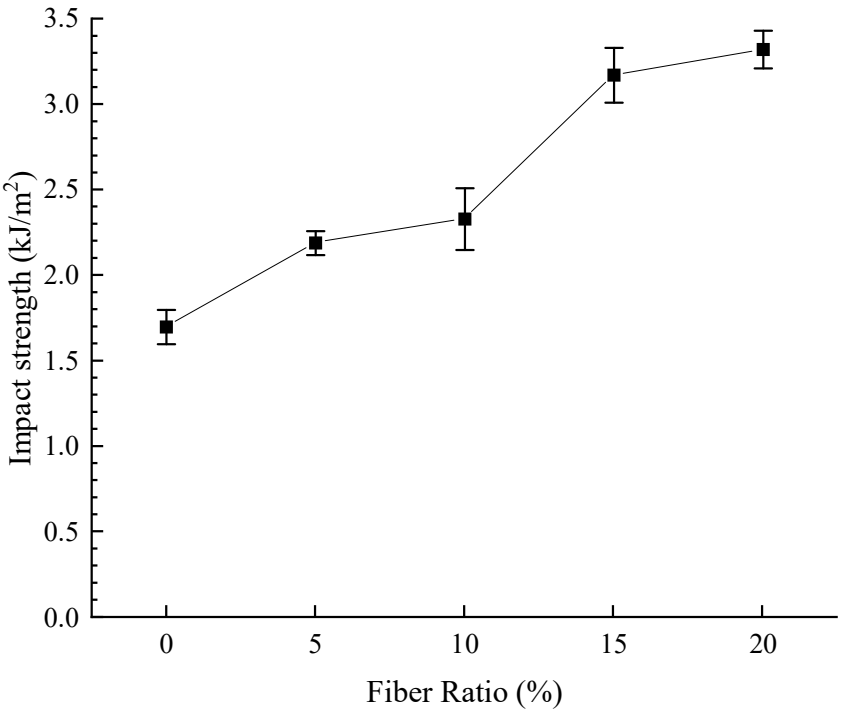

Figure 3.9. Notched impact strength of composite materials at different fiber ratios.

Chapter 4

MECHANICAL PROPERTIES OF FILAMENTOUS BACTERIA ENRICHED IN A MEMBRANE BIOREACTOR

Abstract

Filamentous bacteria can be considered as a kind of natural fiber, but their mechanical properties were rarely studied. In this chapter, a membrane bioreactor (MBR) with low dissolved oxygen, and nitrogen and phosphorus deficiency conditions was used to cultivate and enrich filamentous bacteria. The overgrowth of filamentous bacteria was observed with the sludge volume index as high as 703 mL/g. *Sphaerotilus* spp. were identified as the dominant filamentous bacteria by 16S rRNA gene sequencing with a relative abundance of 19% in the mixed cultures. The morphology of filamentous bacteria was observed using optical microscopy and atomic force microscopy (AFM). The aspect ratio (length to width ratio) of the filamentous bacteria was 346. AFM-based nanoindentation method was used to examine the mechanical properties of filamentous bacteria. The measured Young's modulus of *Sphaerotilus* spp. was 91.4% higher than that of non-filamentous bacteria. The Halpin-Tsai and Tsai-Pagano equations were used to determine the theoretical Young's modulus of filamentous bacteria-reinforced poly (3-hydroxybutyrate-co-3-hydroxyvalerate) (PHBV). The predicted values closely matched the experimental values, indicating that filamentous bacteria were randomly oriented and uniformly distributed in PHBV. This chapter demonstrated that filamentous bacteria enriched in a MBR can be used as reinforcement agents for biocomposite materials.

4.1 Introduction

Many studies over the last several decades reported that the addition of fibers could improve the mechanical properties of poly(3-hydroxybutyrate-co-3-hydroxyvalerate) (PHBV) copolymer (BanLaanen, 1995; Singh et al., 2008; Srubar et al., 2012; Zhao et al., 2021). These fibers are mainly plant based fibers, and usually have poor interfacial adhesion with polymer matrix due to their intrinsic chemical properties, which results in inferior overall mechanical properties of composite materials (Cantero et al., 2003; Zhou et al., 2016). Thus, plant based fibers commonly require chemical modifications, such as alkali treatment, to improve their compatibility and bonding with polymer matrix (Doan et al., 2012). Chemical modification processes are environmentally unfriendly, unsustainable, and costly. Therefore, a new fiber reinforcement, which is abundant and naturally compatible with polymer matrix, is of great interest to the environment and society.

Filamentous bacteria are commonly present in activated sludge, and their presence is essential for ensuring the integrity of activated sludge flocs by forming a rigid backbone (Lou & de los Reyes, 2005). An optimum balance between filamentous bacteria and floc-forming bacteria results in strong flocs that settles well in the sedimentation basin, which is critical in wastewater treatment operation. However, when excessive growth of filamentous bacteria occurs, the balance is disrupted, causing a solid separation problem called “bulking” (Noutsopoulos et al., 2007). Bulking activated sludge is difficult to separate from treated water by gravity in secondary sedimentation tanks, resulting in biomass loss from wastewater treatment systems (Xu et al., 2014). Excessive growth of filamentous bacteria also interferes with oxygen transfer in aeration basins and decreases wastewater treatment efficiency (Wu et al., 2019).

Approximately 30 species of filamentous bacteria have been reported from various activated sludge plants (Richard, 2003). Proliferation of specific filamentous bacteria in mixed cultures has been correlated to various operational and environmental parameters (Jenkins et al., 2003). Excessive growth of *Sphaerotilus* spp. is typically associated with low levels of dissolved oxygen in aeration basins (Li et al., 2021; Seder-Colomina et al., 2015). *Microthrix parvicella* and type 021N are commonly present in plants with low organic loading conditions (Jenkins et al., 2003). The overgrowth of *Thiothrix* spp. and type 021N is commonly associated with discharges of wastewater containing elevated concentrations of sulfides (e.g., septic conditions) (Martins et al., 2004). Many industrial wastewaters (e.g., pulp and paper, fruit and vegetable processing, brewery, petrochemical, etc.) are typically rich in carbon, but deficient in nutrients such as nitrogen and phosphorus. Proliferation of *Thiothrix* spp. and type 021N are common under nitrogen deficient growth conditions (Richard et al., 1985). *Beggiatoa* spp. are also typically present in wastewater containing high sulfide concentrations (Jo et al., 2022; Wang et al., 2022).

Atomic force microscopy (AFM)-based nanoindentation offers the unique opportunity to probe local mechanical properties due to its capability to measure interaction forces as small as pN (Willemsen et al., 2000). It can provide a high-resolution and sensitive approach to understanding the mechanical properties of small biological materials, such as microbial cells (Ding et al., 2017). While AFM-based nanoindentation method is frequently used to study the elastic properties of bacterial cells, the application of AFM nanoindentation has not yet been demonstrated for the mechanical properties of filamentous bacteria to the best of our knowledge. The most relevant research to our study was the use of AFM nanoindentation to measure the

elastic modulus of the fungal hyphae (Couttenier et al., 2022). They reported the Young's modulus of 6.4 ± 3.4 MPa for *Candida albicans* SC5314 hyphae using AFM nanoindentation method. Haneef et al. (2017) evaluated the effects of different nutrient conditions on the Young's modulus of two fungal hyphae, *Ganoderma lucidum* and *Pleurotus ostreatus,* using AFM nanoindentation. The Young's modulus of *G. lucidum* and *P. ostreatus* grown in pure cellulose broth were 12 and 28 MPa, respectively. The Young's modulus values of *G. lucidum* and *P. ostreatus* hyphae decreased to 4 and 17 MP, respectively, when grown on cellulose-potato dextrose broth.

Many types of natural plant-based fibers, such as agave fiber (Torres-Tello et al., 2017), flax fiber (Barkoula et al., 2010), bamboo fiber (S. Singh et al., 2008), and wood fiber (Singh and Mohanty, 2007; Vandi et al., 2019), have been successfully used as reinforcement agents of PHBV. Many filamentous bacteria have dimensions comparable to those of cellulose nanofibers (Khalil et al., 2012; Sharma et al., 2018). Thus, filamentous bacteria with comparable mechanical properties may serve as substitute fibers in biocomposite materials. In chapter 3, activated sludge cultures rich in filamentous bacteria was used as a reinforcement agent. The results showed that the Young's modulus and the impact strength of PHBV improved with the reinforcement by filamentous bacteria-containing mixed cultures. However, the dominant genera of filamentous bacteria in the mixed cultures were not identified in chapter 3.

The overall objective of this chapter is evaluating the Young's modulus of filamentous bacteria enriched in a membrane bioreactor (MBR). Low dissolved oxygen, and nitrogen and phosphorus limited conditions were provided in the MBR to cultivate and maintain a culture rich in filamentous bacteria. The filamentous bacteria were identified by 16S rRNA gene sequencing. The Young's modulus of filamentous

bacteria was determined using AFM nanoindentation. The theoretical Young's modulus of filamentous bacteria-reinforced PHBV was calculated using the Halpin-Tsai and Tsai–Pagano equations to evaluate the reinforcement effects of filamentous bacteria.

4.2 Materials and Methods

4.2.1 Filamentous bacteria cultivation

To obtain mixed cultures rich in filamentous bacteria, activated sludge cultures were established in a bench-top MBR. Since filamentous bacteria are difficult to separate by gravity settling, membrane filtration instead of sedimentation is more suitable for the cultivation of filamentous bacteria-dominated activated sludge. A membrane bioreactor (MBR) system was operated for 29 months to cultivate and maintain filament-dominating cultures. The schematic diagram of MBR system is shown in Figure 4.1. A 3-L MBR unit was constructed from a transparent acrylic polymer. The aeration basin contained a vertically mounted membrane module mounted directly above the air diffuser. Membrane-filtered effluent was withdrawn by a suction pump at a flow rate of 4.2 mL/min to maintain a hydraulic retention time (HRT) of 12 hours. The influent flow rate was also 4.2 mL/min to maintain a constant volume of the MBR. The pH of the aeration basins was maintained to desired values using a pH recorder/controller and strong acid (H_2SO_4) or strong base (NaOH) addition. A mean cell residence time (MCRT) of 25 days was maintained by daily batch wasting of mixed liquor from the MBR. The dissolved oxygen (DO) of the MBR was maintained at 1.5 ± 0.2 mg/L with porous stone diffusers connected to an air pump.

The composition of influent is presented in Table 4.1. The theoretical chemical oxygen demand (COD) of the feed solution was about 300 mg/L. Operation of the MBR was monitored by measuring soluble chemical oxygen demand (COD) values of the influent and effluent, mixed liquor suspended solids (MLSS), mixed liquor volatile suspended solids (MLVSS), pH, and dissolved oxygen (DO) in the MBR. Soluble COD were determined using a spectrophotometer (DR 5000, Hach Company, Loveland, CO. USA) measuring COD of filtrate through a glass fiber filter (GF-A Glass Microfiber Filters, Whatman). MLSS and MLVSS were determined according to Standard Methods (APHA, 2005). Dissolved oxygen (DO) concentration was measured using a DO probe and a YSI DO meter (Yellow Springs, OH, USA). pH was measured using an electrode and Cole-Palmer pH meter (East Bunker Court Vernon Hills, IL, USA) (Maeng and Cha, 2017).

4.2.2 Microbial community analysis

After establishing steady-state filament-dominating cultures in the MBR, 50 mL mixed liquor sample were withdrawn from the aeration basin for microbiological analysis to confirm the presence of filamentous bacteria and the diversity of communities. The mixed liquor was first centrifuged at 8000 ×g for 5 minutes and the supernatant was decanted. The sludge pellet was collected for DNA extraction.

Genomic DNA was extracted and purified using E.Z.N.A™ Mag-Bind Soil DNA Kit (Omega Bio-Tek, Norcross, GA, USA) following the manufacturer's instructions. The quality of the extracted DNA was determined using 2% agarose gel electrophoresis. The Qubit™ dsDNA HS assay kit (Thermo Fisher Scientific, Waltham, MA, USA) and Qubit® 4.0 fluorophotometer (Thermo Fisher Scientific, Waltham, MA, USA) were used to assess the quantity of extracted DNA. The

extracted DNA was amplified using a two-step polymerase chain reaction (PCR) method with a thermocycler (ETC 811, Dongsheng, Beijing, China). The first round of PCR was performed using 341F primer (5′-CCTACGGGNGGCWGCAG-3′) and 805R primer (5′-GACTACHVGGGTATCTAATCC-3′), targeting the V3 and V4 hypervariable regions. The thermal cycling protocol includes initial denaturation at 94 °C for 3 mins, followed by 5 cycles of denaturation at 94 °C for 30 s, annealing at 45 °C for 20 s, and elongation at 65 °C for 30 s. After completion of the initial protocol, additional 20 cycles of denaturation at 94 °C for 20 s and annealing at 55 °C for 20 s were implemented, and this was followed by a final elongation step consisting of 72 °C for 30 s and 72 °C for 5 min. The subsequent round of PCR was performed using Illumina Bridge PCR-compatible primers with the same thermocycler. The PCR conditions consisted of initial denaturation at 94 °C for 3 min, followed by 5 cycles of denaturation at 94 °C for 20 s, annealing at 55 °C for 20 s, and elongation at 72 °C for 30 s. The final extension was also at 72 °C for 5 min.

Hieff NGS™ DNA Selection Beads (Yeasen Biotechnology Co. Ltd., Shanghai, China) were used to purify the amplicons. The quality and quantity of amplicons were determined using the method described above.

Amplicons were sequenced by Illumina MiSeq PE300 platform (San Diego, CA, USA) with 2 × 300 bp paired-end reads. Raw data were denoised and filtered using QIIME 2 (V2018.6) (Bolyen et al., 2019). Operational taxonomic units (OTUs) were assigned based on 97% sequence similarity. The Ribosomal Database Project (RDP) classifier (V2.12) was used to identify and classify different OTUs based on the RDP database (Wang et al., 2007).

4.2.3 Morphology of filamentous bacteria

4.2.3.1 Length of filamentous bacteria

The length distribution of filamentous bacteria was measured to determine the average length of filamentous bacteria in the MBR. One milliliter of the mixed liquor from the MBR was diluted to 15 mL using deionized water. Then 1 mL of diluted mixed liquor was spread on an object slide and subsequently observed by an optical microscope (CX43, Olympus, Tokyo, Japan) equipped with a DP 28 camera (Olympus, Tokyo, Japan) and an image analysis software (Olympus Stream, V2.4.4) under 100x magnification. Filamentous bacteria count was conducted manually in five randomly selected scopes of mixed liquor. A total number of 103 filamentous bacteria were counted, and the length of each filamentous bacterium was measured using the image analysis software.

4.2.3.2 Atomic force microscope

An atomic force microscope (AFM) was used to examine the surface morphology and Young's modulus of the filamentous bacteria. The surface morphology of the filamentous bacteria was examined using AFM tapping mode. One milliliter of mixed liquor sample from the MBR was smeared on a microscopic slide and air-dried. The Dimension Icon AFM (Bruker, Billerica, MA, USA) with a RTESPA-300 probe (Bruker, Billerica, MA, USA) was first operated in tapping mode to perform large-area scans (20 × 20 μm) to locate filamentous bacteria. In total ten scans of different randomly selected area were performed during the tapping mode. The images recorded from tapping mode scanning were used for bacteria width measurements using an image analysis software (NanoScope Analysis, version 1.7). The average Young's modulus of the filamentous bacteria was determined by AFM

nanoindentation performed on 10 randomly selected filamentous bacteria. After filamentous bacteria were located in the tapping mode, the probe was repositioned over the target bacterium, and the AFM was then switched to contact mode. AFM nanoindentation was performed on five randomly selected points on each filamentous bacterium. The force and displacement of the probe was recorded for Young's modulus calculation. The average Young's modulus of the filamentous bacteria was compared to that of ten randomly selected non-filamentous bacteria. Five different points on each non-filamentous bacterium were selected to perform AFM nanoindentation as described above.

4.3 Results and Discussion

Mixed liquor VSS values of MBR were 1320 ± 70 mg/L during the steady-state operation. The effluent VSS was 0 mg/L, indicating good membrane filtration. The average chemical oxygen demand (COD) of MBR influent and effluent were 213 ± 17 mg/L and 8 ± 2 mg/L, respectively. The average pH and DO were maintained at 6.8 ± 0.3 and 1.3 ± 0.2 mg/L, respectively.

A membrane bioreactor (MBR) system was operated at steady-state (± 10% of MLVSS values) for 29 months to cultivate and maintain filament-dominating cultures. Sludge volume index (SVI) measurements of activated sludge were used to monitor settling characteristics of mixed liquors in the MBR. The MBR system began to bulk (SVI > 150 mL/g) in 24 weeks and the bulking persisted (SVI as high as 703 mL/g) throughout the experimental period. Microscopic examination of the mixed liquors revealed large amounts of filamentous bacteria in the CSTR system (Figure 4.2).

4.3.1 Microbial community structure

A mixed liquor sample from the MBR was withdrawn from the aeration basin for microbial genomic analysis. Genomic DNA samples of mixed liquor were extracted and purified using E.Z.N.A™ Mag-Bind Soil DNA Kit (Omega Bio-Tek, Norcross, GA, USA) following the manufacturer's protocol. Once the purified DNA samples met the required concentration and quality ratio, the samples were sequenced for the bacterial and taxonomic identification. A Krona chart using the sequencing results was constructed to illustrate the microbial distribution pattern in the MBR (Figure 4.3) (Kim, 2018).

The most abundant bacterial populations were Betaproteobacteria (54.7% of bacteria) at the class level. This class has been often reported to be dominant in activated sludge communities (Song et al., 2019; Ye & Zhang, 2013). *Sphaerotilus* spp. was revealed as the most abundant genus (19%) of betaproteobacteria. Ferreira et al. (2021) reported that *Sphaerotilus* spp. was commonly detected filamentous bacteria in activated sludge.

Several studies have reported that the excessive growth of *Sphaerotilus* spp. is associated with low dissolved oxygen concentrations, high carbon-to-nitrogen ratio, and phosphorus limitation (Pellegrin et al., 1999). These conditions were provided in our MBR to create a favorable environment for *Sphaerotilus* spp. growth. *Leptothrix* spp., which were also present in the MBR (4% of bacteria), have been reported to be closely related to *Sphaerotilus* spp. (Kämpfer, 1998). It should be noted that the growth of sulfur-oxidizing filamentous bacteria, *Thiothrix* spp. and *type* 021N was not observed in the MBR cultures even though sodium acetate, sodium thiosulfate, and sodium sulfhydrate were added to the MBR medium to simulate favorable growth conditions (e.g., septic conditions) for their growth (Graaff et al., 2020; Martins et al.,

2004). This result suggests that low *Thiothrix* spp. amounts were in the seed sludge, and the environment provided in the MBR was more favorable for *Sphaerotilus* spp.

4.3.2 Characterization of filamentous bacteria

4.3.2.1 Length of filamentous bacteria

The lengths of 103 counted filamentous bacteria were measured to calculate the average length of *Sphaerotilus* spp. Their length distribution is shown in Figure 4.4. The minimum and maximum lengths of measured filamentous bacteria were 124 and 1261 μm, respectively. The average length of the filaments was 520 ± 226 μm. The typical length of *Sphaerotilus* spp. are reported to be from 100 to 1000 μm (Jenkins et al., 2003). Smoothly curved filaments and round-ended cells (Figure 4.2) matched the typical appearance of *Sphaerotilus* spp. in activated sludge. Currently, there has been no consistent conclusions regarding the length of *Leptothrix* spp. Zhou and Li (2020) stated that the length of *Leptothrix* spp. ranged between 5 and 20 μm, whereas Ventolini et al. (2014) reported that *Leptothrix* spp. ranged between 40 and 75 μm in length. However, *Leptothrix* spp. in both ranges were not observed during length measurements, although the sequencing results demonstrated their existence. It is possible that some *Leptothrix* spp. were missed during the bacteria length measurements because they could be as short as 5 μm, thus being confused with other non-filamentous bacteria. Kunoh et al. (2021) revealed that calcium and magnesium, both of which were provided in the MBR medium, could help *Leptothrix* spp. to elongate. Thus, some portions of *Leptothrix* spp. could elongate to more than 100 μm in length, as shown in Figure 4.4.

4.3.2.2 Width and Young's modulus of filamentous bacteria

An atomic force microscope (AFM) was used to examine the surface morphology and the Young's modulus of *Sphaerotilus* spp. A 20 × 20 μm AFM scan of typical *Sphaerotilus* spp. in a mixed liquor sample from the MBR is shown in Figure 4.5. Ten *Sphaerotilus* spp. were randomly selected, and five cross sections of each bacterium were measured to determine the average width of the *Sphaerotilus* spp. The average width of *Sphaerotilus* spp. was 3.01 ± 0.07 μm. The width of *Sphaerotilus* spp. was reported to be 1–3 μm (Jenkins et al., 2003; Pellegrin et al., 1999; STOKES, 1954; Tjaden & Goss, 1969), which was similar to the measurements in this study.

The Young's modulus of the bacteria was determined from the linear portion of the force-displacement unloading curves by fitting the Derjaguin–Muller–Toropov (DMT) model (Derjaguin et al., 1975). The DMT model was used instead of the traditional Hertz, Sneddon, and Johnson–Kendall–Roberts models because bacterial deformation is smaller than the probe radius (Bonilla et al., 2015; Morales-Rivas et al., 2015; Qu & Meredith, 2018; Smolyakov et al., 2016). Typical force-displacement curves of a *Sphaerotilus* spp. and non-filamentous bacterium are compared in Figure 4.6. Due to elastic deformation occurred on both bacteria and the probe, the reduced Young's modulus (E_r) instead of the true Young's modulus (E) of bacteria was determined using Equation 4.1:

$$E_r = \frac{3(F_{tip} - F_{adh})}{4\sqrt{R(\Delta d)^3}} \tag{4.1}$$

where F_{tip} is the force applied on the bacterial surface, F_{adh} is the adhesive force when the tip separates from the bacterial surface, R is the radius of the AFM probe, and Δd is the deformation of the bacteria. The radius of the AFM probe used in this study was

8 nm according to the manufacturer's manual. The true Young's modulus, E, of bacteria was calculated using Equation 4.2:

$$E_r=\left[\frac{1-\nu_b^2}{E}+\frac{1-\nu_p^2}{E_p}\right]^{-1} \quad (4.2)$$

where E_p is the Young's modulus of the AFM probe, and ν_b and ν_p are the Poisson's ratios of bacteria and the probe, respectively. Poisson's ratios of biological samples are normally reported to be between 0.4 and 0.5 (typically close to 0.5) (Elbourne et al., 2019; Kandemir et al., 2018; Limbert et al., 2013; Xia et al., 2018). Therefore, in this study, ν_b of bacteria was assumed to be 0.5. The Young's modulus and Poisson's ratio of probe material (silicon) were reported to be 130.2–187.5 GPa and 0.064–0.361, respectively (Wortman & Evans, 1965), which made the probe part of Equation 4.2 negligible. Thus, the above equation can be simplified as Equation 4.3:

$$E=E_r\left(1-\nu_b^2\right) \quad (4.3)$$

The calculated Young's modulus of filamentous bacteria and non-filamentous bacteria were 5.34 ± 0.68 GPa and 2.79 ± 0.27 GPa, respectively.

This result indicates that *Sphaerotilus* spp. in the MBR cultures are more stiff than non-filamentous bacteria. Similar result was also observed by Cornelissen et al. (2018). Several studies have found that microorganisms with a higher aspect ratio (length to width ratio) tend to have a higher Young's modulus. Elbourne et al. (2019) reported that rod bacteria have a higher Young's modulus than cocci bacteria. Zhao et al. (2005) also found that the Young's modulus of *Aspergillus nidulans* hyphae is much higher than that of yeast. Filamentous microorganisms are more susceptible to external forces because they have greater surface area to volume ratio. Therefore, rigid structures are required to maintain cell integrity.

The sheath of *Sphaerotilus* spp. consists of protein-polysaccharide-lipid complexes rich in ferric hydroxide, manganese dioxide, and disulfide bonds, which play an important role in maintaining a stable structure (Emerson & Ghiorse, 1993b, 1993a; Mulder & Deinema, 1981; ROMANO & PELOQUIN, 1963; Takeda et al., 1998). Table 4.2 compares the Young's moduli of *Sphaerotilus* spp. and several natural fibers. The Young's modulus of *Sphaerotilus* spp. was comparable to that of coconut fiber, palm fiber, and wool. These results suggest that filamentous bacteria commonly found in activated sludge may be a promising substitute for natural fibers as reinforcing agents in composite materials.

4.3.3 Evaluation of reinforcement effects of filamentous bacteria

The theoretical Young's modulus of filamentous bacteria-reinforced PHBV was calculated to evaluate reinforcement effects of filamentous bacteria. The theoretical Young's moduli of PHBV with 5%, 10%, 15%, and 20% sludge ratios were calculated using the Halpin-Tsai and Tsai-Pagano equations (Affdl & Kardos, 1976; Espinach et al., 2014). The PHBV used in this assessment is a commercial PHBV pellets (0.9% polyhydroxyvalerate) from Tianan Biologic Materials (Ningbo, China).

The Tsai-Pagano equation was used to predict the Young's moduli of fiber reinforced composite materials (S. Singh & Mohanty, 2007; Tsai & Pagano, 1968). This equation assumed that fibers in the composite material were randomly oriented and uniformly distributed, which was the nature of extrusion and 3D printing techniques used in composite fabrication in chapter 3. The Young's moduli of composite materials were calculated using Equation 4.4 by assuming 3/8 and 5/8

fibers in the matrix were in the longitudinal and transverse directions, respectively (López et al., 2012; Tsai & Pagano, 1968):

$$E_c = \frac{3}{8}E_l + \frac{5}{8}E_t \quad (4.4)$$

where the longitudinal modulus (E_l) and transverse modulus (E_t) were determined from Halpin-Tsai equations (Equation 4.5 and 4.6). Halpin-Tsai equations were used to predict longitudinal and transverse moduli of composite materials reinforced by aligned short fibers (Affdl & Kardos, 1976) as follows:

$$E_l = E_m\left(\frac{1+\xi\eta_l V_f}{1-\eta_l V_f}\right) \quad (4.5)$$

$$E_t = E_m\left(\frac{1+2\eta_t V_f}{1-\eta_t V_f}\right) \quad (4.6)$$

where E_m is the Young's modulus of the matrix, and V_f is the volume fractions of filamentous bacteria. The E_m of the commercial PHBV is 1.36 GPa, which was determined by 5 replicates tensile tests according to ASTM International D638-14 (Type V specimens, 3 mm thickness, 1 mm/min testing speed). The volume fraction of filamentous bacteria was calculated from the Equation 4.7 as follows:

$$V_f = \frac{\frac{m_s * \omega_f}{\rho_b}}{\frac{m_s}{\rho_b} + \frac{m_m}{\rho_m}} \quad (4.7)$$

where m_s and m_m are mass ratios of the sludge and the matrix, respectively. The density of the PHBV (ρ_m) is 1.25 g/cm^3 according to the manufacturer's information. The ρ_b represents the average density of bacteria, and determined as 1.09 g/cm^3 according to Bakken & Olsen (1983). The ω_f is the abundances of filamentous bacteria (19%) as determined by the microbial community analysis in section 4.3.1. ξ_f in Equation 4.5 is the measure of geometry of the filamentous bacteria, which is calculated by Equation 4.8:

$$\xi = 2\frac{\text{Length of bacteria}}{\text{width of bacteria}} \tag{4.8}$$

The ξ_f is 346 as calculated from the average length (520 μm) and width (3 μm) of filamentous bacteria from section 4.3.2. Parameters η_l and η_t are given by the following expressions:

$$\eta_l = \frac{E_f - E_m}{E_f + \xi E_m} \tag{4.9}$$

$$\eta_t = \frac{E_f - E_m}{E_f + 2E_m} \tag{4.10}$$

where E_f is the Young's modulus of filamentous bacteria (5.34 GPa determined by AFM nanoindentation).

The theorical Young's moduli of filamentous bacteria-reinforced PHBV were verified by being compared with experimental values. Specimens of pure matrix and composite materials were fabricated by extrusion and 3D printing according to ASTM International D638-14 (Type V specimens, 3 mm thickness). Five replicates were tested for pure matrix and each composite material with different fiber ratios. The Young's moduli of specimens were determined by tensile tests using a universal material testing machine (AG-X plus Series, Shimadzu, Kyoto, Japan) with 1 mm/min testing speed. The experimental Young's moduli of filamentous bacteria-reinforced PHBV and theoretical values are compared in Figure 4.7. Tensile moduli were predicted to increase as fiber ratios increased. The calculated tensile modulus of neat PHBV increased from 1.36 GPa to 1.48 GPa when 20% MBR sludge were used as reinforcing agents. The experimental value of 20% MBR sludge reinforced PHBV was 1.52 GPa as determined previously (presented in chapter 3). The theoretical values were close to the experimental values, which indicated that the dimension measurements of filamentous bacteria were accurate. Results also suggested that it

was appropriate to assume filamentous bacteria randomly oriented and uniformly distributed in the composite materials.

Table 4.1. The synthetic wastewater composition of the MBR

Chemical	Concentration (mg/L)
Glucose	100
Glycine	30
Sodium acetate	150
Yeast extract	20
Ammonium chloride	2
Potassium phosphate	2
Sodium thiosulfate	40
Sodium sulfhydrate	10
Sodium lactate	50
Calcium chloride	10
Ferric chloride	0.2
Magnesium sulfate	1
Manganese chloride	0.385
Sodium molybdate	0.01

Table 4.2. Young's modulus of *Sphaerotilus* spp. and some natural fibers

Fibers		Young's modulus (GPa)	Reference
Bacteria	*Sphaerotilus* spp.	5.34 ± 0.67	This study
Plant fibers	Coconut fiber	2.50	(Rao & Rao, 2007)
	Cotton fiber	12	(Wambua et al., 2003)
	Flax fiber	60-80	(Wambua et al., 2003)
	Hemp fiber	70	(Wambua et al., 2003)
	Kenaf fiber	53	(Omrani et al., 2016)
	Palm fiber	2.75	(Goulart et al., 2011)
Animal fiber	Wool	2.3-3.4	(Cheung et al., 2009)
	Spider silk	11-13	(Cheung et al., 2009)

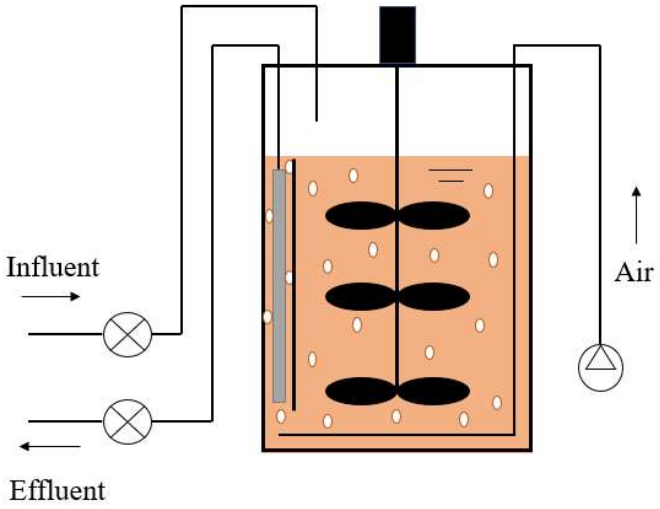

Figure 4.1. Schematic diagram of membrane bioreactor.

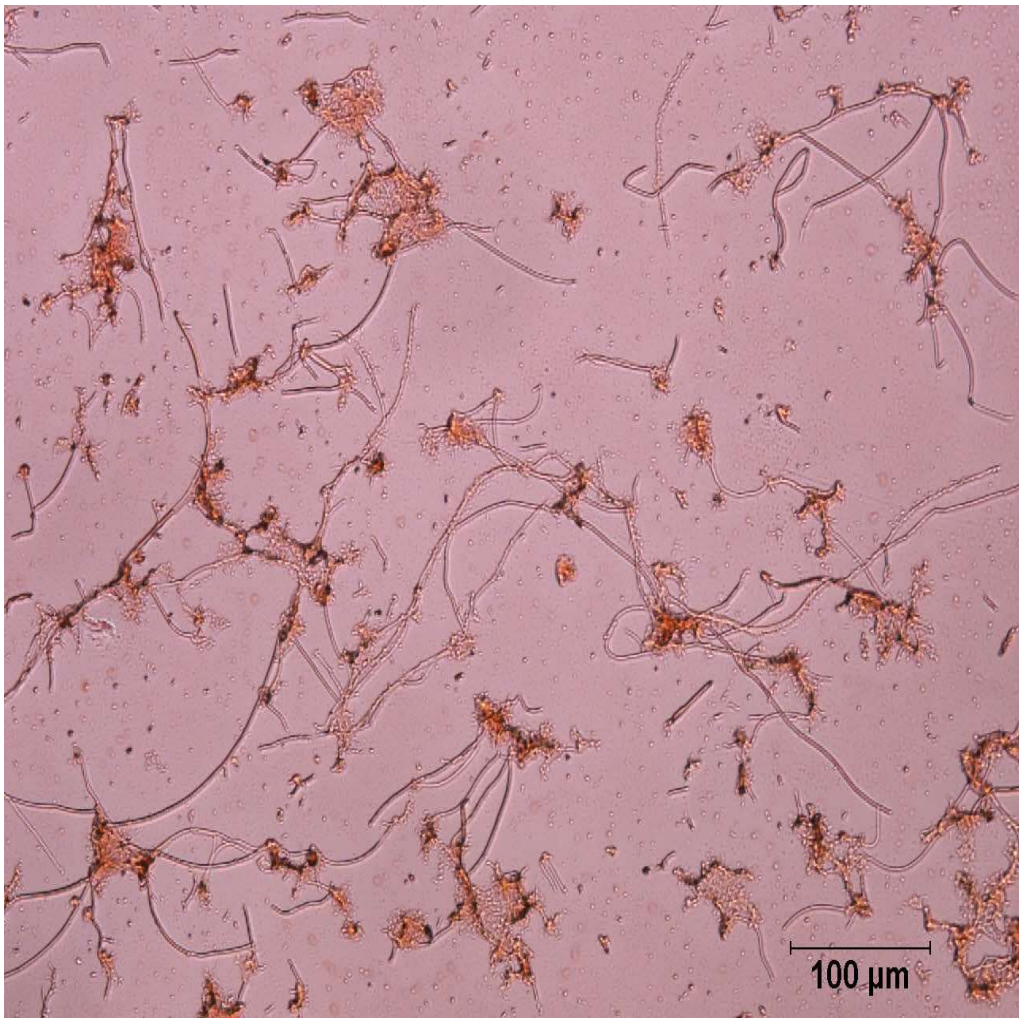

Figure 4.2. Undiluted mixed liquor from the MBR observed by an optical microscope (100×).

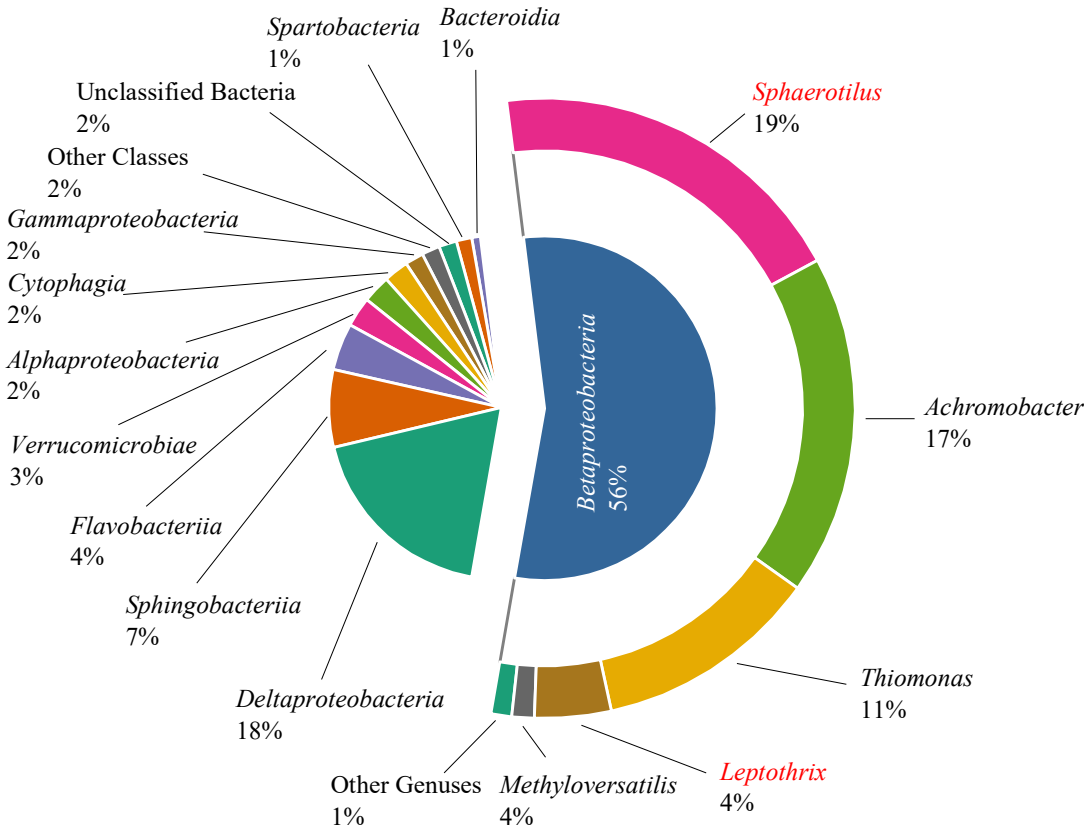

Figure 4.3. Relative abundance at genus level of MBR sludge.

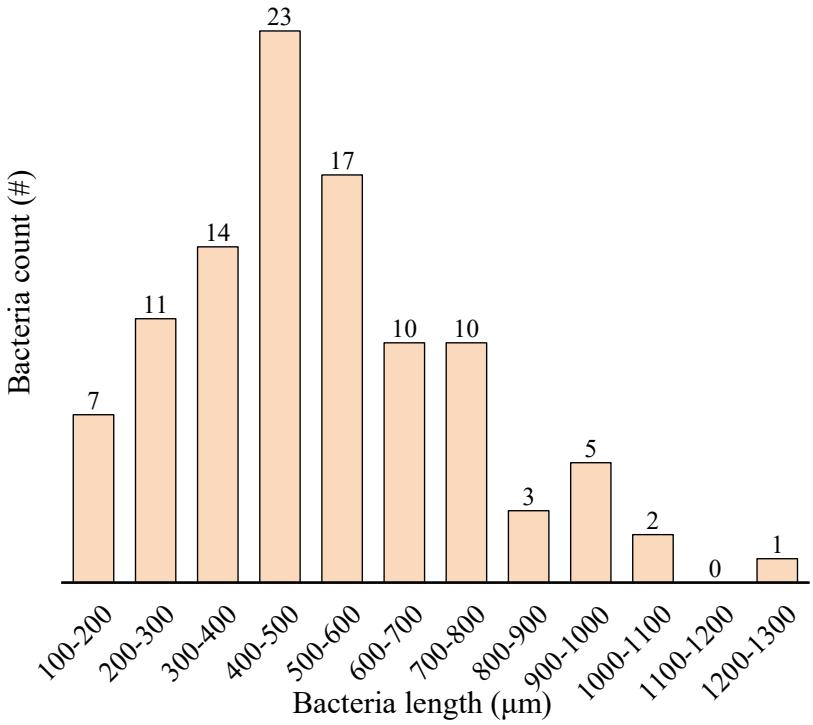

Figure 4.4. Length distribution of filamentous bacteria in the MBR.

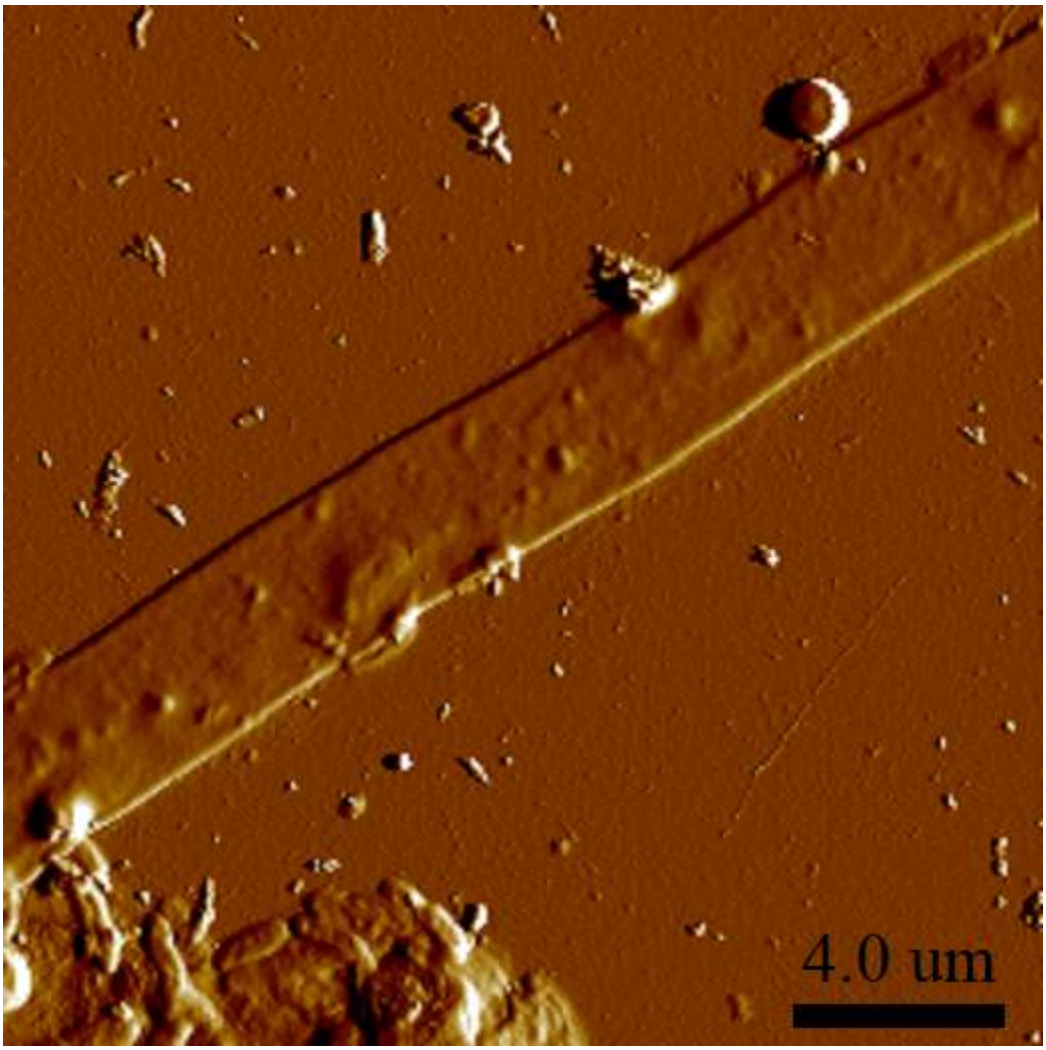

Figure 4.5. Morphology of a typical filamentous bacterium in the MBR via AFM scanning.

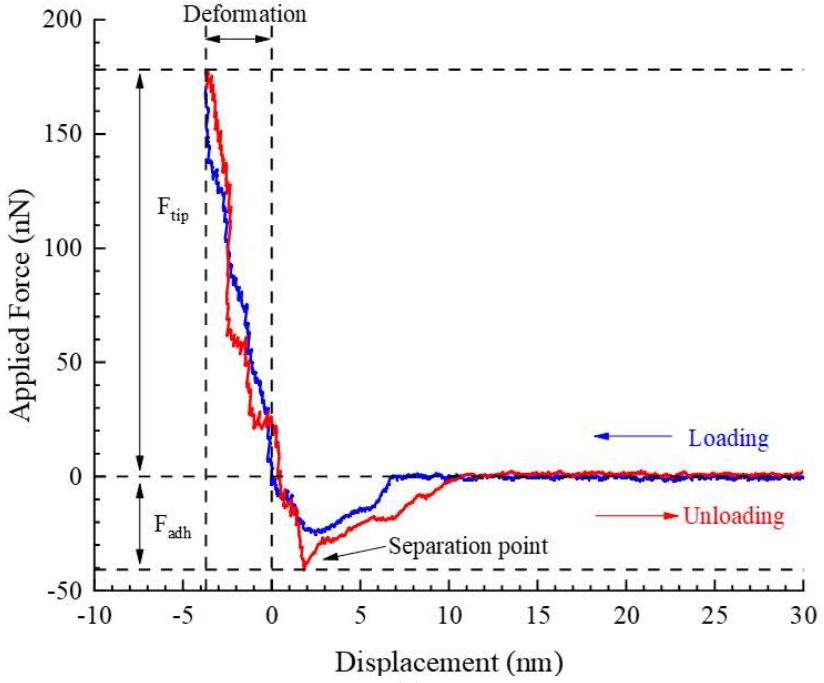

(a)

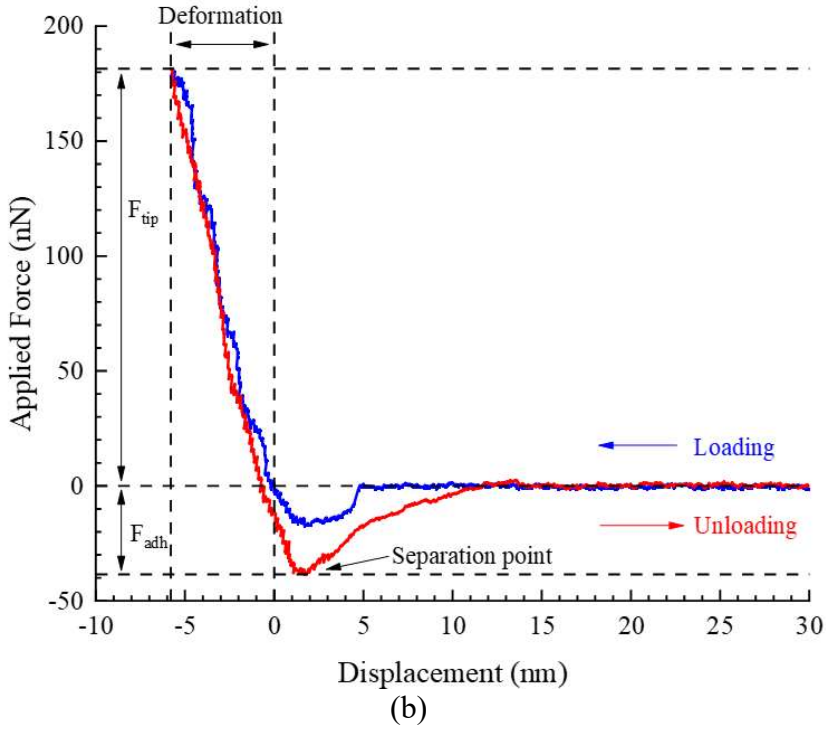

(b)

Figure 4.6. A typical AFM nanoindentation force-displacement curve of: (a) a filamentous bacterium; (b) a non-filamentous bacterium.

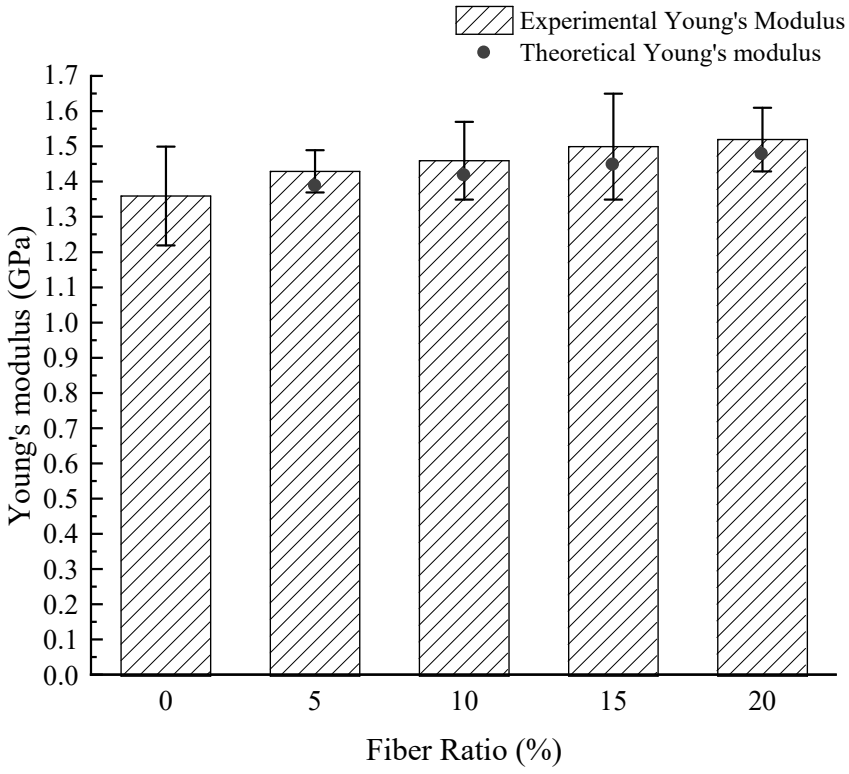

Figure 4.7. Comparison of experimental and theoretical Young's modulus of filamentous bacteria reinforced PHBV.

Chapter 5

BIOCOMPOSITE MATERIALS FROM ACTIVATED SLUDGE: FILAMENTOUS BACTERIA REINFORCED POLY(HYDROXYBUTYRATE-CO-HYDROXYVALERATE)

Abstract

This chapter evaluates the mechanical properties of an all-natural biocomposite material fabricated from activated sludge. A sequencing batch reactor was operated to enrich for polyhydroxyalkanoates (PHA)-accumulating bacteria, and the production of PHBV by the enriched cultures was maximized by a fed-batch reactor. The highest PHA content of 59% dry cell weight was obtained with 68% PHB and 32% PHV. PHBV extracted from the bacterial cells in the fed-batch reactor had a purity of 99.3%. This PHBV was used as the matrix of the composite material. A membrane bioreactor was used to cultivate filamentous bacteria-dominating cultures (19% relative abundance of *Sphaerotilus* spp.). The sludge of the steady-state MBR was freeze-dried and used as the reinforcement agent of the composite material. Differential scanning calorimetry and thermogravimetric analysis of microbial PHBV suggested that the melt extrusion and 3D printing temperatures to be 170 °C and 180 °C, respectively, to minimize the thermal degradation of PHBV. Mechanical tests showed that the tensile modulus and notched impact strength of microbial PHBV improved by 57% and 45%, respectively, following the addition of 20% membrane bioreactor sludge. This chapter demonstrated that filamentous bacteria-dominating mixed culture may be used as reinforcement agents for biocomposite materials.

5.1 Introduction

Most plastics are used in single-use products, which caused several environmental and human health issues (Wang & Li, 2021). Thus, there is an urgent need today for a green alternative to petroleum-based plastics that are environmentally friendly, biodegradable, and economical. At the same time, it is important that we reduce our generation of organic waste, which continue to stress our already limited disposal options and are often disposed of in a manner that produces greenhouse gases.

Poly(3-hydroxybutyrate-co-3-hydroxyvalerate) (PHBV) co-polymer has received considerable attention in recent years due to its biodegradability and properties similar to those of many petroleum-based plastics (McAdam et al., 2020). PHBV can be produced by many bacteria in activated sludge under aerobic dynamic feeding conditions and high-strength organic feeding (Johnson et al., 2009). It has been extensively reported that high PHA content and various hydroxybutyrate-to-hydroxyvalerate (HB-to-HV) ratios can be achieved in activated sludge via the above-mentioned growth strategies (Albuquerque et al., 2007; Fauzi et al., 2019; Tamang et al., 2019; Wijeyekoon et al., 2018; Zhang et al., 2014).

Although considerable research has been conducted on the mechanical properties of commercially available PHBV (usually with a low hydroxyvalerate content), few studies investigated the mechanical properties of microbial PHBV with a high hydroxyvalerate (HV) content. PHBV with a low HV content is stiff and brittle, whereas it becomes softer and more flexible with increasing HV content (Pilla, 2011; Walton, 1991). Therefore, microbial PHBV with a high HV content may be a more promising biopolymer to replace petroleum-based plastics for a wide range of commercial applications.

The PHBV co-polymer typically requires fiber reinforcement to improve its mechanical properties before it can be widely used in high-volume industries (Kinyanjui Muiruri et al., 2023). To date, most research into fiber-reinforced PHA composites have been based on commercially available polyhydroxybutyrate (PHB) or PHBV with low HV contents (Hosokawa et al., 2017; Smith et al., 2020; Torres-Giner et al., 2018; Torres-Tello et al., 2017). The mechanical properties of fiber-reinforced microbial PHBV, particularly of elevated HV contents have not been investigated extensively. Chan et al. (2019) compared the mechanical properties of wood flour-reinforced PHBV composites with 1% HV and 24% HV contents. The PHBV composite with 1% HV exhibited 100% increase in tensile modulus and 19.7% decrease in tensile strength with the addition of 50 wt.% wood flour, whereas the composite with 24% HV exhibited 251% increase in tensile modulus and 11.4% decrease in tensile strength with the same 50% wood flour addition. They concluded that that the use of the softer PHBV matrix (i.e., higher HV contents) resulted in improved tensile properties of wood-flour reinforced composites.

The overall goal of this research is to convert waste sludge into an all-natural composite material that could be a substitute for plastic based composite materials and reduce the amount of waste sludge disposed from WWTPs. Our previous study successfully used filamentous bacteria cultivated from WWTP sludge to reinforce commercial PHBV with 1% HV content. The tensile modulus and impact strength of PHBV with 20% of filamentous-bacteria-dominant sludge improved by 11.99% and 95.29%, respectively. However, filamentous bacteria reinforced PHBV with higher HV content were not assessed.

Microbial PHBV with a high HV content was produced from activated sludge cultures treating synthetic wastewater using a sequencing batch reactor (SBR) and a fed-batch reactor (FBR). Filamentous bacteria were cultivated and enriched in a membrane bioreactor (MBR). The two components were extruded, and 3D printed to fabricate the required specimens for mechanical tests. The thermal and mechanical properties of neat microbial PHBV and its biocomposites were evaluated in this study.

5.2 Materials and Methods

5.2.1 Composite material components preparation

5.2.1.1 Matrix production

5.2.1.1.1 Enrichment of PHA-accumulating bacteria

A sequencing batch reactor (SBR) was used to select and enrich for PHA-accumulating bacteria. A 9-L SBR was constructed using a cylindrical acrylic tube. It was seeded with activated sludge cultures obtained from a local municipal wastewater treatment plant. The reactor content was continuously stirred using a paddle mixer at 150 rpm. The SBR was operated in a 12-h cycle. Each operation cycle consisted of fill (10 min), react (10 h 20 min), settle (1 h 15 min), and decant (15 min) phases. At each fill phase, 7.5 L of feed solution was pumped into the reactor. The detailed composition of the SBR feed solution is listed in Table 5.1. A desired mean cell residence time (MCRT) of 5 days was maintained by wasting 1,560 mL of mixed liquor from the SBR daily. Hydraulic retention time (HRT) of the SBR system was maintained at 0.6 days by decanting 6,720 mL of supernatant after each settle phase and wasting 780 mL of reactor content at the end of each react phase daily. Dissolved

oxygen (DO) concentration in the SBR was maintained above 2.0 mg/L using porous stone diffusers connected to an air pump. The pH of the culture was uncontrolled; however, the pH levels were monitored throughout the cultivation using an electrode and Cole-Palmer pH meter (East Bunker Court Vernon Hills, IL, USA). Operation of the SBR was monitored by measuring soluble chemical oxygen demand (COD) values of the influent and effluent, mixed liquor suspended solids (MLSS), mixed liquor volatile suspended solids (MLVSS), pH, and dissolved oxygen (DO) in the SBR. Soluble COD were determined using a spectrophotometer (DR 5000, Hach Company, Loveland, CO. USA) measuring COD of filtrate through a glass fiber filter (GF-A Glass Microfiber Filters, Whatman). MLSS and MLVSS were determined according to Standard Methods (APHA, 2005). Dissolved oxygen (DO) concentration was measured using a DO probe and a YSI DO meter (Yellow Springs, OH, USA). pH was measured using an electrode and Cole-Palmer pH meter (East Bunker Court Vernon Hills, IL, USA) (Maeng and Cha, 2017).

Acetate and propionate removal rate were monitored as indicators of enriching of PHA-accumulating bacteria in the SBR system. Five mL sample from the SBR was collected on day 0 and day 12 every hour during the react phase, and samples were filtered. Two mL of filtrate was injected into a 7890B gas chromatograph equipped with a flame ionization detector (GC-FID) (Agilent Technologies, Santa Clara, CA, USA) for acetate and propionate analysis. The specification of capillary column was 30 m x 0.32 mm ID x 0.25 μm film thickness (DB-FATWAX UI, Agilent Technologies, Santa Clara, CA, USA), and nitrogen was used as the carrier gas at a constant flow rate of 40 mL/min. Inlet and detector temperatures were 220 °C and 250 °C, respectively. The injected sample volume was 0.1 μL with 1:10 split ratio.

The initial oven temperature was kept at 80 °C for 1 min, and then increased to 180 °C at 10 °C/min for 10 mins. The oven temperature was then increased to 240 °C at 60 °C/min and held for 2 mins.

PHA content in SBR cells were measured 2 months after the SBR operation according to the PHA analysis method reported by Braunegg et al. (1978). Ten mL of the SBR mixed liquor was collected every 30 min during the react phase from 0 h to 3h. The collected mixed liquor was centrifuged at 8000 × g for 5 min, and the supernatant was decanted. The sludge pellets were freeze-dried for 72 h. The pellet was weighed and mixed with 2 mL of chloroform and 2 mL of acidified methanol (3% sulfuric acid) with 40 mg/L benzoic acid as an internal standard in a screw-capped glass vial. Vials were heated at 100 °C for 3.5 h in a water bath, and then cooled down to room temperature. One mL of deionized (DI) water was added to each vial and shaken vigorously for 10 min. The organic phase (lower layer) was syringe-filtered and subsequently used for the GC-FID analysis. The initial oven temperature was 90 °C and kept for 1 min. Subsequently, the oven temperature increased to 150 °C at 8 °C /min and held for 5 min. The injected sample volume was 0.1 µL with 1:20 split ratio. The other conditions were the same as those used for the acetate and propionate analyses described above. Pure PHBV (Sigma-Aldrich, St. Louis, MO, USA) containing 12% of PHV was used as standard.

5.2.1.1.2 PHA production

Fed-batch cultivation strategy was used to maximize PHA production, and the PHA production was conducted on a daily basis. A 4.5-L fed-batch reactor (FBR) was constructed using a cylindrical acrylic tube. The 1560 mL daily wasted sludge from the SBR was centrifuged, and the sludge pellet was resuspended in 2000 mL of FBR

feed solution. This mixed liquor was then transferred into the FBR as the seed sludge for each batch of PHA production. After PHA production completed, all the FBR content was decanted and collected for PHA extraction. The reactor was rinsed with DI water and subsequently used for the next batch of PHA production. The reactor content was continuously stirred with a paddle mixer at 300 rpm during the PHA production. Dissolved oxygen (DO) concentration in the FBR was maintained using porous stone diffusers connected to an air pump. Dissolved oxygen (DO) concentration and pH in the FBR were measured every 10 min throughout the FBR operation using a DO meter (YSI Inc., Yellow Springs, OH, USA) and a pH meter (Cole-Parmer, Vernon Hills, IL, USA), respectively. The feed solution addition was regulated by the DO concentration. After a sudden DO concentration increase was observed, the feed solution was pumped into the reactor. The feed solution addition was paused after DO concentration dropping below 2.0 mg/L. PHA production ended when feed solution addition did not lead to a decrease in DO concentration. The detailed composition of the FBR feed solution is listed in Table 5.2.

The acids concentration and PHA contents were examined to evaluate the PHA production process. Ten mL of the FBR mixed liquor was collected every 30 min throughout the FBR operation. The collected mixed liquor was centrifuged at 8000 × g for 5 min, and the supernatant was collected and filtered. Two mL of the filtrate was collected for acids concentration measurements. The sludge pellets after centrifuged was freeze-dried and subsequently used for PHA content measurements. The acids concentration and PHA contents were determined by GC-FID as described in section 5.2.1.1.1.

5.2.1.1.3 PHA extraction and purification

Intracellular PHA contained in FBR cells were extracted and purified according to the method reported by Burns et al. (2009). The sludge collected from the FBR was centrifuged at 8000 × g for 5 min, and the supernatant was decanted. The cells were lysed by a surfactant treatment to release intracellular PHA content. Sludge pellets collected from the centrifuge were resuspending in a 100 mL solution containing 8 g/L sodium dodecyl sulfate (SDS) and 7.2 g/L EDTA. The mixture was then autoclaved at 121 °C for 30 min. After autoclaving, the mixture was centrifuged, washed with 50 mL DI water, and washed thrice with 20 mL acetone. The washed pellet was then dried in an oven at 60 °C for 8 h.

The crude PHA was extracted from the lysed cellular substances using chloroform extraction. The dried pellet was mixed with 40 mL chloroform in a screw-capped glass vial. The vial was heated at 70 °C for 2 h in a water-bath, and then cooled down to room temperature. The heated mixture was then filtered, and the filtrate was collected in a 100 mL beaker. This beaker was heated at 60 °C in a water-bath until the chloroform completely evaporated. The solid left in the beaker after filtrate evaporation was the crude PHA. Crude PHA was purified using the anti-solvent precipitation method. The crude PHA was mixed with 30 mL chloroform in a 100 mL beaker. After the crude PHA was completely dissolved, 30 mL of cold methanol (4 °C) was added into the beaker to precipitate PHA. The mixture was then filtered again, and the filtered residues were collected as the purified PHA. The purity of the purified PHA was determined using GC-FID as described above.

5.2.1.2 Reinforcement production

Activated sludge cultures used to enrich filamentous bacteria were established in a bench-scale membrane bioreactor (MBR) on a synthetic wastewater. The 3-L MBR was constructed with a cylindrical acrylic tube, and initially seeded with the recycle sludge from a local municipal wastewater treatment plant.

An initial total suspended solid (TSS) concentration of 2000 mg/L was used. The reactor content was continuously stirred with a paddle mixer at 400 rpm. The dissolved oxygen (DO) concentration in the MBR was maintained at 1.5 ± 0.2 mg/L with porous stone diffusers connected to an air pump. The pH of the reactor content was maintained at 7.0 ± 0.5 using 0.1 M sulfuric acid or 0.1 M sodium hydroxide solutions. The synthetic influent wastewater contained of 100 mg/L of glucose, 30mg/L of glycine, 150 mg/L of sodium acetate trihydrate, 20 mg/L yeast exact, 2 mg/L of ammonium chloride, 2 mg/L of potassium phosphate monobasic, 40 mg/L of sodium thiosulfate, 10 mg/L of sodium sulfhydrate, 50 mg/L of sodium lactate, 10 mg/L of calcium chloride dihydrate, 0.2 mg/L of ferric chloride hexahydrate, 1 mg/L of magnesium sulfate heptahydrate, 0.385 mg/L of manganese chloride and 0.01 mg/L of sodium molybdate dihydrate. The hydraulic retention time (HRT) and mean cell residence time (MCRT) were maintained at 12 hours and 25 days, respectively. A constant MCRT was maintained by daily batch wasting of mixed liquor from the MBR.

Operation of the MBR was monitored by measuring soluble chemical oxygen demand (COD) values of the influent and effluent, mixed liquor suspended solids (MLSS), mixed liquor volatile suspended solids (MLVSS), pH, and dissolved oxygen (DO) in the MBR. Soluble COD were determined using a spectrophotometer (DR 5000, Hach Company, Loveland, CO. USA) measuring COD of filtrate through a glass fiber filter (GF-A Glass Microfiber Filters, Whatman). MLSS and MLVSS were

determined according to Standard Methods (APHA, 2005). Dissolved oxygen (DO) concentration was measured using a DO probe and a YSI DO meter (Yellow Springs, OH, USA). pH was measured using an electrode and Cole-Palmer pH meter (East Bunker Court Vernon Hills, IL, USA) (Maeng and Cha, 2017).

The MBR was operated for 29 months at steady state (± 10% of target MLVSS values). The sludge containing *Sphaerotilus* spp. was collected daily from the MBR. The collected sludge was centrifuged, and the supernatant was decanted. The sludge pellet was then freeze dried for 72 hours. A ball mill (JC-QM-2, Jvchuang Group Co., Ltd) with 3 mm Zirconia balls was used to grinded activated sludge into fine power for composite fabrication (Kumar et al., 2018). The freeze-dried pellet was ground in the ball mill for 10 minutes, and the dry sludge power was collected for subsequent composite fabrication.

Sludge containing *Sphaerotilus* spp. was observed using a scanning electron microscope (SEM) (Auriga 60 CrossBeam, Carl Zeiss Inc., Dublin, CA, USA). A vacuum filtration system was used to filter 20 mL of mixed liquor from the MBR with a 0.22 μm filter membrane. The sludge pellet on the filter membrane was lyophilized for 72 h. The dried sludge was fixed on a metal stub, sputter-coated with gold in a vacuum evaporator, and subsequently observed using the SEM.

5.2.2 PHA thermal assessments

5.2.2.1 Differential scanning calorimetry

The thermal properties of the PHBV samples were examined using a differential scanning calorimeter (Q2000, TA Instruments, New Castle, DE, USA) under a constant nitrogen flow rate of 50 mL/min. The differential scanning

calorimetry (DSC) test was conducted by using a heat-cool-heat method. A 10-mg polymer sample was first heated from -60 °C to 200 °C at 10 °C/min and kept isothermal for 3 minutes. The sample was then cooled back to -60 °C and held isothermal for 3 minutes before reheating. The crystallization temperature (T_c) and entropy of crystallization were determined during the cooling cycle. The sample was heated to 200 °C again in the reheating cycle to determine the melting temperature (T_m) and entropy of melting. The degree of crystallization (X_c (%)) was calculated as Equation 5.1:

$$X_c = \frac{\Delta H_m}{\Delta H_m^0} \times 100\% \quad (5.1)$$

where ΔH_m is the total enthalpy of melting, and ΔH_m^0 is the melting enthalpy of 100 % crystalline PHBV (146 J/g) (Berthet et al., 2015).

5.2.2.2 Thermogravimetric analysis

Thermogravimetric analysis (TGA) was performed using a Hitachi STA 7200 thermogravimetric analyzer (Hitachi High-Tech Science Corp., Tokyo, Japan). TGA tests were conducted with purified microbial PHBV (10 mg). The sample was heated from room temperature to 800 °C at a heating rate of 10 °C /min under an argon atmosphere.

5.2.3 Composite material fabrication

Specimens of composite materials were fabricated by an extrusion-3D printing technique. Purified microbially PHA and milled MBR sludge were dried in an oven at 60 °C for 6 hours before processing. Four different polymer-sludge mixtures were prepared for extrusion by mixing different amounts of purified PHBV and MBR sludge in a bench-top grinder. The MBR sludge contents in mixtures were 5%, 10%,

15%, and 20% by weight. The polymer-sludge mixtures were fed into the Wellzoom filament extrusion system (Wellzoom 2021 models Desktop Extruder Line II, Shenzhen Mistar Technology Co. Ltd., Shenzhen, China) to obtain composite filaments with a diameter of 1.75 ± 0.05 mm for the 3D printer. The temperatures of the two heating chambers of the extruder were 170 °C and 160 °C, respectively, to melt the matrix and to minimize thermal degradation. The maximum sludge content was 20% because higher sludge content made it difficult to maintain the required filament diameter for 3D printing. The extruded filaments were cooled down in the water bath, then collected, and subsequently dried in an oven at 60 °C for 4 h before 3D printing.

Specimens for mechanical studies were fabricated by a fused deposition modeling (FDM) 3D printer (Chiron, Anycubic Technology Co., Shenzhen, China). The models of specimens were designed by Ultimaker Cura (V3.2.1) software, and then sent to the 3D printer. Filaments from the extruder were placed layer by layer to achieve required dimensions for mechanical testing. The height of the first layer was set as 0.3 mm. All the following layers were 0.1 mm in height. The temperature of the printing nozzle and the bed were set at 180 °C and 60 °C, respectively. The printing speed was 100 mm/s.

5.2.4 Materials mechanical properties

Tensile strength of specimens was determined by a universal material testing machine (AG-X plus Series, Shimadzu, Kyoto, Japan). All tensile tests were conducted according to ASTM International D638-14 (Type V specimens). The specimen thickness was 3 mm and tested at a strain rate of 1 mm/min. Five specimens were tested for each polymer-sludge composite. The stress-strain curve of each test

was recorded, and the linear portion of the curve was used to calculate Young's modulus of each specimen by Equation 5.2:

$$E=\frac{\Delta\sigma}{\Delta\varepsilon} \tag{5.2}$$

where $\Delta\sigma$ was the change in tensile strength of the material, and $\Delta\varepsilon$ was the change in strain of the material.

The notched impact tests were conducted using an impact tester (HIT5.5P, Zwick, Ulm, Germany) with a 2.75 J pendulum impactor. The specimen was 3 mm thick, while other dimensions were the same as defined by ASTM International D256-10. Other procedures in impact tests all followed ASTM International D256-10. Five replicates were tested for each polymer-sludge composite.

5.3 Results and Discussion

5.3.1 Enrichment of PHA-accumulating bacteria and PHA production

After seeding the SBR units, acetate removal percentage during the react phase were compared at day 0 and day 12 to assess the activity of PHA-accumulating cultures in the SBR units (Figure 5.1). The intermittently fed SBR sludge exhibited much higher acetate uptake rate than activated sludge from a continually fed systems (seed cultures) when exposed to excess substrate. At 12 days of operation, acetate in feed solution decreased rapidly, resulting in more than 80% of feed acetate removal in 1 h. On the other hand, the seed cultures obtained from a completely mixed activated sludge treatment system (day 0 sludge) took 5 h to consume 90% of feed acetate. Acetate removal by the SBR sludge was characterized by a rapid initial removal followed by a subsequent slower removal rate. After 2 h, the acetate was depleted and the famine conditions in the SBR lasted for the remaining 10 h until the next react

phase. Niekerk et al. (1987), experimenting with an intermittently fed system, reported that most of the substrate removed during the short "feast" phase were stored as PHA polymer since only a small fraction of the removed substrate was actually metabolized during this phase. The stored PHA was then metabolized during the subsequent endogenous phase restoring the substrate storage capacity before the next feeding cycle. Thus, bacteria with PHA-storing abilities have a competitive advantage over bacteria that do not have PHA-storing abilities (Sehgal & Gupta, 2020).

Substrate utilization rates and PHA accumulation of the SBR cultures were assessed after 2 months of SBR operation (Figure 5.2). Both PHB and PHV were detected in the SBR sludge, and their amounts were expressed as percent dry cell weight (DCW). Low amounts of PHB (1.5%) and PHV (1.4%) were detected at the beginning of feed phase, indicating that intracellular PHA was not completely depleted during the famine stage. During react phase, both acetate and propionate were depleted after 1.5 h, while intracellular PHB and PHV increased to 7.9% and 6.1%, respectively. This rapid consumption of fatty acids and simultaneous synthesis of PHA suggests acetate and propionate as the precursors of PHB and PHV. This result is consistent with those reported in literature (Christensen et al., 2021; Ma et al., 2018; Narancic et al., 2016; Shozui et al., 2010; Sullivan et al., 2022). Anjum et al. (2016) reported that bacteria converted a portion of carbon sources to PHB and PHV via β-oxidation, and catabolized PHB as well as PHV for energy production after exogenous carbon sources were exhausted.

The SBR system was operated at steady-state (± 10% of the target MCRT) for 29 months to select PHA-accumulating-bacteria-dominant cultures. The MLVSS values of SBR mixed liquor were 1540 ± 40 mg/L during the steady-state operation.

The effluent VSS was 30 ± 5 mg/L, indicating good settleability of the SBR sludge. The actual MCRT of the SBR was calculated as 4.9 days. The average chemical oxygen demand (COD) of SBR influent and effluent were 1425 ± 51 mg/L and 18 ± 3 mg/L, respectively. The COD removal rate of the SBR was 99%, indicating good wastewater treatment efficiency of the SBR. pH and DO were monitored during the SBR operation. The average pH and DO in the reactor were maintained at 7.6 ± 0.2 and 2.1 ± 0.4 mg/L, respectively.

Fed-batch reactor (FBR) operation and performance parameters during mixed culture fermentation of PHA are shown in Figure 5.3. The addition of FBR medium was dissolved oxygen (DO) regulated. An increase in DO concentrations during fermentation normally indicates decrease in oxygen demand of heterotrophic microorganisms because of substrate exhaustion (Wang et al., 2019). The fatty acid concentration profile confirmed that the substrate addition was well-timed. The intracellular PHA content reached 59% DCW at 7 h of FBR operation. The PHB and PHV fractions were 68% and 32%, respectively. The PHA content and composition reached steady state levels after 6 h. Therefore, subsequent FBR fermentation runs for the PHA production were carried out for 6 h. The overall intracellular PHA extraction efficiency was 40%, with a purity of 99.3%, which is similar to the values obtained by Pagliano et al. (2021).

5.3.2 Enrichment of filamentous bacteria

The membrane bioreactor (MBR) system was operated at steady-state (± 10% variation in MLVSS values of MBR mixed liquor) for 29 months to cultivate and maintain filament-dominating cultures. The MLVSS values of MBR mixed liquor were 1320 ± 70 mg/L during the steady-state operation. The effluent VSS was 0 mg/L,

indicating good membrane filtration. The average chemical oxygen demand (COD) of MBR influent and effluent were 213 ± 17 mg/L and 8 ± 2 mg/L, respectively. The average pH and DO were maintained at 6.8 ± 0.3 and 1.3 ± 0.2 mg/L, respectively.

A membrane bioreactor (MBR) was used to cultivate and enrich filamentous bacteria. Low dissolved oxygen, and nitrogen and phosphorus limited conditions were provided in the MBR, resulting in proliferation of filamentous bacteria. An SEM image of the lyophilized mixed cultures harvested from SBR is shown in Figure 5.4. Our previous study identified *Sphaerotilus* spp. as the dominant filamentous bacteria in the MBR cultures using 16S rRNA gene sequencing. A relative abundance of these filamentous bacteria was 19% in the mixed culture.

5.3.3 Thermal property characterizations

Differential scanning calorimetry (DSC) thermogram of the purified microbial PHBV (MPHBV) is shown in Figure 5.5. A sub-ambient T_g (-8.4 °C) and a cold crystallization peak (T_c at 66.4 °C) were observed in the second heating scan, indicating that MPHBV crystallized incompletely during the cooling scan and shifted into the crystal structure during the second heating scan (Lorenzo et al., 2012). There were two melting temperatures (127.4 °C and 155.9 °C) detected in the second heating scan, while only one melting peak was observed during the first heating scan with a melting temperature of 166.9 °C (figure not shown). This phenomenon is similar to PHBV with HV content range from 15% to 24% reported by Guho et al. (2020). The differences in the MPHBV melting behavior between the first and second heating scans were another evidence that the crystal structure of the co-polymer is changing during the DSC test. Figures 5.6 and 5.7 compare the thermogravimetric analysis (TGA) and derivative thermogravimetry (DTG) thermograms of MPHBV with those

of commercial PHBV (CPHBV) purchased from Tianan Biologic Materials (Ningbo, China), respectively. The onset temperatures of thermal degradation (T_d) of MPHBV and CPHBV, at which weight loss of the sample was 5%, were 240.8 ℃ and 276.1 ℃, respectively (Figure 5.6). The rate of weight loss reached its maximum at the peak decomposition temperature (T_p) of 270.2 ℃ and 294.0 ℃ for MPHBV and CPHBV, respectively (Figure 5.7).

The thermal properties of the MPHBV and CPHBV are summarized in Table 5.3. MPHBV containing 31.7% HV had a lower melting temperature than CPHBV, which contained 1% HV. Similarly, Chan et al. (2004) reported that a lower melting temperature of PHB copolymer with increasing content of hydroxyvalerate (HV). The degree of crystallization (X_c) of MPHBV was determined as 23.4% based on the DSC assessment. This value was lower than that of CPHBV (64.9%) due to high HV content of MPHBV. The higher HV content limited the PHB-lattice formation owing to hydrogen bonding between HV and hydroxybutyrate (HB) (Guho et al., 2020). The T_d and T_p values of MPHBV were lower than those of CPHBV as summarized in Table 5.3. The thermal decomposition temperature of PHBV had no clear correlation with the HV content (Wang et al., 2013); however, it increases with increasing molecular weight (Carrasco et al., 2006). The lower T_d and T_p values of the MPHBV indicated that it had a smaller molecular weight than that of CPHBV. Therefore, heating zones of the extruder were set at 170 °C and 160 °C, respectively, based on the thermal properties of MPHBV. The temperature of the 3D printer nozzle was also set to 180 °C accordingly.

5.3.4 Mechanical property characterizations

The mechanical properties of the MPHBV reinforced with 0, 5, 10, 15, and 20% of filament-dominating MBR sludge are shown in Figures 5.8 to 5.10. Tensile strength of the MPHBV decreased as the amount of MBR sludge increased (Figure 5.8). The average tensile strength of the neat MPHBV was 17.7 ± 0.4 MPa, which was comparable to the values reported in the literature for PHBV copolymers with elevated HV contents (Chan et al., 2019). The average tensile strength values of PHBV composites gradually decreased with higher amounts of filamentous sludge addition, which is consistent with the general observations reported with fiber-reinforced composites (Seggiani et al., 2017; Vandi et al., 2019; C. S. Wu et al., 2017). The average tensile strength decreased to 15.7 ± 0.3 MPa with 20% MBR sludge addition. The addition of filamentous sludge decreased the elongation at break when compared to that of the neat PHBV specimen (Figure 5.9). The elongation at break value decreased from 14.1 ± 0.7 % to 3.4 ± 0.3 % with 20 % filamentous bacteria content.

On the other hand, blending with the filament-dominating MBR sludge improved the tensile modulus of MPHBV (Figure 5.10). The tensile modulus of the neat MPHBV increased by 57% with the addition of 20% MBR sludge (from 811 ± 24 MPa to 1271 ± 39 MPa). This increase in tensile modulus of the filament-reinforced MPHBV composites may be attributed to the nucleating effect of filaments in the MBR sludge. The addition of fibers increases the number of polymer nucleation sites, thereby increasing the degree of polymer crystallization. A higher degree of crystallization generally leads to a higher tensile modulus (Batista et al., 2016; Dong et al., 2020). However, introducing filament-dominating MBR sludge into the PHBV may have increased the heterogeneity of the polymer microstructure. This would weaken the stress transfer within the composite material and result in a decrease in

tensile strength and elongation at break (S. Singh & Mohanty, 2007). A Student's t-test assuming equal variance was performed to check the statistical difference of Young's modulus between the neat microbial PHBV and microbial PHBV composite specimens with 20% bulking sludge. The two-tailed t-test with a degree of freedom of 8 showed a t-value of 22.3 and a p-value of 1.8×10^{-8}, which indicated a significant statistical difference in Young's modulus between microbial PHBV without and with 20% bulking sludge reinforcement.

In comparison to the neat commercial PHBV (CPHBV), the neat MPHBV with 32% HV content exhibited substantially lower tensile strength and tensile modulus (Figures 5.11 and 5.12). On the other hand, significantly higher elongation at break was observed with the neat MPHBV than that of the neat CPHBV (Figure 5.13). These differences in mechanical properties of the two copolymers may be attributed to the HV contents. Similar results were reported in previous literature (Abbasi et al., 2022; Barkoula et al., 2010; Chan et al., 2019; Zhuikov et al., 2020). Lv et al. (2016) reported that high HV percentage in the MPHBV hindered the formation of HB crystal lattices, thus, decreasing the degree of crystallization. They postulated that this decreased crystallization allowed the polymer chain to move and be more flexible, resulting in a higher elongation at break as well as lower stiffness. The two melting peaks in the DSC thermogram (Figure 5.5) also reflected the different crystal structures of MPHBV and CPHBV.

The notched impact strength of composite materials improved with increasing filamentous MBR sludge (Figure 5.14). The impact strength of neat MPHBV, which was 3.61 ± 0.15 kJ/m^2, increased to 5.22 ± 0.14 kJ/m^2 with the addition of 20% MBR sludge. Thus, adding filamentous bacteria significantly increased the energy needed to

break the composite, suggesting good interfacial adhesion between the PHBV and microbial filaments. Barkoula et al. (2010) reported that as the fiber ratio increased, more fibers are expected to act as bridges to prolong the fracture process of composites due to fiber debonding and pull-out, which increased the impact strength of the composites. Also, weaker stress transfer due to elevated fiber ratio can cause multiple microcracks within the composites during impacts, which can dissipate energy and increase the impact resistance of the composites (Russo et al., 2013; Torres-Tello et al., 2017).

The notched impact strength of neat MPHBV was significantly higher than that of neat CPHBV (1.7 ± 0.1 kJ/m^2) as shown in Figure 5.15. This observation is consistent with the findings of Chan et al. (2019). The extra energy required to completely break neat MPHBV was due to the more flexible polymer chains of MPHBV with a higher HV percentage.

Table 5.4 summarizes the effect of various fiber reinforcements on mechanical properties of PHA-based composites. Microbial PHBV reinforced with 20% MBR sludge has higher improvement in tensile modulus and lower reduction in tensile strength when compared with PHA reinforced with 20% raw palm fiber (C. S. Wu et al., 2017). The tensile modulus improvement of the microbial PHBV reinforced with 20% MBR sludge was similar to that of 30% bamboo fibers reinforced PHBV (S. Singh et al., 2008) and 30% maple wood fiber reinforced PHBV (S. Singh & Mohanty, 2007). Table 5.4 indicates that the reinforcement effects of filamentous bacteria growing in activated sludge were comparable to those of plant fibers as reinforcing agents for PHBV composites.

Table 5.1. Medium compositions of the SBR

Chemical	Concentration (mg/L)
Sodium acetate trihydrate	2754
Sodium propionate	648
Ammonium chloride	321
Magnesium sulfate heptahydrate	123
Ethylene diamine tetraacetic acid	100
Potassium phosphate monobasic	68
Potassium chloride	53.64
Zinc sulfate heptahydrate	44
Yeast extract	40
Allylthiourea	40
Calcium chloride dihydrate	14.7
Ferrous sulfate heptahydrate	10
Manganese chloride tetrahydrate	9.9
Cobalt chloride hexahydrate	3.22
Copper sulfate pentahydrate	3.14
Ammonium molybdate tetrahydrate	2.2

Table 5.2. Medium compositions of the FBR

Chemical	Concentration (mg/L)
Acetate acid	7875
Propionate acid	2475
Magnesium sulfate heptahydrate	123
Ethylene diamine tetraacetic acid	100
Potassium phosphate monobasic	68
Potassium chloride	53.64
Zinc sulfate heptahydrate	44
Yeast extract	40
Allylthiourea	40
Calcium chloride dihydrate	14.7
Ferrous sulfate heptahydrate	10
Manganese chloride tetrahydrate	9.9
Cobalt chloride hexahydrate	3.22
Copper sulfate pentahydrate	3.14
Ammonium molybdate tetrahydrate	2.2

Table 5.3. Comparison of thermal properties between microbial PHBV and commercial PHBV

	T_g (°C)	T_c (°C)	T_{m1} (°C)	T_{m2} (°C)	X_c (%)	T_d (°C)	T_p (°C)
Commercial PHBV (1% HV)*	NA	123	173.1	NA	64.9	276.1	294
Microbial PHBV (31.7% HV)	-8.4	66.4	127.4	155.9	23.4	240.8	270.2

*Data from chapter 3.

Table 5.4. Effects of different natural fibers on mechanical properties of PHBV composites

Matrix	Reinforcement	Fiber loading (%)	Tensile strength variation	Tensile modulus variation	Impact strength variation	Reference
PHBV (13% HV)	Recycled cellulose fiber	15%	-26.92%	30%	-40.43%	(Bhardwaj et al., 2006)
PHA	Raw palm fiber	20%	-16.17%	-4.20%	-	(C. S. Wu et al., 2017)
PHBV (8% HV)	Bamboo pulp fiber	20%	42.00%	31.43%	223.80%	(Long Jiang et al., 2008)
PHBV (8% HV)	Flax fiber	20%	1.67%	142.10%	113.20%	(Barkoula et al., 2010)
PHBV (32% HV)	Filamentous bacteria	20%	-11.39%	56.77%	44.60%	This study
PHBV	Bamboo fiber	30%	-11.68%	67.65%	-29.21%	(S. Singh et al., 2008)
PHBV	Maple wood fiber	30%	-15.51%	90.20%	-12.54%	(S. Singh & Mohanty, 2007)
PHBV (12% HV)	Agave fiber	30%	1.95%	47.91%	65.86%	(Torres-Tello et al., 2017)
PHBV (1% HV)	Oak wood fiber	36%	-38.51%	127%	-	(Srubar et al., 2012)
PHBV (2% HV)	Raw kenaf fiber	40%	-	-	175%	(Russo et al., 2013)

-: not reported

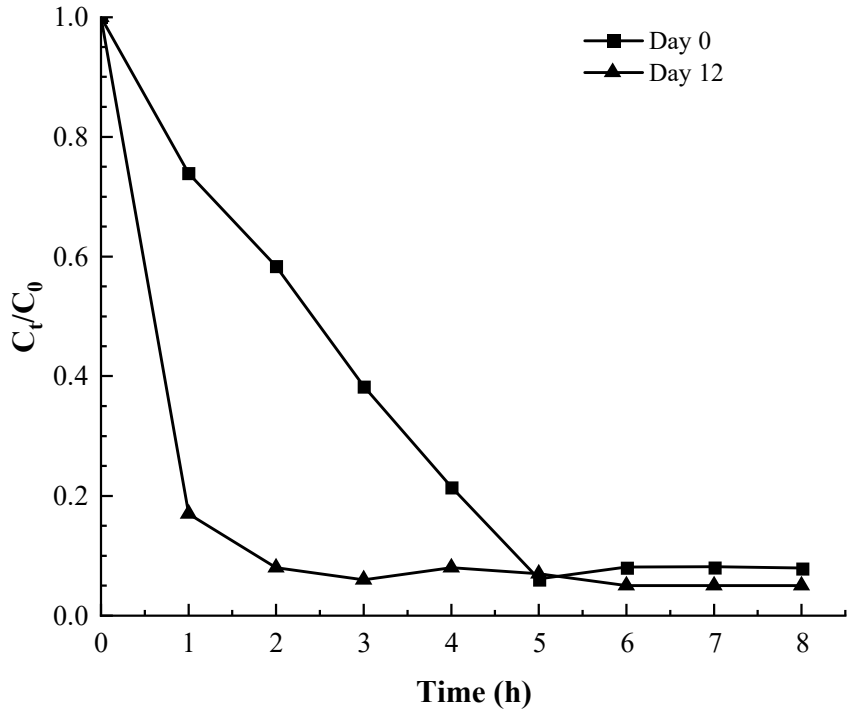

Figure 5.1. Acetate removal percentage changed with time at day 0 and day 12 after SBR operation.

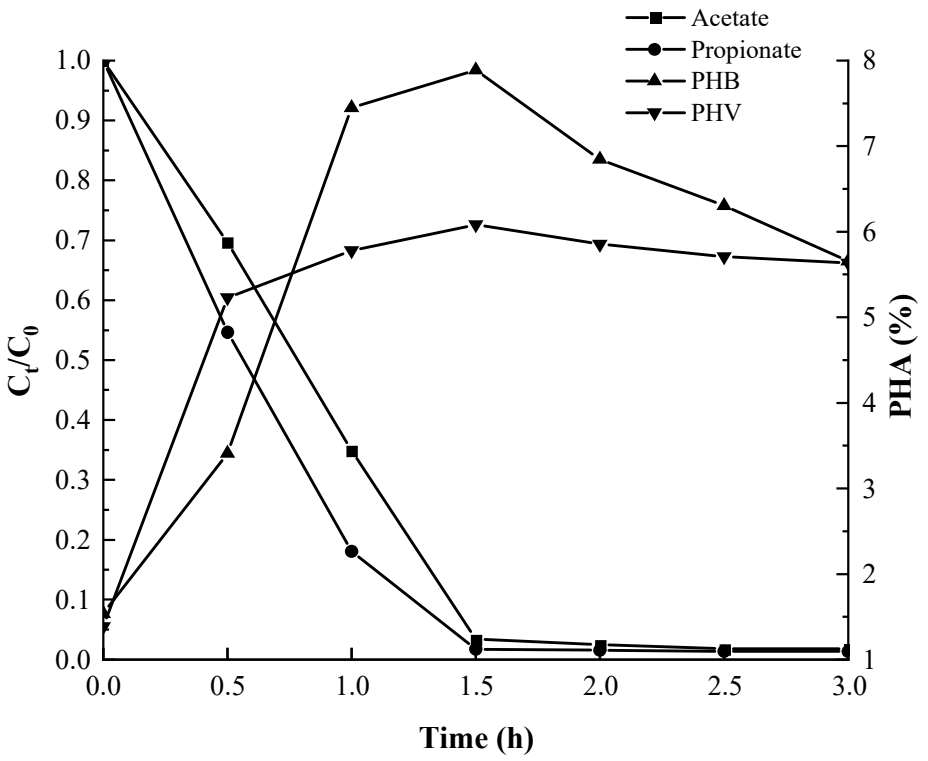

Figure 5.2. Fatty acids consumption and PHA accumulation in the SBR after two months of operation.

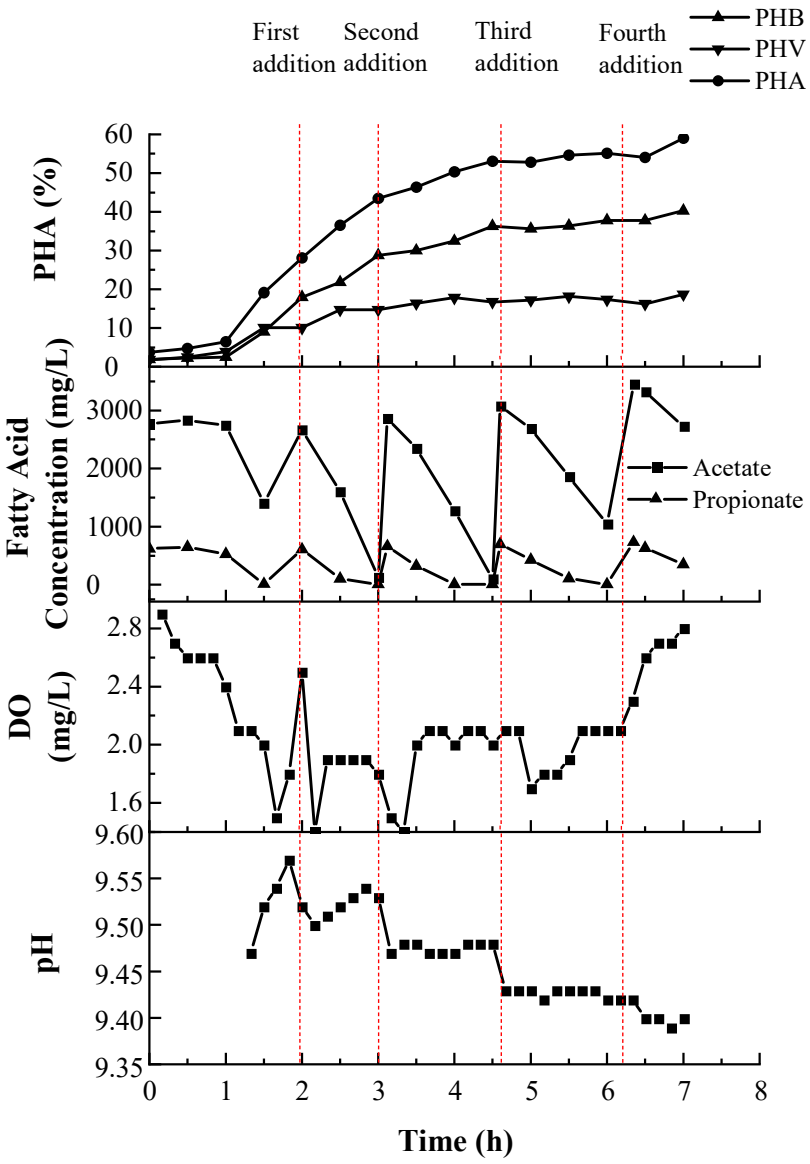

Figure 5.3. PHA production and operation parameters of fermentation in the FBR.

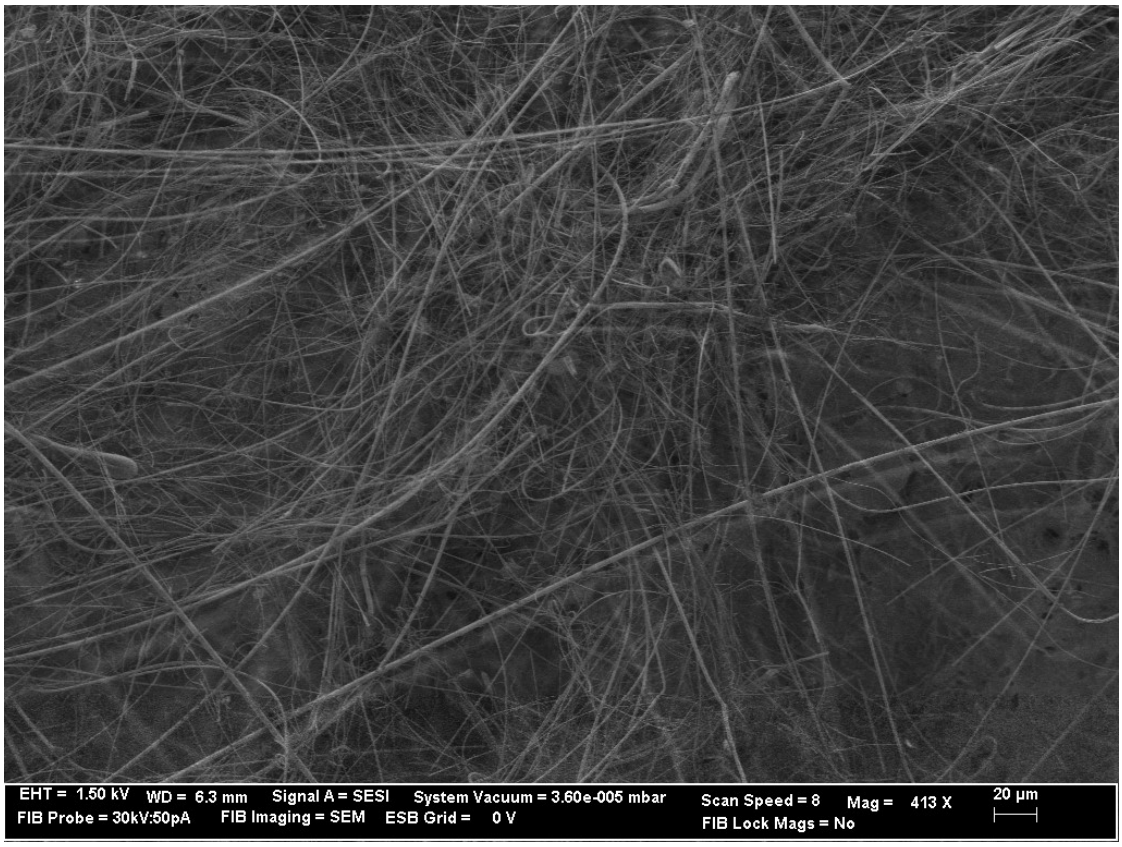

Figure 5.4. SEM image of lyophilized MBR cultures.

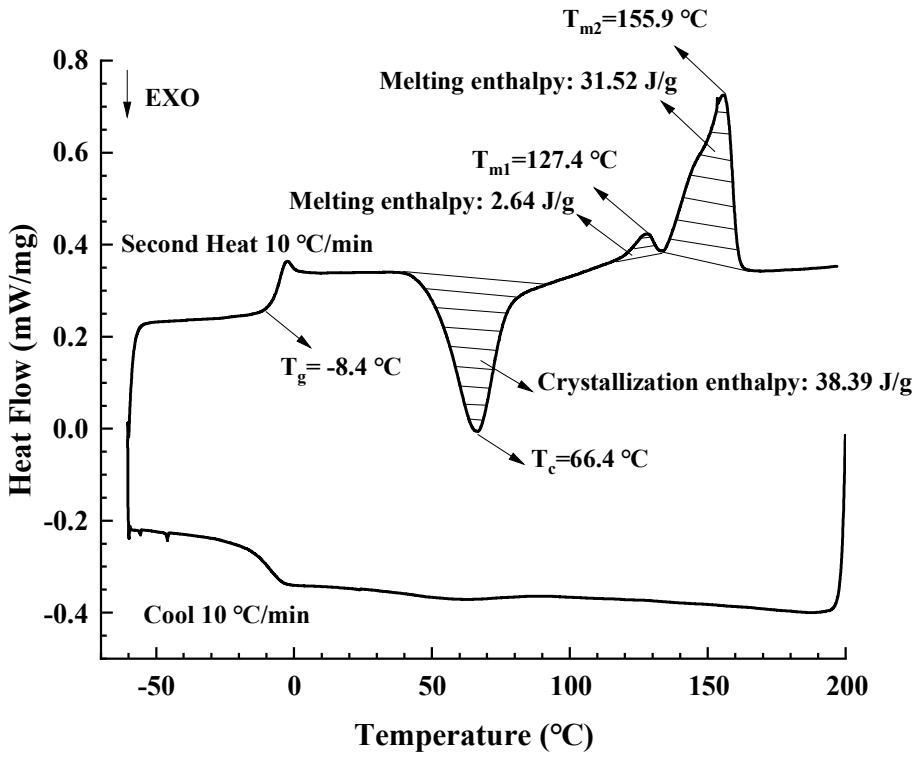

Figure 5.5. DSC thermogram of microbial PHBV.

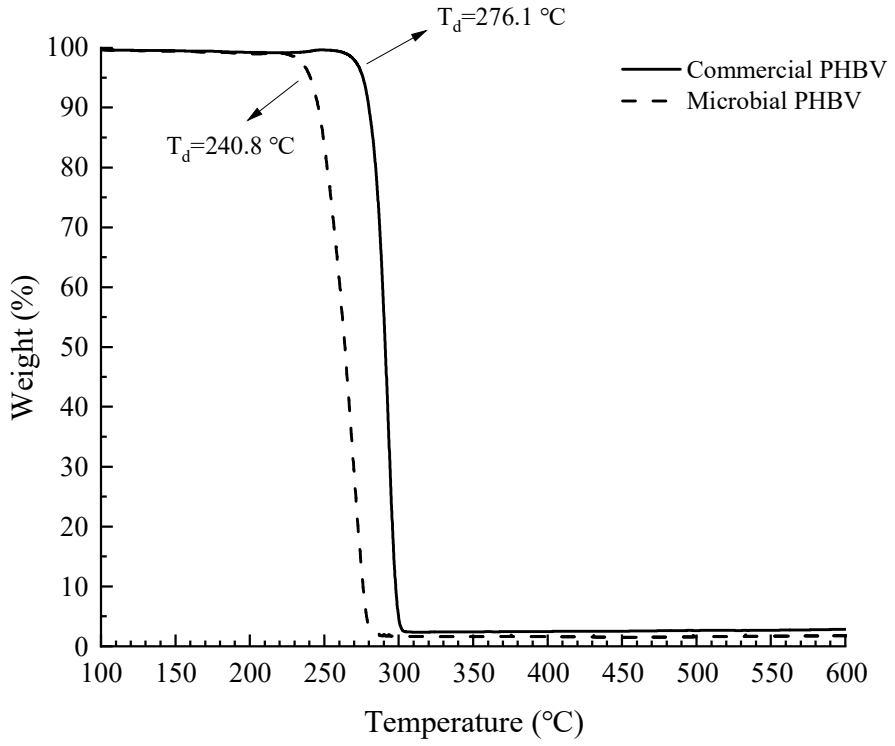

Figure 5.6. TGA thermograms of microbial and commercial PHBV.

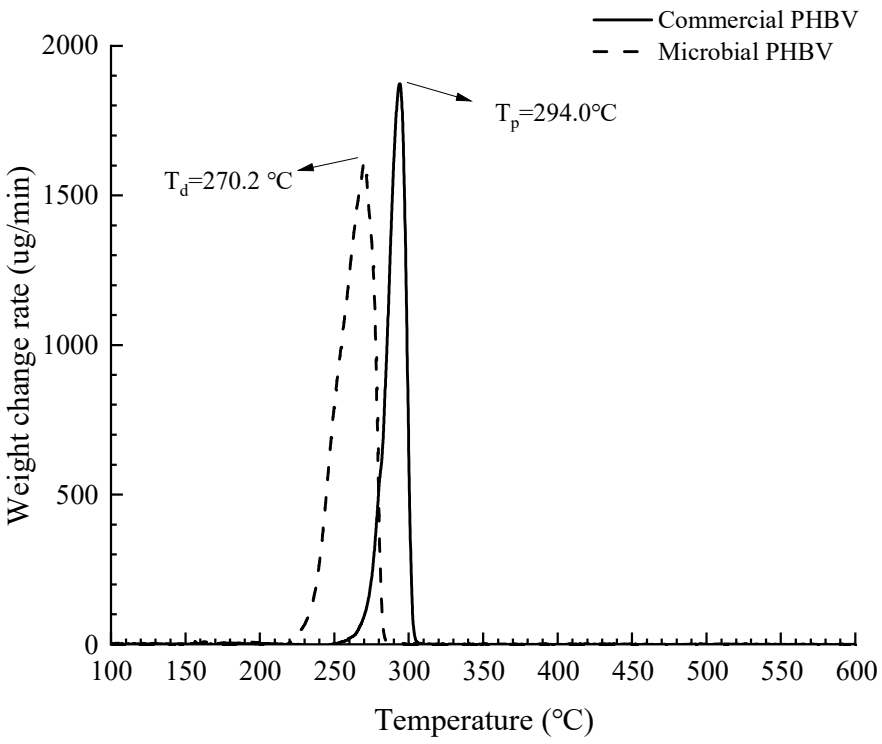

Figure 5.7. DTG thermograms of microbial and commercial PHBV.

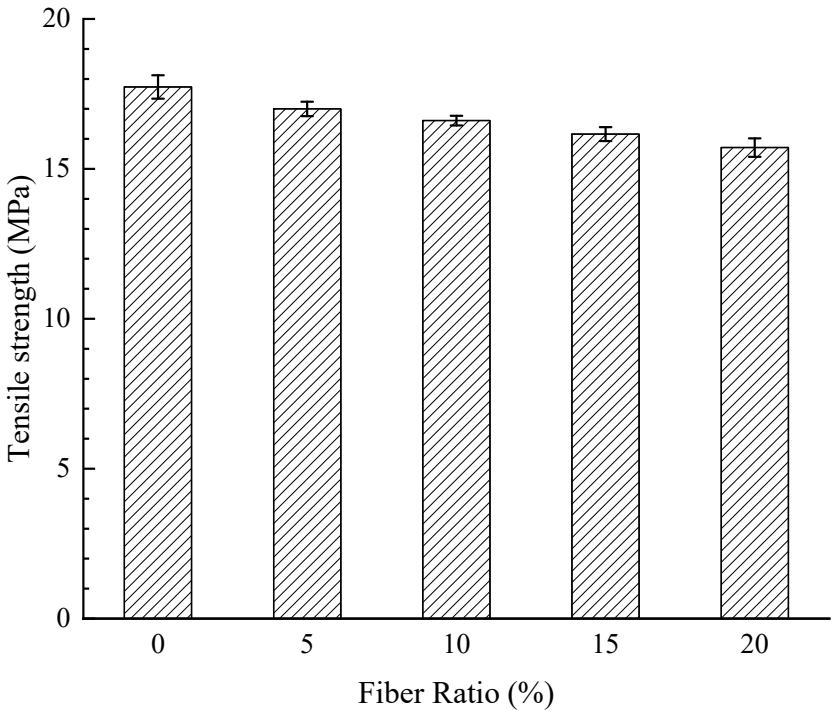

Figure 5.8. Tensile strength of microbial PHBV with different filament-dominating MBR sludge contents.

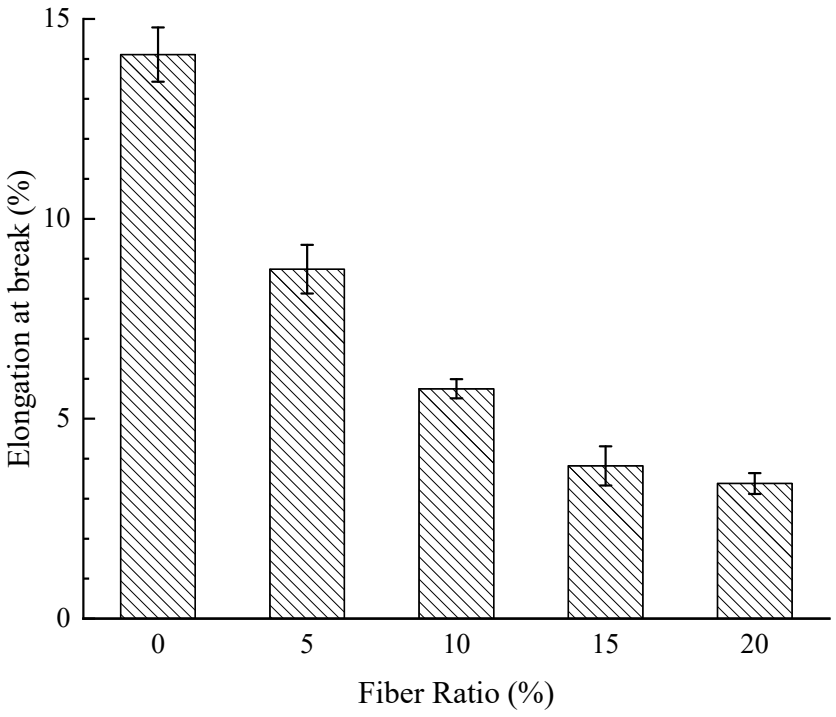

Figure 5.9. Elongation at break of microbial PHBV with different filament-dominating MBR sludge contents.

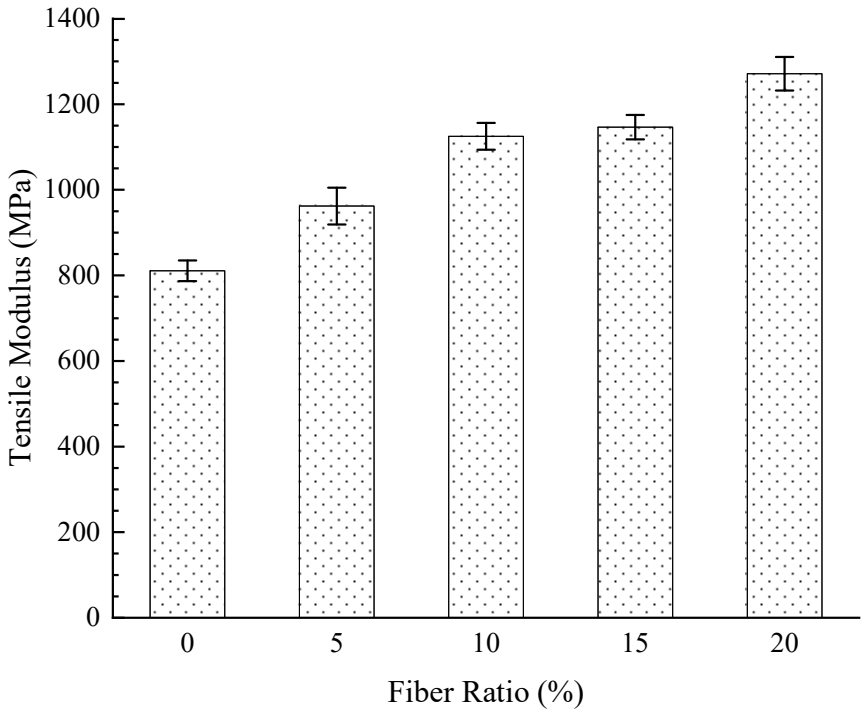

Figure 5.10. Tensile modulus of microbial PHBV with different filament-dominating MBR sludge contents.

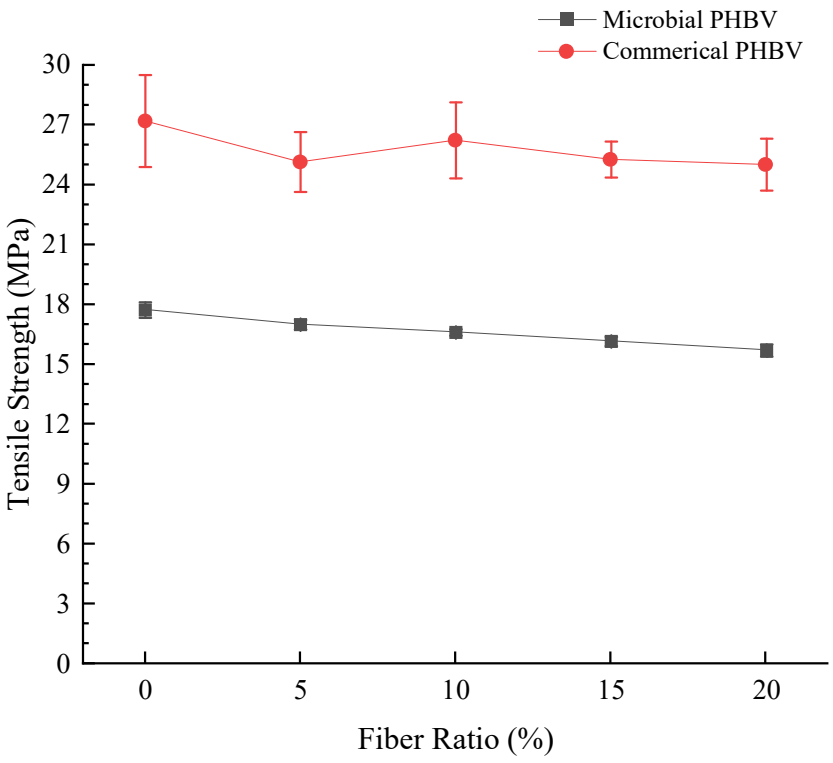

Figure 5.11. Comparison of tensile strength between microbial PHBV and commercial PHBV with different fiber ratio.

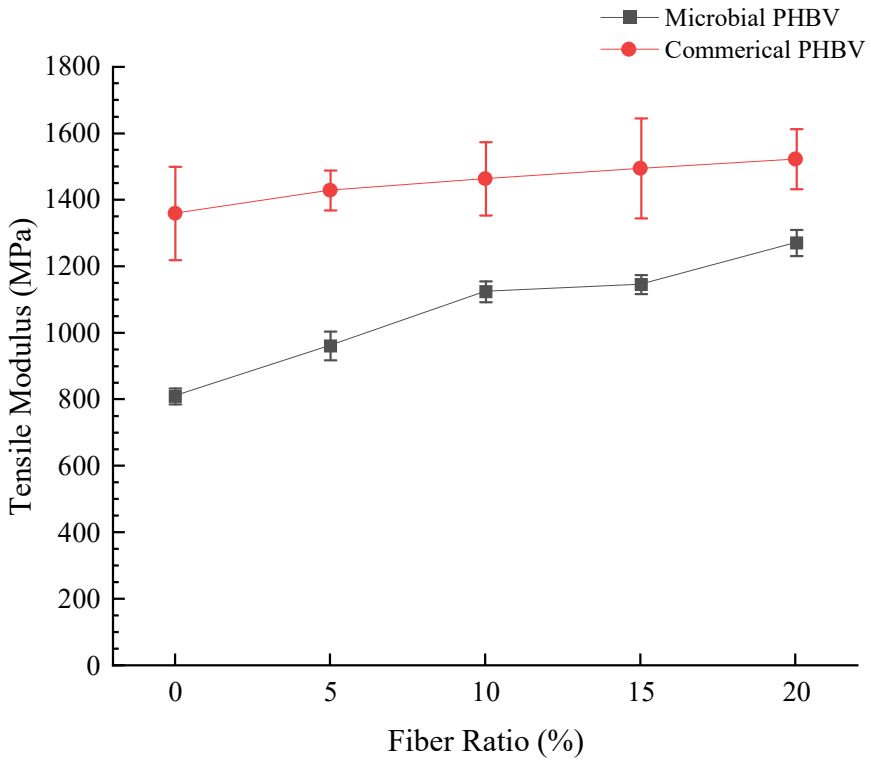

Figure 5.12. Comparison of tensile modulus between microbial PHBV and commercial PHBV with different fiber ratio.

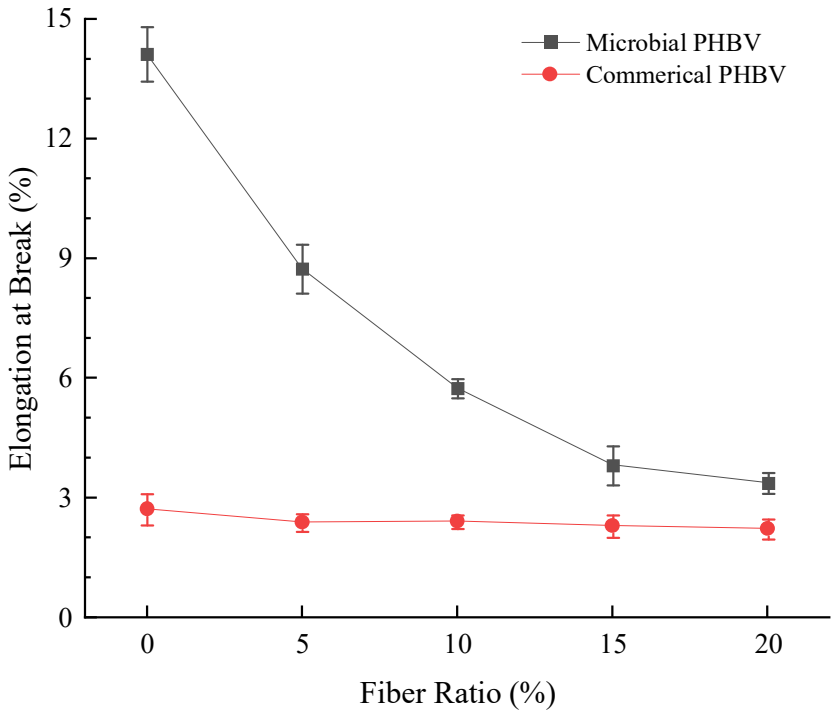

Figure 5.13. Comparison of elongation at break between microbial PHBV and commercial PHBV with different fiber ratio.

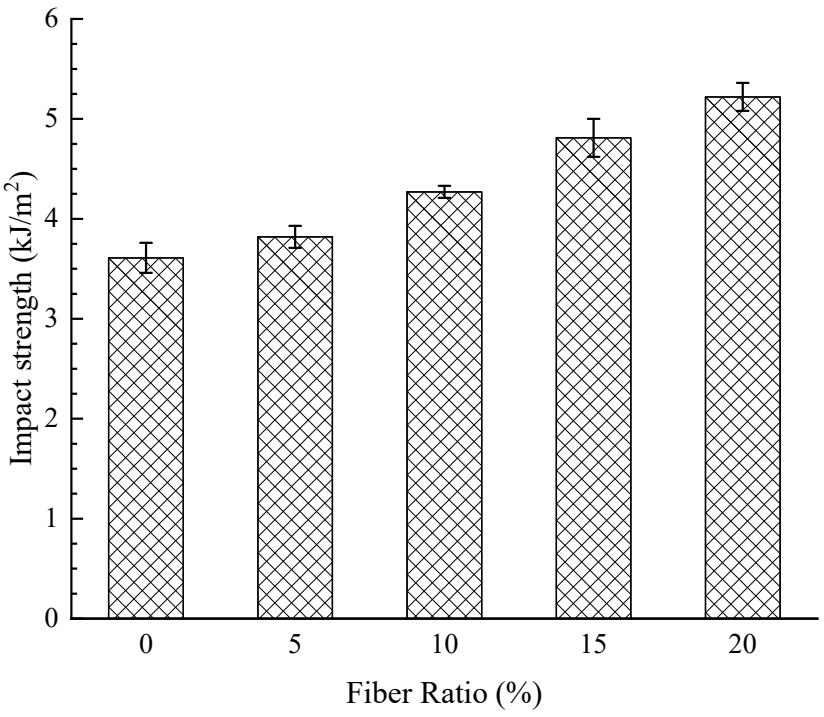

Figure 5.14. Impact strength of microbial PHBV with different filament-dominating MBR sludge contents.

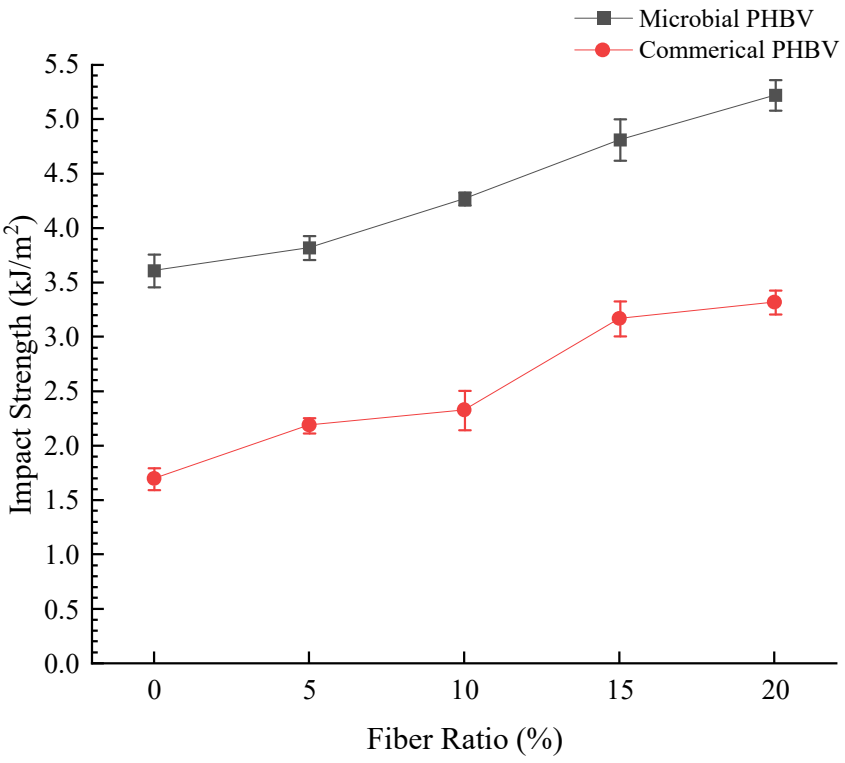

Figure 5.15. Comparison of impact strength between microbial PHBV and commercial PHBV with different fiber ratio.

Chapter 6

SUMMARY OF RESULTS

6.1 Filamentous Bacteria Reinforced Commercial PHBV

The reinforcing effects of filamentous bacteria on mechanical properties of commercial PHBV composites were evaluated. The composite specimens were fabricated using 3D printing after melt extrusion. The results of DSC and TGA of PHBV and filamentous bacteria suggested the processing temperature of these composite materials to be around 185 °C to minimize thermal degradation. We evaluated the tensile properties and notched impact strength of PHBV composites containing different amounts of filamentous bacteria. The tensile modulus and notched impact strength of the composites increased with higher fiber content. In contrast, the tensile strength and elongation at break of the composite decreased with increasing filamentous bacteria content. These results demonstrated that filamentous bacteria growing in wastewater treatment systems may be used as reinforcement agents for PHBV biocomposite materials.

6.2 Filamentous Bacteria Cultivation and Characterization

A membrane bioreactor was used to cultivate and enrich filamentous bacteria. Low dissolved oxygen, and nitrogen and phosphorus limited conditions in the MBR resulting in excessive proliferation of *Sphaerotilus* spp. with the sludge volume index as high as 703 mL/g. 16S rRNA gene sequencing identified that *Sphaerotilus* spp. were the dominant filamentous bacteria with a relative abundance 19% in the mixed

cultures. Optical microscopy and atomic force microscopy were used to study the morphology of filamentous bacteria. The aspect ratio (length to width ratio) of the filamentous bacteria was 346. The Young's modulus of *Sphaerotilus* spp. was determined using AFM-based nanoindentation. The measured Young's modulus of *Sphaerotilus* spp. was 91.4% higher than that of non-filamentous bacteria. The theoretical Young's moduli of filamentous bacteria-reinforced poly (3-hydroxybutyrate-co-3-hydroxyvalerate) were predicted using Halpin-Tsai and Tsai-Pagano equations. The predicted values closely matched the experimental values. This indicated that filamentous bacteria were randomly oriented and uniformly distributed in the matrix.

6.3 Filamentous Bacteria Reinforced Microbial PHBV

An all-natural composite material was fabricated using microbial PHBV as the matrix and filamentous bacteria as the reinforcement material. A sequencing batch reactor was operated to enrich for polyhydroxyalkanoates (PHA)-accumulating bacteria, and the production of PHBV by the enriched cultures was maximized by a fed-batch reactor. The highest PHA content of 59% dry cell weight was obtained with 68 % PHB and 32% PHV. PHBV extracted from the bacterial cells in the fed-batch reactor had a purity of 99.3%. A membrane bioreactor was used to cultivate filamentous bacteria-dominating cultures (19% relative abundance of *Sphaerotilus* spp.). Differential scanning calorimetry and thermogravimetric analysis of microbial PHBV suggested that the melt extrusion and 3D printing temperatures to be 170 °C and 180 °C, respectively, to minimize the thermal degradation of PHBV. Mechanical tests showed that the tensile modulus and notched impact strength of microbial PHBV improved by 57% and 45%, respectively, following the addition of 20% membrane

bioreactor sludge. These results demonstrated that an all-natural composite material may be fabricated from activated sludge using microbial PHBV as the matrix and filamentous bacteria as the reinforcement material.

Chapter 7

APPLICATION AND FUTURE WORK

7.1 Projected Production of Biocomposite Material

Biocomposite materials examined in this dissertation may be directly produced in wastewater treatment plants with appropriate design. The daily production of the composite materials can be projected based on results from this study. The following section describes the projected production of biocomposite materials from a model wastewater treatment plant. A SBR is designed to select and enrich PHA-accumulating bacteria. Its volume (V) is determined by the Equation 7.1:

$$V = HRT \times Q \tag{7.1}$$

where the influent flow rate (Q) is assumed to be 250,000 m^3/d, and HRT is 0.6 days. The SBR volume is calculated to be 150,000 m^3. The substrate consumption rate (U) in the SBR is calculated by the Equation 7.2:

$$\frac{1}{MCRT} = UY - k_d \tag{7.2}$$

where MCRT is 5 days, yield coefficie (Y) is 0.5 g biomass/g BOD (Metcalf & Eddy, 2013), and decay constant (k_d) is 0.02 d^{-1} (Friedrich & Takács, 2013). U is calculated as 0.44 d^{-1}. The mixed liquor suspended solids (MLSS) concentration of the SBR is calculated using the Equation 7.3:

$$U = \frac{Q\,(S_0 - S_e)}{V\,(MLSS)} \tag{7.3}$$

where biochemical oxygen demand (BOD) of the influent wastewater (S_o) is 200 mg/L based on the average value reported by New Castle County, Delaware (Delaware

Department of Natural Resources and Environmental Control, 2020), biochemical oxygen demand of the effluent wastewater (S_e) is 2 mg/L based on 99% BOD removal efficiency found in this study. The MLSS in the SBR was determined to be 750 mg/L using the Equation 7.3. The daily waste sludge production is determined by Equations 7.4 and 7.5:

$$\text{MCRT}=\frac{V \times \text{MLSS}}{(Q-Q_w)\,X_e+Q_w\,X_w} \tag{7.4}$$

$$\text{Sludge Production}=Q_w\,X_r \tag{7.5}$$

where Q_w is the sludge wasting rate, X_e is the biomass concentration in effluent (using 30 mg/L from chapter 5), and X_w is the biomass concentration of the waste sludge. The X_w is identical to the MLSS in the SBR in this study, due to sludge directly wasted from the reactor. The sludge production from the SBR is determined to be 15,625 kg/d, and all the sludge is used in PHA production in an FBR. The PHA production for the FBR will be 3,688 kg/d, applying 59% PHA content in bacterial cells and 40% overall extraction efficiency based on results of this study.

A MBR is designed to cultivate and enrich filamentous bacteria-dominant sludge. The calculation of the sludge production of the MBR follows the same process as that of the SBR. The volume of the MBR is determined to be 7,500 m^3 by assuming Q to be 15,000 m^3/d and HRT to be 0.5 days. The U value of the MBR is calculated to be 0.12 d^{-1}, using the same Y and k_d as the SBR, but a MCRT of 25 days. The MLSS of the MBR is determined to be 3,200 mg/L, using the same S_o as the SBR and 96% BOD removal rate. The daily waste sludge production is determined to be 960 kg/d, using 0 mg/L as X_e of the MBR. The X_w is identical to the MLSS in the MBR due to sludge directly wasted from the reactor.

The projected daily composite material production is 4,610 kg/d combining daily PHA and MBR sludge production. The total wastewater flow rate of this designed wastewater treatment plant is 265,000 m^3/d, which is 67% of the designed influent wastewater flow rate (397,468 m^3/d), and close to the average influent wastewater flow rate (260,058 m^3/d) of Wilmington wastewater treatment plant, Delaware (Delaware Department of Natural Resources and Environmental Control, 2020).

There are some major issues that need to be addressed before the proposed model wastewater treatment plant can achieve the overall goal of this research. First, the average BOD concentration of domestic wastewater is not high enough for intracellular PHA content reaching 59% as observed in this study. Second, producing microbial PHA requires no ammonium in FBR feedstocks, which is not possible in real wastewater. The above two issues could be solved by using external carbon sources with high concentration of fatty acids and low concentration of nitrogen, such as acidogenic digestate from food waste or waste activated sludge digestion. Additionally, PHA needs to be extracted before composite fabrication. This process requires large usage of organic solvents, which raises questions about the sustainability of the process. This issue may be addressed by developing a new method to directly use intracellular PHA without extraction.

7.2 Potential Application of Biocomposite Materials

The potential application of the biocomposite material fabricated in this study are proposed by comparing its mechanical properties with other petroleum-based plastic materials. The tensile strength and tensile modulus of 20% filamentous bacteria reinforced microbial PHBV is 15.7 MPa and 1.3 GPa, respectively. Current,

polypropylene (PP) and rigid polyvinyl chloride (PVC) were widely used in producing motor vehicle interior trim (Shinde and Patel, 2020). The tensile modulus and tensile strength of PP are 1.5 GPa and 38 MPa, respectively (Chodák & Blackburn, 2009; Keskin et al., 2017). The tensile modulus and tensile strength of rigid PVC are 3.4 GPa and 16.5 MPa, respectively (Wilkes et al., 2005; Zampino et al., 2021). The mechanical properties of the biocomposite material fabricated in this study are comparable to those of PP and rigid PVC. Therefore, the 20% filamentous bacteria reinforced microbial PHBV may be used as a substitute for PP and rigid PVC in fabricating interior trim of motor vehicles. Low-density polyethylene (LDPE) is a widely used packaging material (Dietrich et al., 2018; Selke & Hernandez, 2001). Its tensile modulus and tensile strength are 0.2 GPa and 10 MPa, respectively (Chodák & Blackburn, 2009). The 20% filamentous bacteria reinforced microbial PHBV has higher tensile modulus and tensile strength than those of LDPE, which suggests that this biocomposite material may be used as a substitute for LDPE in packaging materials.

7.3 Recommendations for Future Study

In this dissertation, filamentous bacteria were used as a reinforcement agent of PHAs to fabricate a novel biocomposite material. Although this composite material gets improved in tensile modulus and impact strength compared to neat PHAs, more studies are needed to help facilitate the application of this composite material. The maximum fiber content of the composite material in this study is 20% for both commercial and microbial PHAs due to higher fiber contents resulting in a failure in extrusion process. Other fabrication methods, such as injection molding and compression molding, can be investigated to achieve a higher fiber content and may

result in better overall mechanical properties. The *Sphaerotilus* spp. is enriched in the MBR and used as reinforcement agent in this study. Study in the future could cultivate and enrich other filamentous bacteria, such as type 021N, *Thiothrix* spp., *Beggiatoa* spp. and *Microthrix parvicella*, as reinforcement agent of PHAs. Different combinations of PHAs and filamentous bacteria may generate new filamentous bacteria reinforced PHAs with superior mechanical properties. The microbial PHBV was produced using pure chemical-based feed solution in this study, which leads to a high cost of PHA production. The next step may be using waste by-product as feed solution, such as acidogenic digestate from food waste or activated sludge, to further decrease the production cost of PHA. This will also make the PHAs production more environmentally friendly and sustainable. Directly using intracellular PHA without extraction is another study that may be investigated in the future. Previous study has reported that *Sphaerotilus natans*, type 021N, *Beggiatoa* spp. and *Microthrix parvicella* are able to accumulate PHA within their cells (Jenkins et al., 2003). Therefore, fabricating biocomposite materials using filamentous bacteria and their intracellular PHA may avoid the PHA extraction, thus eliminating the organic solvents usage.

REFERENCES

Abbasi, M., Pokhrel, D., Coats, E. R., Guho, N. M., & McDonald, A. G. (2022). Effect of 3-Hydroxyvalerate Content on Thermal, Mechanical, and Rheological Properties of Poly(3-hydroxybutyrate-co-3-hydroxyvalerate) Biopolymers Produced from Fermented Dairy Manure. *Polymers*, *14*(19). https://doi.org/10.3390/polym14194140

Abdul Khalil, H. P. S., Bhat, A. H., & Ireana Yusra, A. F. (2012). Green composites from sustainable cellulose nanofibrils: A review. In *Carbohydrate Polymers* (Vol. 87, Issue 2, pp. 963–979). https://doi.org/10.1016/j.carbpol.2011.08.078

Abu Aldam, S., Dey, M., Javaid, S., Ji, Y., & Gupta, S. (2020). On the Synthesis and Characterization of Polylactic Acid, Polyhydroxyalkanoate, Cellulose Acetate, and Their Engineered Blends by Solvent Casting. *Journal of Materials Engineering and Performance*, *29*(9), 5542–5556. https://doi.org/10.1007/s11665-020-04594-3

Affdl, J. C. H., & Kardos, J. L. (1976). The Halpin-Tsai equations: A review. In *Polymer Engineering & Science* (Vol. 16, Issue 5, pp. 344–352). https://doi.org/10.1002/pen.760160512

Ajmal, A. W., Masood, F., & Yasin, T. (2018). Influence of sepiolite on thermal, mechanical and biodegradation properties of poly-3-hydroxybutyrate-co-3-hydroxyvalerate nanocomposites. *Applied Clay Science*, *156*, 11–19. https://doi.org/10.1016/j.clay.2018.01.010

Akiyama, M., Taima, Y., & Doi, Y. (1992). Production of poly(3-hydroxyalkanoates) by a bacterium of the genus Alcaligenes utilizing long-chain fatty acids. *Applied Microbiology and Biotechnology*, *37*(6), 698–701. https://doi.org/10.1007/BF00174830

Albuquerque, M. G. E., Eiroa, M., Torres, C., Nunes, B. R., & Reis, M. A. M. (2007). Strategies for the development of a side stream process for polyhydroxyalkanoate (PHA) production from sugar cane molasses. *Journal of Biotechnology*, *130*(4), 411–421. https://doi.org/10.1016/j.jbiotec.2007.05.011

Albuquerque, M. G. E., Martino, V., Pollet, E., Avérous, L., & Reis, M. A. M. (2011). Mixed culture polyhydroxyalkanoate (PHA) production from volatile fatty acid (VFA)-rich streams: Effect of substrate composition and feeding regime on PHA productivity, composition and properties. *Journal of Biotechnology*, *151*(1), 66–76. https://doi.org/10.1016/j.jbiotec.2010.10.070

Albuquerque, M. G. E., Torres, C. A. V., & Reis, M. A. M. (2010). Polyhydroxyalkanoate (PHA) production by a mixed microbial culture using sugar molasses: Effect of the influent substrate concentration on culture selection. *Water Research*, *44*(11), 3419–3433. https://doi.org/10.1016/j.watres.2010.03.021

Anjum, A., Zuber, M., Zia, K. M., Noreen, A., Anjum, M. N., & Tabasum, S. (2016). Microbial production of polyhydroxyalkanoates (PHAs) and its copolymers: A review of recent advancements. In *International Journal of Biological Macromolecules* (Vol. 89, pp. 161–174). https://doi.org/10.1016/j.ijbiomac.2016.04.069

Ansari, S., & Fatma, T. (2018). Characterization of Nostoc muscorum NCCU-442 Derived Poly-3- hydroxybutyrate (PHB) and Polyethylene Glycol (PEG) Blends. *The Natural Products Journal*, *10*(3), 200–207. https://doi.org/10.2174/2210315508666180810145127

APHA. (2005). Standard Methods for the Examination of Water and Wastewater. *Standard Methods*. https://doi.org/ISBN 9780875532356

Arthurson, V. (2008). Proper sanitization of sewage sludge: A critical issue for a sustainable society. In *Applied and Environmental Microbiology* (Vol. 74, Issue 17, pp. 5267–5275). https://doi.org/10.1128/AEM.00438-08

Ashby, R. D., Foglia, T. A., Solaiman, D. K. Y., Liu, C. K., Nuñez, A., & Eggink, G. (2000). Viscoelastic properties of linseed oil-based medium chain length poly(hydroxyalkanoate) films: Effects of epoxidation and curing. *International Journal of Biological Macromolecules*, *27*(5), 355–361. https://doi.org/10.1016/S0141-8130(00)00140-9

Asrar, J., Valentin, H. E., Berger, P. A., Tran, M., Padgette, S. R., & Garbow, J. R. (2002). Biosynthesis and properties of poly(3-hydroxybutyrate-co-3-hydroxyhexanoate) polymers. *Biomacromolecules*, *3*(5), 1006–1012. https://doi.org/10.1021/bm025543a

Bakken, L. R., & Olsen, R. A. (1983). Buoyant densities and dry-matter contents of microorganisms: Conversion of a measured biovolume into biomass. In *Applied and Environmental Microbiology* (Vol. 45, Issue 4). https://doi.org/10.1128/aem.45.4.1188-1195.1983

Barkoula, N. M., Garkhail, S. K., & Peijs, T. (2010). Biodegradable composites based on flax/polyhydroxybutyrate and its copolymer with hydroxyvalerate. *Industrial Crops and Products*, *31*(1), 34–42. https://doi.org/10.1016/j.indcrop.2009.08.005

Basko, M., Duda, A., Kazmierski, S., & Kubisa, P. (2013). Cationic copolymerization of racemic-β-butyrolactone with L,L-lactide: One-pot synthesis of block copolymers. *Journal of Polymer Science, Part A: Polymer Chemistry*, *51*(22), 4873–4884. https://doi.org/10.1002/pola.26916

Batista, N. L., Olivier, P., Bernhart, G., Rezende, M. C., & Botelho, E. C. (2016). Correlation between degree of crystallinity, morphology and mechanical properties of PPS/carbon fiber laminates. *Materials Research*, *19*(1), 195–201. https://doi.org/10.1590/1980-5373-MR-2015-0453

Bengtsson, S., Werker, A., Christensson, M., & Welander, T. (2008). Production of polyhydroxyalkanoates by activated sludge treating a paper mill wastewater. *Bioresource Technology*, *99*(3), 509–516. https://doi.org/10.1016/j.biortech.2007.01.020

Berthet, M. A., Gontard, N., & Angellier-Coussy, H. (2015). Impact of fibre moisture content on the structure/mechanical properties relationships of PHBV/wheat straw fibres biocomposites. *Composites Science and Technology*, *117*, 386–391. https://doi.org/10.1016/j.compscitech.2015.07.015

Bharathiraja, B., Yogendran, D., Ranjith Kumar, R., Chakravarthy, M., & Palani, S. (2014). Biofuels from sewage sludge- A review. *International Journal of ChemTech Research*, *6*(9), 4417–4427.

Bhardwaj, R., Mohanty, A. K., Drzal, L. T., Pourboghrat, F., & Misra, M. (2006). Renewable resource-based green composites from recycled cellulose fiber and poly(3-hydroxybutyrate-co-3-hydroxyvalerate) bioplastic. *Biomacromolecules*, *7*(6), 2044–2051. https://doi.org/10.1021/bm050897y

Bhubalan, K., Lee, W. H., Loo, C. Y., Yamamoto, T., Tsuge, T., Doi, Y., & Sudesh, K. (2008). Controlled biosynthesis and characterization of poly(3-hydroxybutyrate-co-3-hydroxyvalerate-co-3-hydroxyhexanoate) from mixtures of palm kernel oil and 3HV-precursors. *Polymer Degradation and Stability*, *93*(1), 17–23. https://doi.org/10.1016/j.polymdegradstab.2007.11.004

Bhubalan, K., Rathi, D. N., Abe, H., Iwata, T., & Sudesh, K. (2010). Improved synthesis of P(3HB-co-3HV-co-3HHx) terpolymers by mutant Cupriavidus necator using the PHA synthase gene of Chromobacterium sp. USM2 with high affinity towards 3HV. *Polymer Degradation and Stability*, *95*(8), 1436–1442. https://doi.org/10.1016/j.polymdegradstab.2009.12.018

Bin Bakri, M. K., Jayamani, E., & Kakar, A. (2018). Potential in the development of borneo acacia wood reinforced polyhydroxyalkanoates bio-composites. *Key Engineering Materials*, *779 KEM*, 19–24. https://doi.org/10.4028/www.scientific.net/KEM.779.19

Bledzki, A. K., & Jaszkiewicz, A. (2010). Mechanical performance of biocomposites based on PLA and PHBV reinforced with natural fibres - A comparative study to PP. *Composites Science and Technology*, *70*(12), 1687–1696. https://doi.org/10.1016/j.compscitech.2010.06.005

Bolyen, E., Rideout, J. R., Dillon, M. R., Bokulich, N. A., Abnet, C. C., Al-Ghalith, G. A., Alexander, H., Alm, E. J., Arumugam, M., Asnicar, F., Bai, Y., Bisanz, J. E., Bittinger, K., Brejnrod, A., Brislawn, C. J., Brown, C. T., Callahan, B. J., Caraballo-Rodríguez, A. M., Chase, J., … Caporaso, J. G. (2019). Reproducible, interactive, scalable and extensible microbiome data science using QIIME 2. In *Nature Biotechnology* (Vol. 37, Issue 8, pp. 852–857). https://doi.org/10.1038/s41587-019-0209-9

Bonilla, M. R., Stokes, J. R., Gidley, M. J., & Yakubov, G. E. (2015). Interpreting atomic force microscopy nanoindentation of hierarchical biological materials using multi-regime analysis. *Soft Matter*, *11*(7), 1281–1292. https://doi.org/10.1039/c4sm02440k

Braunegg, G., Sonnleitner, B., & Lafferty, R. M. (1978). A rapid gas chromatographic method for the determination of poly-β-hydroxybutyric acid in microbial biomass. *European Journal of Applied Microbiology and Biotechnology*, *6*(1), 29–37. https://doi.org/10.1007/BF00500854

Budzianowski, W. M. (2016). A review of potential innovations for production, conditioning and utilization of biogas with multiple-criteria assessment. In *Renewable and Sustainable Energy Reviews* (Vol. 54, pp. 1148–1171). https://doi.org/10.1016/j.rser.2015.10.054

Burniol-Figols, A., Varrone, C., Le, S. B., Daugaard, A. E., Skiadas, I. V., & Gavala, H. N. (2018). Combined polyhydroxyalkanoates (PHA) and 1,3-propanediol production from crude glycerol: Selective conversion of volatile fatty acids into PHA by mixed microbial consortia. *Water Research*, *136*, 180–191. https://doi.org/10.1016/j.watres.2018.02.029

Burns, K. L., Oldham, C. D., & May, S. W. (2009). Bacterial production of poly(3-hydroxybutyrate). *Journal of Chemical Education*, *86*(5), 603–605. https://doi.org/10.1021/ed086p603

Burzic, I., Pretschuh, C., Kaineder, D., Eder, G., Smilek, J., Másilko, J., & Kateryna, W. (2019). Impact modification of PLA using biobased biodegradable PHA biopolymers. *European Polymer Journal*, *114*, 32–38. https://doi.org/10.1016/j.eurpolymj.2019.01.060

Campbell, H. W. (2000). Sludge management - Future issues and trends. *Water Science and Technology*, *41*(8), 1–8. https://doi.org/10.2166/wst.2000.0135

Cantero, G., Arbelaiz, A., Llano-Ponte, R., & Mondragon, I. (2003). Effects of fibre treatment on wettability and mechanical behaviour of flax/polypropylene composites. *Composites Science and Technology*, *63*(9), 1247–1254. https://doi.org/10.1016/S0266-3538(03)00094-0

Cao, Q., Zhang, J., Liu, H., Wu, Q., Chen, J., & Chen, G. Q. (2014). The mechanism of anti-osteoporosis effects of 3-hydroxybutyrate and derivatives under simulated microgravity. *Biomaterials*, *35*(28), 8273–8283. https://doi.org/10.1016/j.biomaterials.2014.06.020

Carrasco, F., Dionisi, D., Martinelli, A., & Majone, M. (2006). Thermal stability of polyhydroxyalkanoates. *Journal of Applied Polymer Science*, *100*(3), 2111–2121. https://doi.org/10.1002/app.23586

Castilho, L. R., Mitchell, D. A., & Freire, D. M. G. (2009). Production of polyhydroxyalkanoates (PHAs) from waste materials and by-products by submerged and solid-state fermentation. *Bioresource Technology*, *100*(23), 5996–6009. https://doi.org/10.1016/j.biortech.2009.03.088

Cenens, C., Smets, I. Y., & Van Impe, J. F. (2000). Modeling the competition between floc-forming and filamentous bacteria in activated sludge waste water treatment systems - II. A prototype mathematical model based on kinetic selection and filamentous backbone theory. *Water Research*, *34*(9), 2535–2541. https://doi.org/10.1016/S0043-1354(99)00422-4

Chan, C. H., KummerÏwe, C., & Kammer, H. W. (2004). Crystallization and melting behavior of poly(3-hydroxybutyrate)-based blends. *Macromolecular Chemistry and Physics*, *205*(5), 664–675. https://doi.org/10.1002/macp.200300062

Chan, C. M., Vandi, L. J., Pratt, S., Halley, P., Ma, Y., Chen, G. Q., Richardson, D., Werker, A., & Laycock, B. (2019). Understanding the effect of copolymer content on the processability and mechanical properties of polyhydroxyalkanoate (PHA)/wood composites. *Composites Part A: Applied Science and Manufacturing*, *124*. https://doi.org/10.1016/j.compositesa.2019.05.005

Chaturvedi, K., Ganguly, K., Kulkarni, A. R., Rudzinski, W. E., Krauss, L., Nadagouda, M. N., & Aminabhavi, T. M. (2015). Oral insulin delivery using deoxycholic acid conjugated PEGylated polyhydroxybutyrate co-polymeric nanoparticles. *Nanomedicine*, *10*(10), 1569–1583. https://doi.org/10.2217/nnm.15.36

Chen, G.-Q. (2010). *Plastics Completely Synthesized by Bacteria: Polyhydroxyalkanoates* (pp. 17–37). https://doi.org/10.1007/978-3-642-03287-5_2

Chen, G. Q., Hajnal, I., Wu, H., Lv, L., & Ye, J. (2015a). Engineering Biosynthesis Mechanisms for Diversifying Polyhydroxyalkanoates. In *Trends in Biotechnology* (Vol. 33, Issue 10, pp. 565–574). https://doi.org/10.1016/j.tibtech.2015.07.007

Chen, L. J., & Wang, M. (2002). Production and evaluation of biodegradable composites based on PHB-PHV copolymer. *Biomaterials*, *23*(13), 2631–2639. https://doi.org/10.1016/S0142-9612(01)00394-5

Chen, Z., Huang, L., Wen, Q., & Guo, Z. (2015). Efficient polyhydroxyalkanoate (PHA) accumulation by a new continuous feeding mode in three-stage mixed microbial culture (MMC) PHA production process. *Journal of Biotechnology*, *209*, 68–75. https://doi.org/10.1016/j.jbiotec.2015.06.382

Cheung, H. yan, Ho, M. po, Lau, K. tak, Cardona, F., & Hui, D. (2009). Natural fibre-reinforced composites for bioengineering and environmental engineering applications. *Composites Part B: Engineering*, *40*(7), 655–663. https://doi.org/10.1016/j.compositesb.2009.04.014

Chodák, I., & Blackburn, R. S. (2009). Sustainable synthetic fibres: The case of poly(hydroxyalkanoates) (PHA) and other fibres. In *Sustainable Textiles: Life Cycle and Environmental Impact* (pp. 88–112). https://doi.org/10.1533/9781845696948.1.88

Christensen, M., Jablonski, P., Altermark, B., Irgum, K., & Hansen, H. (2021). High natural PHA production from acetate in Cobetia sp. MC34 and Cobetia marina DSM 4741T and in silico analyses of the genus specific PhaC2 polymerase variant. *Microbial Cell Factories*, *20*(1). https://doi.org/10.1186/s12934-021-01713-0

Chu, L., & He, W. (2021). Toxic metals in soil due to the land application of sewage sludge in China: Spatiotemporal variations and influencing factors. *Science of the Total Environment*, *757*. https://doi.org/10.1016/j.scitotenv.2020.143813

Colombo, B., Pereira, J., Martins, M., Torres-Acosta, M. A., Dias, A. C. R. V., Lemos, P. C., Ventura, S. P. M., Eisele, G., Alekseeva, A., Adani, F., & Serafim, L. S. (2020). Recovering PHA from mixed microbial biomass: Using non-ionic surfactants as a pretreatment step. *Separation and Purification Technology*, *253*. https://doi.org/10.1016/j.seppur.2020.117521

Colombo, B., Sciarria, T. P., Reis, M., Scaglia, B., & Adani, F. (2016). Polyhydroxyalkanoates (PHAs) production from fermented cheese whey by using a mixed microbial culture. *Bioresource Technology*, *218*, 692–699. https://doi.org/10.1016/j.biortech.2016.07.024

Colombo, B., Villegas Calvo, M., Pepè Sciarria, T., Scaglia, B., Savio Kizito, S., D'Imporzano, G., & Adani, F. (2019). Biohydrogen and polyhydroxyalkanoates (PHA) as products of a two-steps bioprocess from deproteinized dairy wastes. *Waste Management*, *95*, 22–31. https://doi.org/10.1016/j.wasman.2019.05.052

Cornelissen, R., Bøggild, A., Thiruvallur Eachambadi, R., Koning, R. I., Kremer, A., Hidalgo-Martinez, S., Zetsche, E. M., Damgaard, L. R., Bonné, R., Drijkoningen, J., Geelhoed, J. S., Boesen, T., Boschker, H. T. S., Valcke, R., Nielsen, L. P., D'Haen, J., Manca, J. V., & Meysman, F. J. R. (2018). The Cell Envelope Structure of Cable Bacteria. *Frontiers in Microbiology*, *9*. https://doi.org/10.3389/fmicb.2018.03044

Couttenier, E., Bachellier-Bassi, S., d'Enfert, C., & Villard, C. (2022). Bending stiffness of Candida albicans hyphae as a proxy of cell wall properties. *Lab on a Chip*, *22*(20), 3898–3909. https://doi.org/10.1039/d2lc00219a

de Graaff, D. R., van Loosdrecht, M. C. M., & Pronk, M. (2020). Stable granulation of seawater-adapted aerobic granular sludge with filamentous Thiothrix bacteria. *Water Research*, *175*. https://doi.org/10.1016/j.watres.2020.115683

Debuissy, T., Pollet, E., & Avérous, L. (2017). Synthesis and characterization of block poly(ester-ether-urethane)s from bacterial poly(3-hydroxybutyrate) oligomers. *Journal of Polymer Science, Part A: Polymer Chemistry*, *55*(11), 1949–1961. https://doi.org/10.1002/pola.28567

Defoirdt, T., Boon, N., Sorgeloos, P., Verstraete, W., & Bossier, P. (2009). Short-chain fatty acids and poly-β-hydroxyalkanoates: (New) Biocontrol agents for a sustainable animal production. In *Biotechnology Advances* (Vol. 27, Issue 6, pp. 680–685). https://doi.org/10.1016/j.biotechadv.2009.04.026

Defoirdt, T., Halet, D., Vervaeren, H., Boon, N., Van De Wiele, T., Sorgeloos, P., Bossier, P., & Verstraete, W. (2007). The bacterial storage compound poly-β-hydroxybutyrate protects Artemia franciscana from pathogenic Vibrio campbellii. *Environmental Microbiology*, *9*(2), 445–452. https://doi.org/10.1111/j.1462-2920.2006.01161.x

Dehouche, N., Idres, C., Kaci, M., Zembouai, I., & Bruzaud, S. (2020). Effects of various surface treatments on Aloe Vera fibers used as reinforcement in poly(3-hydroxybutyrate-co-3-hydroxyhexanoate) (PHBHHx) biocomposites. *Polymer Degradation and Stability*, *175*. https://doi.org/10.1016/j.polymdegradstab.2020.109131

Delaware Department of Natural Resources and Environmental Control. (2020). *Delaware Statewide Assessments of Wastewater Facilities and Current Status and Future Needs 2020-2025*. https://documents.dnrec.delaware.gov/fab/Documents/DE-WWTP-Needs-Assessment-4-10-20.pdf

Demirbas, A., Edris, G., & Alalayah, W. M. (2017). Sludge production from municipal wastewater treatment in sewage treatment plant. *Energy Sources, Part A: Recovery, Utilization and Environmental Effects*, *39*(10), 999–1006. https://doi.org/10.1080/15567036.2017.1283551

Derjaguin, B. V., Muller, V. M., & Toporov, Y. P. (1975). Effect of contact deformations on the adhesion of particles. *Journal of Colloid And Interface Science*, *53*(2), 314–326. https://doi.org/10.1016/0021-9797(75)90018-1

Di Lorenzo, M. L., Gazzano, M., & Righetti, M. C. (2012). The role of the rigid amorphous fraction on cold crystallization of poly(3-hydroxybutyrate). *Macromolecules*, *45*(14), 5684–5691. https://doi.org/10.1021/ma3010907

Dietrich, K., Dumont, M. J., Del Rio, L. F., & Orsat, V. (2017). Producing PHAs in the bioeconomy — Towards a sustainable bioplastic. *Sustainable Production and Consumption*, *9*, 58–70. https://doi.org/10.1016/j.spc.2016.09.001

Dietrich, M. L., Sarmoria, C., Brandolin, A., & Asteasuain, M. (2018). High-Pressure Polymerization of Ethylene in Tubular Reactors: Prediction of the Bivariate Distributions of Molecular Weight-Branches with a Rigorous Reactor Model. In *Computer Aided Chemical Engineering* (Vol. 44, pp. 1447–1452). https://doi.org/10.1016/B978-0-444-64241-7.50236-6

Ding, Y., Xu, G. K., & Wang, G. F. (2017). On the determination of elastic moduli of cells by AFM based indentation. *Scientific Reports*, *7*. https://doi.org/10.1038/srep45575

Doan, T. T. L., Brodowsky, H., & Mäder, E. (2012). Jute fibre/epoxy composites: Surface properties and interfacial adhesion. *Composites Science and Technology*, *72*(10), 1160–1166. https://doi.org/10.1016/j.compscitech.2012.03.025

Dobrogojski, J., Spychalski, M., Luciński, R., & Borek, S. (2018). Transgenic plants as a source of polyhydroxyalkanoates. In *Acta Physiologiae Plantarum* (Vol. 40, Issue 9). https://doi.org/10.1007/s11738-018-2742-4

Domiński, A., Konieczny, T., Zięba, M., Klim, M., & Kurcok, P. (2019). Anionic polymerization of β-butyrolactone initiated with sodium phenoxides. The effect of the initiator basicity/nucleophilicity on the ROP mechanism. *Polymers*, *11*(7). https://doi.org/10.3390/polym11071221

Dong, J., Liu, J., Li, X., Liang, Q., & Xu, X. (2020). Relationship between the Young's Modulus and the Crystallinity of Cross-Linked Poly(ε-caprolactone) as an Immobilization Membrane for Cancer Radiotherapy. *Global Challenges*, *4*(8), 2000008. https://doi.org/10.1002/gch2.202000008

Du, G. C., Chen, J., Yu, J., & Lun, S. (2001). Feeding strategy of propionic acid for production of poly(3-hydroxybutyrate-co-3-hydroxyvalerate) with Ralstonia eutropha. *Biochemical Engineering Journal*, *8*(2), 103–110. https://doi.org/10.1016/S1369-703X(01)00091-2

Ecker, J. V., Burzic, I., Haider, A., Hild, S., & Rennhofer, H. (2019). "Improving the impact strength of PLA and its blends with PHA in fused layer modelling ." *Polymer Testing*, *78*. https://doi.org/10.1016/j.polymertesting.2019.105929

Elbourne, A., Chapman, J., Gelmi, A., Cozzolino, D., Crawford, R. J., & Truong, V. K. (2019). Bacterial-nanostructure interactions: The role of cell elasticity and adhesion forces. *Journal of Colloid and Interface Science*, *546*, 192–210. https://doi.org/10.1016/j.jcis.2019.03.050

Emerson, D., & Ghiorse, W. C. (1993a). Role of disulfide bonds in maintaining the structural integrity of the sheath of Leptothrix discophora SP-6. *Journal of Bacteriology*, *175*(24), 7819–7827. https://doi.org/10.1128/jb.175.24.7819-7827.1993

Emerson, D., & Ghiorse, W. C. (1993b). Ultrastructure and chemical composition of the sheath of Leptothrix discophora SP-6. *Journal of Bacteriology*, *175*(24), 7808–7818. https://doi.org/10.1128/jb.175.24.7808-7818.1993

Erhard, G. (2006). Designing with plastics. In *Designing with Plastics* (Vol. 117, Issue 12, pp. 1–517). https://doi.org/10.3139/9783446412828

Espinach, F. X., Julián, F., Alcalá, M., Tresserras, J., & Mutjé, P. (2014). High stiffness performance alpha-grass pulp fiber reinforced thermoplastic starch-based fully biodegradable composites. In *BioResources* (Vol. 9, Issue 1, pp. 738–755). https://doi.org/10.15376/biores.9.1.738-755

Facca, A. G., Kortschot, M. T., & Yan, N. (2006). Predicting the elastic modulus of natural fibre reinforced thermoplastics. *Composites Part A: Applied Science and Manufacturing*, *37*(10), 1660–1671. https://doi.org/10.1016/j.compositesa.2005.10.006

Fang, F., Xu, R. Z., Huang, Y. Q., Wang, S. N., Zhang, L. L., Dong, J. Y., Xie, W. M., Chen, X., & Cao, J. S. (2019). Production of polyhydroxyalkanoates and enrichment of associated microbes in bioreactors fed with rice winery wastewater at various organic loading rates. *Bioresource Technology*, *292*. https://doi.org/10.1016/j.biortech.2019.121978

Fang, J., Tschan, M. J. L., Roisnel, T., Trivelli, X., Gauvin, R. M., Thomas, C. M., & Maron, L. (2013). Yttrium catalysts for syndioselective β-butyrolactone polymerization: On the origin of ligand-induced stereoselectivity. *Polymer Chemistry*, *4*(2), 360–367. https://doi.org/10.1039/c2py20590d

Fericelli, P. D. (2011). Comparison of sludge treatment by gasification vs. incineration. *Ninth LACCEI Latin American and Caribbean Conference (LACCEI'2011)*, 1–10. http://www.laccei.org/LACCEI2011-Medellin/StudentPapers/PM022_Fericelli_SP.pdf

Ferreira, R., Amado, R., Padrão, J., Ferreira, V., Dias, N. M., Melo, L. D. R., Santos, S. B., & Nicolau, A. (2021). The first sequenced Sphaerotilus natans bacteriophage-characterization and potential to control its filamentous bacterium host. *FEMS Microbiology Ecology*, *97*(4). https://doi.org/10.1093/femsec/fiab029

Fradinho, J. C., Oehmen, A., & Reis, M. A. M. (2014). Photosynthetic mixed culture polyhydroxyalkanoate (PHA) production from individual and mixed volatile fatty acids (VFAs): Substrate preferences and co-substrate uptake. *Journal of Biotechnology*, *185*, 19–27. https://doi.org/10.1016/j.jbiotec.2014.05.035

Freches, A., & Lemos, P. C. (2017). Microbial selection strategies for polyhydroxyalkanoates production from crude glycerol: Effect of OLR and cycle length. *New Biotechnology*, *39*, 22–28. https://doi.org/10.1016/j.nbt.2017.05.011

Friedrich, M., & Takács, I. (2013). A new interpretation of endogenous respiration profiles for the evaluation of the endogenous decay rate of heterotrophic biomass in activated sludge. *Water Research*, *47*(15), 5639–5646. https://doi.org/10.1016/j.watres.2013.06.043

Fukui, T., Kichise, T., Yoshida, Y., & Doi, Y. (1997). Biosynthesis of poly(3-hydroxybutyrate-co-3-hydroxyvalerate-co-3-hydroxy-heptanoate) terpolymers by recombinant Alcaligenes eutrophus. *Biotechnology Letters*, *19*(11), 1093–1097. https://doi.org/10.1023/A:1018436426032

G. W. Ehrenstein, R. P. T. (2001). Polymeric materials: structure, properties, applications. In *Hanser Verlag*.

Galván, A., Urbina, P., & De Castro, F. (2000). Characterization of filamentous microorganisms in rotating biological contactor biofilms of wastewater treatment plants. *Bioprocess Engineering*, *22*(3), 257–260. https://doi.org/10.1007/s004490050729

García-Quiles, L., Cuello, Á. F., & Castell, P. (2019). Sustainable materials with enhanced mechanical properties based on industrial polyhydroxyalkanoates reinforced with organomodified sepiolite and montmorillonite. *Polymers*, *11*(4). https://doi.org/10.3390/polym11040696

García, I. L., López, J. A., Dorado, M. P., Kopsahelis, N., Alexandri, M., Papanikolaou, S., Villar, M. A., & Koutinas, A. A. (2013). Evaluation of by-products from the biodiesel industry as fermentation feedstock for poly(3-hydroxybutyrate-co-3-hydroxyvalerate) production by Cupriavidus necator. *Bioresource Technology*, *130*, 16–22. https://doi.org/10.1016/j.biortech.2012.11.088

Gaval, G., & Pernelle, J. J. (2003). Impact of the repetition of oxygen deficiencies on the filamentous bacteria proliferation in activated sludge. *Water Research*, *37*(9), 1991–2000. https://doi.org/10.1016/S0043-1354(02)00421-9

Gilbert, M. (1994). Crystallinity in poly(vinyl chloride). *Journal of Macromolecular Science, Part C*, *34*(1), 77–135. https://doi.org/10.1080/15321799408009633

Giusti, L. (2009). A review of waste management practices and their impact on human health. In *Waste Management* (Vol. 29, Issue 8, pp. 2227–2239). https://doi.org/10.1016/j.wasman.2009.03.028

Glasauer, S. M., Burford, E. P., & Gadd, G. M. (2022). Transformation of metals and metalloids by microorganisms. In *Reference Module in Earth Systems and Environmental Sciences*. https://doi.org/10.1016/b978-0-12-822974-3.00011-2

González, E., Herencias, C., & Prieto, M. A. (2020). A polyhydroxyalkanoate-based encapsulating strategy for 'bioplasticizing' microorganisms. *Microbial Biotechnology*, *13*(1), 185–198. https://doi.org/10.1111/1751-7915.13492

Goulart, S. A. S., Oliveira, T. A., Teixeira, A., Miléo, P. C., & Mulinari, D. R. (2011). Mechanical behaviour of polypropylene reinforced palm fibers composites. *Procedia Engineering*, *10*, 2034–2039. https://doi.org/10.1016/j.proeng.2011.04.337

Gridneva, E., Chernousova, E., Dubinina, G., Akimov, V., Kuever, J., Detkova, E., & Grabovich, M. (2011). Taxonomic investigation of representatives of the genus Sphaerotilus: Descriptions of Sphaerotilus montanus sp. nov., Sphaerotilus hippei sp. nov., Sphaerotilus natans subsp. natans subsp. nov. and Sphaerotilus natans subsp. sulfidivorans subsp. nov., and. *International Journal of Systematic and Evolutionary Microbiology*, *61*(4), 916–925. https://doi.org/10.1099/ijs.0.023887-0

Guho, N. M., Pokhrel, D., Abbasi, M., McDonald, A. G., Alfaro, M., Brinkman, C. K., & Coats, E. R. (2020). Pilot-scale production of poly-3-hydroxybutyrate-co-3-hydroxyvalerate from fermented dairy manure: Process performance, polymer characterization, and scale-up implications. *Bioresource Technology Reports*, *12*. https://doi.org/10.1016/j.biteb.2020.100588

Guo, W. Q., Yang, S. S., Xiang, W. S., Wang, X. J., & Ren, N. Q. (2013). Minimization of excess sludge production by in-situ activated sludge treatment processes - A comprehensive review. *Biotechnology Advances*, *31*(8), 1386–1396. https://doi.org/10.1016/j.biotechadv.2013.06.003

Guo, Y., Wang, L., Chen, Y., Luo, P., & Chen, T. (2019). Properties of Luffa Fiber Reinforced PHBV biodegradable composites. *Polymers*, *11*(11). https://doi.org/10.3390/polym11111765

Haneef, M., Ceseracciu, L., Canale, C., Bayer, I. S., Heredia-Guerrero, J. A., & Athanassiou, A. (2017). Advanced Materials from Fungal Mycelium: Fabrication and Tuning of Physical Properties. *Scientific Reports*, *7*. https://doi.org/10.1038/srep41292

Hong, J., Hong, J., Otaki, M., & Jolliet, O. (2009). Environmental and economic life cycle assessment for sewage sludge treatment processes in Japan. *Waste Management*, *29*(2), 696–703. https://doi.org/10.1016/j.wasman.2008.03.026

Hosokawa, M. N., Darros, A. B., Moris, V. A. D. S., & De Paiva, J. M. F. (2017). Polyhydroxybutyrate composites with random mats of sisal and coconut fibers. *Materials Research*, *20*(1), 279–290. https://doi.org/10.1590/1980-5373-MR-2016-0254

Iqbal, H. M. N., Kyazze, G., Tron, T., & Keshavarz, T. (2014). A preliminary study on the development and characterisation of enzymatically grafted P(3HB)-ethyl cellulose based novel composites. *Cellulose*, *21*(5), 3613–3621. https://doi.org/10.1007/s10570-014-0337-9

Israni, N., Thapa, S., & Shivakumar, S. (2018). Biolytic extraction of poly(3-hydroxybutyrate) from Bacillus megaterium Ti3 using the lytic enzyme of Streptomyces albus Tia1. *Journal of Genetic Engineering and Biotechnology*, *16*(2), 265–271. https://doi.org/10.1016/j.jgeb.2018.07.004

Ivorra-Martinez, J., Verdu, I., Fenollar, O., Sanchez-Nacher, L., Balart, R., & Quiles-Carrillo, L. (2020). Manufacturing and properties of binary blend from bacterial polyester poly(3-hydroxybutyrate-co-3-hydroxyhexanoate) and poly(caprolactone) with improved toughness. *Polymers*, *12*(5). https://doi.org/10.3390/POLYM12051118

Jaffredo, C. G., Carpentier, J. F., & Guillaume, S. M. (2012). Controlled ROP of β-butyrolactone simply mediated by amidine, guanidine, and phosphazene organocatalysts. *Macromolecular Rapid Communications*, *33*(22), 1938–1944. https://doi.org/10.1002/marc.201200410

Jain, S., Jain, S., Wolf, I. T., Lee, J., & Tong, Y. W. (2015). A comprehensive review on operating parameters and different pretreatment methodologies for anaerobic digestion of municipal solid waste. In *Renewable and Sustainable Energy Reviews* (Vol. 52, pp. 142–154). https://doi.org/10.1016/j.rser.2015.07.091

Jenkins, D., Richard, M. G., & Daigger, G. T. (2003). Manual on the Causes and Control of Activated Sludge Bulking, Foaming, and Other Solids Separation Problems. In *Manual on the Causes and Control of Activated Sludge Bulking, Foaming, and Other Solids Separation Problems*. https://doi.org/10.1201/9780203503157

Jiang, Long, Huang, J., Qian, J., Chen, F., Zhang, J., Wolcott, M. P., & Zhu, Y. (2008). Study of poly(3-hydroxybutyrate-co-3-hydroxyvalerate) (PHBV)/bamboo pulp fiber composites: Effects of nucleation agent and compatibilizer. *Journal of Polymers and the Environment*, *16*(2), 83–93. https://doi.org/10.1007/s10924-008-0086-7

Jiang, Lu, Luo, Z., Loh, X. J., Wu, Y. L., & Li, Z. (2019). PHA-Based thermogel as a controlled zero-order chemotherapeutic delivery system for the effective treatment of melanoma. *ACS Applied Bio Materials*, *2*(8), 3591–3600. https://doi.org/10.1021/acsabm.9b00467

Jiang, Y., Mikova, G., Kleerebezem, R., van der Wielen, L. A. M., & Cuellar, M. C. (2015). Feasibility study of an alkaline-based chemical treatment for the purification of polyhydroxybutyrate produced by a mixed enriched culture. *AMB Express*, *5*(1). https://doi.org/10.1186/s13568-015-0096-5

Jo, J., Price-Whelan, A., & Dietrich, L. E. P. (2022). Gradients and consequences of heterogeneity in biofilms. In *Nature Reviews Microbiology* (Vol. 20, Issue 10, pp. 593–607). https://doi.org/10.1038/s41579-022-00692-2

Johnson, K., Jiang, Y., Kleerebezem, R., Muyzer, G., & Van Loosdrecht, M. C. M. (2009). Enrichment of a mixed bacterial culture with a high polyhydroxyalkanoate storage capacity. *Biomacromolecules*, *10*(4), 670–676. https://doi.org/10.1021/bm8013796

Joyyi, L., Ahmad Thirmizir, M. Z., Salim, M. S., Han, L., Murugan, P., Kasuya, K. ichi, Maurer, F. H. J., Zainal Arifin, M. I., & Sudesh, K. (2017). Composite properties and biodegradation of biologically recovered P(3HB-co-3HHx) reinforced with short kenaf fibers. *Polymer Degradation and Stability*, *137*, 100–108. https://doi.org/10.1016/j.polymdegradstab.2017.01.004

Jung, H. R., Jeon, J. M., Yi, D. H., Song, H. S., Yang, S. Y., Choi, T. R., Bhatia, S. K., Yoon, J. J., Kim, Y. G., Brigham, C. J., & Yang, Y. H. (2019). Poly(3-hydroxybutyrate-co-3-hydroxyvalerate-co-3-hydroxyhexanoate) terpolymer production from volatile fatty acids using engineered Ralstonia eutropha. *International Journal of Biological Macromolecules*, *138*, 370–378. https://doi.org/10.1016/j.ijbiomac.2019.07.091

Jung, Y. M., & Lee, Y. H. (2000). Utilization of oxidative pressure for enhanced production of poly-β-hydroxybutyrate and poly(3-hydroxybutyrate-3-hydroxyvalerate) in Ralstonia eutropha. *Journal of Bioscience and Bioengineering*, *90*(3), 266–270. https://doi.org/10.1016/S1389-1723(00)80080-8

Kachrimanidou, V., Kopsahelis, N., Papanikolaou, S., Kookos, I. K., De Bruyn, M., Clark, J. H., & Koutinas, A. A. (2014). Sunflower-based biorefinery: Poly(3-hydroxybutyrate) and poly(3-hydroxybutyrate-co-3-hydroxyvalerate) production from crude glycerol, sunflower meal and levulinic acid. *Bioresource Technology*, *172*, 121–130. https://doi.org/10.1016/j.biortech.2014.08.044

Kadouri, D., Jurkevitch, E., Okon, Y., & Castro-Sowinski, S. (2005). Ecological and agricultural significance of bacterial polyhydroxyalkanoates. In *Critical Reviews in Microbiology* (Vol. 31, Issue 2, pp. 55–67). https://doi.org/10.1080/10408410590899228

Kalia, V. C., Ray, S., Patel, S. K. S., Singh, M., & Singh, G. P. (2019). Applications of polyhydroxyalkanoates and their metabolites as drug carriers. In *Biotechnological Applications of Polyhydroxyalkanoates* (pp. 35–48). https://doi.org/10.1007/978-981-13-3759-8_3

Kalia, V. C., Singh Patel, S. K., Shanmugam, R., & Lee, J. K. (2021). Polyhydroxyalkanoates: Trends and advances toward biotechnological applications. In *Bioresource Technology* (Vol. 326). https://doi.org/10.1016/j.biortech.2021.124737

Kamdem, D. P., Jiang, H., Cui, W., Freed, J., & Matuana, L. M. (2004). Properties of wood plastic composites made of recycled HDPE and wood flour from CCA-treated wood removed from service. *Composites Part A: Applied Science and Manufacturing*, *35*(3), 347–355. https://doi.org/10.1016/j.compositesa.2003.09.013

Kämpfer, P. (1998). Some chemotaxonomic and physiological properties of the genus Sphaerotilus. *Systematic and Applied Microbiology*, *21*(2), 245–250. https://doi.org/10.1016/S0723-2020(98)80029-5

Kandemir, N., Vollmer, W., Jakubovics, N. S., & Chen, J. (2018). Mechanical interactions between bacteria and hydrogels. *Scientific Reports*, *8*(1). https://doi.org/10.1038/s41598-018-29269-x

Kaygusuz, B., & Özerinç, S. (2019). Improving the ductility of polylactic acid parts produced by fused deposition modeling through polyhydroxyalkanoate additions. *Journal of Applied Polymer Science*, *136*(43). https://doi.org/10.1002/app.48154

Kehail, A. A., & Brigham, C. J. (2018). Anti-biofilm Activity of Solvent-Cast and Electrospun Polyhydroxyalkanoate Membranes Treated with Lysozyme. *Journal of Polymers and the Environment*, *26*(1), 66–72. https://doi.org/10.1007/s10924-016-0921-1

Keskin, G., Klzll, G., Bechelany, M., Pochat-Bohatier, C., & Öner, M. (2017). Potential of polyhydroxyalkanoate (PHA) polymers family as substitutes of petroleum based polymers for packaging applications and solutions brought by their composites to form barrier materials. *Pure and Applied Chemistry*, *89*(12), 1841–1848. https://doi.org/10.1515/pac-2017-0401

Kim, I. (2018). *Denitrification by zero-valent iron-supported mixed cultures* [University of Delaware]. https://search.proquest.com/docview/2191512701?accountid=10457

Kinyanjui Muiruri, J., Chee Chuan Yeo, J., Yun Debbie Soo, X., Wang, S., Liu, H., Kong, J., Cao, J., Hoon Tan, B., Suwardi, A., Li, Z., Xu, J., Jun Loh, X., & Zhu, Q. (2023). Recent advances of sustainable Short-chain length polyhydroxyalkanoates (Scl-PHAs) – Plant biomass composites. *European Polymer Journal*, *187*(February), 111882. https://doi.org/10.1016/j.eurpolymj.2023.111882

Kittikorn, T., Malakul, R., Stromberg, E., Ek, M., & Karlsson, S. (2018). Enhancement of mechanical, thermal and antibacterial properties of sisal/ polyhydroxybutyrate-co-valerate biodegradable composite. *Journal of Metals, Materials and Minerals*, *28*(1), 52–61. https://doi.org/10.14456/jmmm.2018.8

Koller, M., Niebelschütz, H., & Braunegg, G. (2013). Strategies for recovery and purification of poly[(R)-3-hydroxyalkanoates] (PHA) biopolyesters from surrounding biomass. In *Engineering in Life Sciences* (Vol. 13, Issue 6, pp. 549–562). https://doi.org/10.1002/elsc.201300021

Kosseva, M. R., & Rusbandi, E. (2018). Trends in the biomanufacture of polyhydroxyalkanoates with focus on downstream processing. In *International Journal of Biological Macromolecules* (Vol. 107, Issue PartA, pp. 762–778). https://doi.org/10.1016/j.ijbiomac.2017.09.054

Kourmentza, C., Ntaikou, I., Lyberatos, G., & Kornaros, M. (2015). Polyhydroxyalkanoates from Pseudomonas sp. using synthetic and olive mill wastewater under limiting conditions. *International Journal of Biological Macromolecules*, *74*, 202–210. https://doi.org/10.1016/j.ijbiomac.2014.12.032

Kourmentza, Constantina, Plácido, J., Venetsaneas, N., Burniol-Figols, A., Varrone, C., Gavala, H. N., & Reis, M. A. M. (2017). Recent advances and challenges towards sustainable polyhydroxyalkanoate (PHA) production. In *Bioengineering* (Vol. 4, Issue 2). https://doi.org/10.3390/bioengineering4020055

Krishnan, S., Chinnadurai, G. S., Ravishankar, K., Raghavachari, D., & Perumal, P. (2021). Statistical augmentation of polyhydroxybutyrate production by Isoptericola variabilis: Characterization, moulding, in vitro cytocompatibility and biodegradability evaluation. *International Journal of Biological Macromolecules*, *166*, 80–97. https://doi.org/10.1016/j.ijbiomac.2020.10.089

Kumar, M., Rathour, R., Singh, R., Sun, Y., Pandey, A., Gnansounou, E., Andrew Lin, K. Y., Tsang, D. C. W., & Thakur, I. S. (2020). Bacterial polyhydroxyalkanoates: Opportunities, challenges, and prospects. In *Journal of Cleaner Production* (Vol. 263). https://doi.org/10.1016/j.jclepro.2020.121500

Kumar, P., Singh, M., Mehariya, S., Patel, S. K. S., Lee, J. K., & Kalia, V. C. (2014). Ecobiotechnological Approach for Exploiting the Abilities of Bacillus to Produce Co-polymer of Polyhydroxyalkanoate. *Indian Journal of Microbiology*, *54*(2), 151–157. https://doi.org/10.1007/s12088-014-0457-9

Kunasundari, B., & Sudesh, K. (2011). Isolation and recovery of microbial polyhydroxyalkanoates. In *Express Polymer Letters* (Vol. 5, Issue 7, pp. 620–634). https://doi.org/10.3144/expresspolymlett.2011.60

Kunoh, T., Yamamoto, T., Sugimoto, S., Ono, E., Nomura, N., & Utada, A. S. (2021). Leptothrix cholodnii Response to Nutrient Limitation. *Frontiers in Microbiology*, *12*. https://doi.org/10.3389/fmicb.2021.691563

Kwon, H. S., Jung, S. G., Kim, H. Y., Parker, S. A., Batt, C. A., & Kim, Y. R. (2014). A multi-functional polyhydroxybutyrate nanoparticle for theranostic applications. *Journal of Materials Chemistry B*, *2*(25), 3965–3971. https://doi.org/10.1039/c4tb00304g

Lakshman, K., & Shamala, T. R. (2006). Extraction of polyhydroxyalkanoate from Sinorhizobium meliloti cells using Microbispora sp. culture and its enzymes. *Enzyme and Microbial Technology*, *39*(7), 1471–1475. https://doi.org/10.1016/j.enzmictec.2006.03.037

Laycock, B., Halley, P., Pratt, S., Werker, A., & Lant, P. (2014). The chemomechanical properties of microbial polyhydroxyalkanoates. In *Progress in Polymer Science* (Vol. 39, Issue 2, pp. 397–442). https://doi.org/10.1016/j.progpolymsci.2013.06.008

Lee, J. K., Patel, S. K. S., Sung, B. H., & Kalia, V. C. (2020). Biomolecules from municipal and food industry wastes: An overview. In *Bioresource Technology* (Vol. 298). https://doi.org/10.1016/j.biortech.2019.122346

Lee, S., Jeon, E., Yun, H. S., & Lee, J. (2011). Improvement of fatty acid biosynthesis by engineered recombinant Escherichia coli. *Biotechnology and Bioprocess Engineering*, *16*(4), 706–713. https://doi.org/10.1007/s12257-011-0034-6

Lemes, A. P., Montanheiro, T. L. D. A., Durán, N., & da Silva, A. P. (2019). Phbv/mwcnt films: Hydrophobicity, thermal and mechanical properties as a function of mwcnt concentration. *Journal of Composites Science*, *3*(1). https://doi.org/10.3390/jcs3010012

Leo, Z. Z., Li, Z., Tian, H. L., Li, M., & Chen, G. Q. (2005). Molecular cloning and functional analysis of (R)-3-hydroxyacyl-acyl carrier protein:coenzyme A transacylase from Pseudomonas mendocina LZ. *FEMS Microbiology Letters*, *252*(2), 299–307. https://doi.org/10.1016/j.femsle.2005.09.006

Leong, Y. K., Show, P. L., Ooi, C. W., Ling, T. C., & Lan, J. C. W. (2014). Current trends in polyhydroxyalkanoates (PHAs) biosynthesis: Insights from the recombinant Escherichia coli. *Journal of Biotechnology*, *180*, 52–65. https://doi.org/10.1016/j.jbiotec.2014.03.020

Li, C., He, W., Liang, D. D., Tian, Y., Yadav, R. S., Li, D., Liu, J., & Feng, Y. (2021). The anaerobic and starving treatment eliminates filamentous bulking and recovers biocathode biocatalytic activity with residual organic loading in microbial electrochemical system. *Chemical Engineering Journal*, *404*. https://doi.org/10.1016/j.cej.2020.127072

Li, W., Cicek, N., Levin, D. B., Logsetty, S., & Liu, S. (2020). Bacteria-triggered release of a potent biocide from core-shell polyhydroxyalkanoate (PHA)-based nanofibers for wound dressing applications. *Journal of Biomaterials Science, Polymer Edition*, *31*(3), 394–406. https://doi.org/10.1080/09205063.2019.1693882

Li, Z., Yang, J., & Loh, X. J. (2016). Polyhydroxyalkanoates: Opening doors for a sustainable future. In *NPG Asia Materials* (Vol. 8, Issue 4). https://doi.org/10.1038/am.2016.48

Lim, J., You, M., Li, J., & Li, Z. (2017). Emerging bone tissue engineering via Polyhydroxyalkanoate (PHA)-based scaffolds. In *Materials Science and Engineering C* (Vol. 79, pp. 917–929). https://doi.org/10.1016/j.msec.2017.05.132

Limbert, G., Bryan, R., Cotton, R., Young, P., Hall-Stoodley, L., Kathju, S., & Stoodley, P. (2013). On the mechanics of bacterial biofilms on non-dissolvable surgical sutures: A laser scanning confocal microscopy-based finite element study. *Acta Biomaterialia*, *9*(5), 6641–6652. https://doi.org/10.1016/j.actbio.2013.01.017

Liu, Y. C., Lin, C. H., Ko, B. T., & Ho, R. M. (2010). Ring-opening polymerization of β-butyrolactone catalyzed by efficient magnesium and zinc complexes derived from tridentate anilido-aldimine ligand. *Journal of Polymer Science, Part A: Polymer Chemistry*, *48*(23), 5339–5347. https://doi.org/10.1002/pola.24334

Lopaschuk, G. D., Ussher, J. R., Folmes, C. D. L., Jaswal, J. S., & Stanley, W. C. (2010). Myocardial fatty acid metabolism in health and disease. In *Physiological Reviews* (Vol. 90, Issue 1, pp. 207–258). https://doi.org/10.1152/physrev.00015.2009

López-Abelairas, M., García-Torreiro, M., Lú-Chau, T., Lema, J. M., & Steinbüchel, A. (2015). Comparison of several methods for the separation of poly(3-hydroxybutyrate) from Cupriavidus necator H16 cultures. *Biochemical Engineering Journal*, *93*, 250–259. https://doi.org/10.1016/j.bej.2014.10.018

López, J. P., Méndez, J. A., Espinach, F. X., Julián, F., Mutjé, P., & Vilaseca, F. (2012). Tensile strength characteristics of polypropylene composites reinforced with stone groundwood fibers from softwood. *BioResources*, *7*(3), 3188–3200.

Lou, I. C., & de los Reyes, F. L. (2005). Integrating Decay, Storage, Kinetic Selection, and Filamentous Backbone Factors in a Bacterial Competition Model. *Water Environment Research*, *77*(3), 287–296. https://doi.org/10.2175/106143005x41870

Lu, H. I., Rasmussen, J., Wright, M. J., Patterson, D., & Doyle, J. M. (2011). A cold and slow molecular beam. In *Physical Chemistry Chemical Physics* (Vol. 13, Issue 42). https://doi.org/10.1039/c1cp21206k

Lu, Y., Xie, Q., Tang, L., Yu, J., Wang, J., Yang, Z., Fan, C., & Zhang, S. (2021). The reduction of nitrobenzene by extracellular electron transfer facilitated by Fe-bearing biochar derived from sewage sludge. *Journal of Hazardous Materials*, *403*. https://doi.org/10.1016/j.jhazmat.2020.123682

Lv, Y., Zhu, H., An, M. fang, Xu, H. jun, Zhang, L., & Wang, Z. bao. (2016). Multiple endothermic peaks resulted from different crystal structures in an isomorphous copolymer poly(3-hydroxybutyrate-co-3-hydroxyvalerate). *Chinese Journal of Polymer Science (English Edition)*, *34*(12), 1510–1522. https://doi.org/10.1007/s10118-016-1866-5

Ma, W., Wang, J., Li, Y., Yin, L., & Wang, X. (2018). Poly(3-hydroxybutyrate-co-3-hydroxyvalerate) co-produced with l-isoleucine in Corynebacterium glutamicum WM001. *Microbial Cell Factories*, *17*(1). https://doi.org/10.1186/s12934-018-0942-7

Madison, L. L., & Huisman, G. W. (1999). Metabolic Engineering of Poly(3-Hydroxyalkanoates): From DNA to Plastic. *Microbiology and Molecular Biology Reviews*, *63*(1), 21–53. https://doi.org/10.1128/mmbr.63.1.21-53.1999

Maeng, M. H., & Cha, D. K. (2017). Transesterification of Waste Activated Sludge for Biosolids Reduction and Biodiesel Production. *Water Environment Research*, *90*(2), 180–186. https://doi.org/10.2175/106143017x14902968254881

Mannina, G., Presti, D., Montiel-Jarillo, G., Carrera, J., & Suárez-Ojeda, M. E. (2020). Recovery of polyhydroxyalkanoates (PHAs) from wastewater: A review. In *Bioresource Technology* (Vol. 297). https://doi.org/10.1016/j.biortech.2019.122478

Mármol, G., Gauss, C., & Fangueiro, R. (2020). Potential of cellulose microfibers for PHA and PLA biopolymers reinforcement. *Molecules*, *25*(20). https://doi.org/10.3390/molecules25204653

Martins, A. M. P., Pagilla, K., Heijnen, J. J., & Van Loosdrecht, M. C. M. (2004). Filamentous bulking sludge - A critical review. In *Water Research* (Vol. 38, Issue 4, pp. 793–817). https://doi.org/10.1016/j.watres.2003.11.005

Marudkla, J., Patjawit, A., Chuensangjun, C., & Sirisansaneeyakul, S. (2018). Optimization of poly(3-hydroxybutyrate) extraction from Cupriavidus necator DSM 545 using sodium dodecyl sulfate and sodium hypochlorite. *Agriculture and Natural Resources*, *52*(3), 266–273. https://doi.org/10.1016/j.anres.2018.09.009

Mazur, K., & Kuciel, S. (2019). Mechanical and hydrothermal aging behaviour of polyhydroxybutyrate-co-valerate (PHBV) composites reinforced by natural fibres. *Molecules*, *24*(19). https://doi.org/10.3390/molecules24193538

McAdam, B., Fournet, M. B., McDonald, P., & Mojicevic, M. (2020). Production of polyhydroxybutyrate (PHB) and factors impacting its chemical and mechanical characteristics. In *Polymers* (Vol. 12, Issue 12, pp. 1–20). https://doi.org/10.3390/polym12122908

Meereboer, K. W., Misra, M., & Mohanty, A. K. (2020). Review of recent advances in the biodegradability of polyhydroxyalkanoate (PHA) bioplastics and their composites. In *Green Chemistry* (Vol. 22, Issue 17, pp. 5519–5558). https://doi.org/10.1039/d0gc01647k

Metcalf, & Eddy. (2013). Metcalf and Eddy, AECOM - Wastewater Engineering_ Treatment and Resource Recovery-McGraw-Hill (2014).pdf. *Wastewater Engineering: Treatment and Reuse McGraw Hill. New York, NY.*, 2044.

Miller, S. A., Billington, S. L., & Lepech, M. D. (2013). Improvement in environmental performance of poly(β-hydroxybutyrate)- co-(β-hydroxyvalerate) composites through process modifications. *Journal of Cleaner Production*, *40*, 190–198. https://doi.org/10.1016/j.jclepro.2012.08.033

Mohamad Fauzi, A. H., Chua, A. S. M., Yoon, L. W., Nittami, T., & Yeoh, H. K. (2019). Enrichment of PHA-accumulators for sustainable PHA production from crude glycerol. *Process Safety and Environmental Protection*, *122*, 200–208. https://doi.org/10.1016/j.psep.2018.12.002

Montano-Herrera, L., Pratt, S., Arcos-Hernandez, M. V., Halley, P. J., Lant, P. A., Werker, A., & Laycock, B. (2014). In-line monitoring of thermal degradation of PHA during melt-processing by Near-Infrared spectroscopy. *New Biotechnology*, *31*(4), 357–363. https://doi.org/10.1016/j.nbt.2013.10.005

Moore, T., Adhikari, R., & Gunatillake, P. (2005). Chemosynthesis of bioresorbable poly(γ-butyrolactone) by ring-opening polymerisation: A review. In *Biomaterials* (Vol. 26, Issue 18, pp. 3771–3782). https://doi.org/10.1016/j.biomaterials.2004.10.002

Morales-Rivas, L., González-Orive, A., Garcia-Mateo, C., Hernández-Creus, A., Caballero, F. G., & Vázquez, L. (2015). Nanomechanical characterization of nanostructured bainitic steel: Peak Force Microscopy and Nanoindentation with AFM. In *Scientific Reports* (Vol. 5). https://doi.org/10.1038/srep17164

Morgan-Sagastume, F. (2016). Characterisation of open, mixed microbial cultures for polyhydroxyalkanoate (PHA) production. In *Reviews in Environmental Science and Biotechnology* (Vol. 15, Issue 4, pp. 593–625). https://doi.org/10.1007/s11157-016-9411-0

Moura, A., Bolba, C., Demori, R., Lima, L. P. F. C., & Santana, R. M. C. (2018). Effect of Rice Husk Treatment with Hot Water on Mechanical Performance in Poly(hydroxybutyrate)/Rice Husk Biocomposite. *Journal of Polymers and the Environment*, *26*(6), 2632–2639. https://doi.org/10.1007/s10924-017-1156-5

Mukheem, A., Muthoosamy, K., Manickam, S., Sudesh, K., Shahabuddin, S., Saidur, R., Akbar, N., & Sridewi, N. (2018). Fabrication and characterization of an electrospun PHA/graphene silver nanocomposite scaffold for antibacterial applications. *Materials*, *11*(9). https://doi.org/10.3390/ma11091673

Mulchandani, A., & Westerhoff, P. (2016). Recovery opportunities for metals and energy from sewage sludges. *Bioresource Technology*, *215*, 215–226. https://doi.org/10.1016/j.biortech.2016.03.075

Mulder, E. G., & Deinema, M. H. (1981). The Sheathed Bacteria. In *The Prokaryotes* (pp. 425–440). Springer, Berlin, Heidelberg. https://doi.org/10.1007/978-3-662-13187-9_27

Munir, S., & Jamil, N. (2018). Polyhydroxyalkanoates (PHA) production in bacterial co-culture using glucose and volatile fatty acids as carbon source. *Journal of Basic Microbiology*, *58*(3), 247–254. https://doi.org/10.1002/jobm.201700276

Munir, S., & Jamil, N. (2020). Polyhydroxyalkanoate (PHA) production in open mixed cultures using waste activated sludge as biomass. *Archives of Microbiology*, *202*(7), 1907–1913. https://doi.org/10.1007/s00203-020-01912-0

Murugan, P., Han, L., Gan, C. Y., Maurer, F. H. J., & Sudesh, K. (2016). A new biological recovery approach for PHA using mealworm, Tenebrio molitor. *Journal of Biotechnology*, *239*, 98–105. https://doi.org/10.1016/j.jbiotec.2016.10.012

Murugan, P., Ong, S. Y., Hashim, R., Kosugi, A., Arai, T., & Sudesh, K. (2020). Development and evaluation of controlled release fertilizer using P(3HB-co-3HHx) on oil palm plants (nursery stage) and soil microbes. *Biocatalysis and Agricultural Biotechnology*, *28*. https://doi.org/10.1016/j.bcab.2020.101710

Narancic, T., Scollica, E., Kenny, S. T., Gibbons, H., Carr, E., Brennan, L., Cagney, G., Wynne, K., Murphy, C., Raberg, M., Heinrich, D., Steinbüchel, A., & O'Connor, K. E. (2016). Understanding the physiological roles of polyhydroxybutyrate (PHB) in Rhodospirillum rubrum S1 under aerobic chemoheterotrophic conditions. *Applied Microbiology and Biotechnology*, *100*(20), 8901–8912. https://doi.org/10.1007/s00253-016-7711-5

Nielsen, L. E., & Stockton, F. D. (1963). Theory of the modulus of crystalline polymers. *Journal of Polymer Science Part A: General Papers*, *1*(6), 1995–2002. https://doi.org/10.1002/pol.1963.100010616

Nielsen, P. H., Aquino de Muro, M., & Nielsen, J. L. (2000). Studies on the in situ physiology of Thiothrix spp. present in activated sludge. *Environmental Microbiology*, *2*(4), 389–398. https://doi.org/10.1046/j.1462-2920.2000.00120.x

Nielsen, Per Halkjær, Kragelund, C., Seviour, R. J., & Nielsen, J. L. (2009). Identity and ecophysiology of filamentous bacteria in activated sludge. In *FEMS Microbiology Reviews* (Vol. 33, Issue 6, pp. 969–998). https://doi.org/10.1111/j.1574-6976.2009.00186.x

Nishida, M., Tanaka, T., Hayakawa, Y., Ogura, T., Ito, Y., & Nishida, M. (2019). Multi-scale instrumental analyses of plasticized polyhydroxyalkanoates (PHA) blended with polycaprolactone (PCL) and the effects of crosslinkers and graft copolymers. *RSC Advances*, *9*(3), 1551–1561. https://doi.org/10.1039/C8RA10045D

Noutsopoulos, C., Andreadakis, A., Mamais, D., & Gavalakis, E. (2007). Identification of type and causes of filamentous bulking under Mediterranean conditions. *Environmental Technology*, *28*(1), 115–122. https://doi.org/10.1080/09593332808618771

Ojha, N., & Das, N. (2020). Fabrication and characterization of biodegradable PHBV/SiO2 nanocomposite for thermo-mechanical and antibacterial applications in food packaging. *IET Nanobiotechnology*, *14*(9), 785–795. https://doi.org/10.1049/iet-nbt.2020.0066

Omrani, E., Menezes, P. L., & Rohatgi, P. K. (2016). State of the art on tribological behavior of polymer matrix composites reinforced with natural fibers in the green materials world. In *Engineering Science and Technology, an International Journal* (Vol. 19, Issue 2, pp. 717–736). https://doi.org/10.1016/j.jestch.2015.10.007

Ong, S. Y., Kho, H. P., Riedel, S. L., Kim, S. W., Gan, C. Y., Taylor, T. D., & Sudesh, K. (2018). An integrative study on biologically recovered polyhydroxyalkanoates (PHAs) and simultaneous assessment of gut microbiome in yellow mealworm. *Journal of Biotechnology*, *265*, 31–39. https://doi.org/10.1016/j.jbiotec.2017.10.017

Pagliano, G., Galletti, P., Samorì, C., Zaghini, A., & Torri, C. (2021). Recovery of Polyhydroxyalkanoates From Single and Mixed Microbial Cultures: A Review. In *Frontiers in Bioengineering and Biotechnology* (Vol. 9). https://doi.org/10.3389/fbioe.2021.624021

Pan, C., Tan, G. Y. A., Ge, L., Chen, C. L., & Wang, J. Y. (2016). Microbial removal of carboxylic acids from 1,3-propanediol in glycerol anaerobic digestion effluent by PHAs-producing consortium. *Biochemical Engineering Journal*, *112*, 269–276. https://doi.org/10.1016/j.bej.2016.04.031

Panaitescu, D. M., Ionita, E. R., Nicolae, C. A., Gabor, A. R., Ionita, M. D., Trusca, R., Lixandru, B. E., Codita, I., & Dinescu, G. (2018). Poly(3-hydroxybutyrate) modified by nanocellulose and plasma treatment for packaging applications. *Polymers*, *10*(11). https://doi.org/10.3390/polym10111249

Panaitescu, D. M., Trusca, R., Gabor, A. R., Nicolae, C. A., & Casarica, A. (2020). Biocomposite foams based on polyhydroxyalkanoate and nanocellulose: Morphological and thermo-mechanical characterization. *International Journal of Biological Macromolecules*, *164*, 1867–1878. https://doi.org/10.1016/j.ijbiomac.2020.07.273

Pantaloni, D., Rudolph, A. L., Shah, D. U., Baley, C., & Bourmaud, A. (2021). Interfacial and mechanical characterisation of biodegradable polymer-flax fibre composites. *Composites Science and Technology*, *201*, 108529. https://doi.org/10.1016/j.compscitech.2020.108529

Pellegrin, V., Juretschko, S., Wagner, M., & Cottenceau, G. (1999). Morphological and biochemical properties of a Sphaerotilus sp. isolated from paper mill slimes. *Applied and Environmental Microbiology*, *65*(1), 156–162. https://doi.org/10.1128/aem.65.1.156-162.1999

Peoples, O. P., & Sinskey, A. J. (1989). Poly-β-hydroxybutyrate (PHB) biosynthesis in Alcaligenes eutrophus H16. Identification and characterization of the PHB polymerase gene (phbC). *Journal of Biological Chemistry*, *264*(26), 15298–15303.

Perez-Zabaleta, M., Khatami, K., & Cetecioglu, Z. (2020). From waste to bioplastics: bio-based conversion of volatile fatty acids to polyhydroxyalkanoates. *Access Microbiology*, *2*(7A). https://doi.org/10.1099/acmi.ac2020.po0900

Peterson, A., & Fischer, C. (2010). Conversion of natural products including cellulose to hydrocarbons, hydrogen and/or other related compounds (Patent No. US 8,546,625 B2). In *US Patent 2010/0228067 A1* (US 8,546,625 B2). http://www.google.com/patents/US8546625

Pickering, K. L., Efendy, M. G. A., & Le, T. M. (2016). A review of recent developments in natural fibre composites and their mechanical performance. *Composites Part A: Applied Science and Manufacturing*, *83*, 98–112. https://doi.org/10.1016/j.compositesa.2015.08.038

Pilla, S. (2011). Handbook of Bioplastics and Biocomposites Engineering Applications. In *Handbook of Bioplastics and Biocomposites Engineering Applications*. https://doi.org/10.1002/9781118203699

Pramanik, N., Dutta, K., Basu, R. K., & Kundu, P. P. (2016). Aromatic π-Conjugated Curcumin on Surface Modified Polyaniline/Polyhydroxyalkanoate Based 3D Porous Scaffolds for Tissue Engineering Applications. *ACS Biomaterials Science and Engineering*, *2*(12), 2365–2377. https://doi.org/10.1021/acsbiomaterials.6b00595

Qu, Z., & Meredith, J. C. (2018). The atypically high modulus of pollen exine. *Journal of the Royal Society Interface*, *15*(146). https://doi.org/10.1098/rsif.2018.0533

Raberg, M., Bechmann, J., Brandt, U., Schlüter, J., Uischner, B., Voigt, B., Hecker, M., & Steinbüchel, A. (2011). Versatile metabolic adaptations of Ralstonia eutropha H16 to a loss of PdhL, the E3 component of the pyruvate dehydrogenase complex. *Applied and Environmental Microbiology*, *77*(7), 2254–2263. https://doi.org/10.1128/AEM.02360-10

Raheem, A., Sikarwar, V. S., He, J., Dastyar, W., Dionysiou, D. D., Wang, W., & Zhao, M. (2018). Opportunities and challenges in sustainable treatment and resource reuse of sewage sludge: A review. *Chemical Engineering Journal*, *337*(December 2017), 616–641. https://doi.org/10.1016/j.cej.2017.12.149

Rai, R., Roether, J. A., Knowles, J. C., Mordan, N., Salih, V., Locke, I. C., Gordge, M. P., McCormick, A., Mohn, D., Stark, W. J., Keshavarz, T., Boccaccini, A. R., & Roy, I. (2017). Highly elastomeric poly(3-hydroxyoctanoate) based natural polymer composite for enhanced keratinocyte regeneration. *International Journal of Polymeric Materials and Polymeric Biomaterials*, *66*(7), 326–335. https://doi.org/10.1080/00914037.2016.1217530

Rao, K. M. M., & Rao, K. M. (2007). Extraction and tensile properties of natural fibers: Vakka, date and bamboo. *Composite Structures*, *77*(3), 288–295. https://doi.org/10.1016/j.compstruct.2005.07.023

Ratledge, C., & Kristiansen, B. (2006). *Basic Biotechnology, 3rd edition*. CambriCambridge University Press. http://doi.org/10.1017/CBO9780511802409

Ray, S., & Kalia, V. C. (2017a). Co-metabolism of substrates by Bacillus thuringiensis regulates polyhydroxyalkanoate co-polymer composition. *Bioresource Technology*, *224*, 743–747. https://doi.org/10.1016/j.biortech.2016.11.089

Ray, S., & Kalia, V. C. (2017b). Microbial Cometabolism and Polyhydroxyalkanoate Co-polymers. In *Indian Journal of Microbiology* (Vol. 57, Issue 1, pp. 39–47). https://doi.org/10.1007/s12088-016-0622-4

Ray, S., Patel, S. K. S., Singh, M., Singh, G. P., & Kalia, V. C. (2019). Exploiting polyhydroxyalkanoates for tissue engineering. In *Biotechnological Applications of Polyhydroxyalkanoates* (pp. 271–282). https://doi.org/10.1007/978-981-13-3759-8_10

Raza, Z. A., Khalil, S., & Abid, S. (2020). Recent progress in development and chemical modification of poly(hydroxybutyrate)-based blends for potential medical applications. *International Journal of Biological Macromolecules*, *160*, 77–100. https://doi.org/10.1016/j.ijbiomac.2020.05.114

Raza, Z. A., Riaz, S., & Banat, I. M. (2018). Polyhydroxyalkanoates: Properties and chemical modification approaches for their functionalization. In *Biotechnology Progress* (Vol. 34, Issue 1, pp. 29–41). https://doi.org/10.1002/btpr.2565

Rebocho, A. T., Pereira, J. R., Neves, L. A., Alves, V. D., Sevrin, C., Grandfils, C., Freitas, F., & Reis, M. A. M. (2020). Preparation and characterization of films based on a natural p(3hb)/mcl-pha blend obtained through the co-culture of cupriavidus necator and pseudomonas citronellolis in apple pulp waste. *Bioengineering*, *7*(2). https://doi.org/10.3390/bioengineering7020034

Reddy, S. V., Thirumala, M., & Mahmood, S. K. (2009). A novel Bacillus sp. accumulating poly (3-hydroxybutyrate-co-3- hydroxyvalerate) from a single carbon substrate. *Journal of Industrial Microbiology and Biotechnology*, *36*(6), 837–843. https://doi.org/10.1007/s10295-009-0561-8

Ren, Q., Sierro, N., Witholt, B., & Kessler, B. (2000). FabG, an NADPH-dependent 3-ketoacyl reductase of Pseudomonas aeruginosa, provides precursors for medium-chain-length poly-3-hydroxyalkanoate biosynthesis in Escherichia coli. *Journal of Bacteriology*, *182*(10), 2978–2981. https://doi.org/10.1128/JB.182.10.2978-2981.2000

Ribeiro, P. L. L., de Souza Silva, G., & Druzian, J. I. (2016). Evaluation of the effects of crude glycerol on the production and properties of novel polyhydroxyalkanoate copolymers containing high 11-hydroxyoctadecanoate by Cupriavidus necator IPT 029 and Bacillus megaterium IPT 429. *Polymers for Advanced Technologies*, *27*(4), 542–549. https://doi.org/10.1002/pat.3725

Richard, M. (2003). Activated Sludge Microbiology Problems and Their Control. *USEPA National Operator Trainers Conference*, 1–21.

Richard, M. G., Shimizu, G. P., & Jenkins, D. (1985). The growth physiology of the filamentous organism type 021N and its significance to activated sludge bulking. *Journal of the Water Pollution Control Federation*, *57*(12), 1152–1162.

Rieth, L. R., Moore, D. R., Lobkovsky, E. B., & Coates, G. W. (2002). Single-site β-diiminate zinc catalysts for the ring-opening polymerization of β-butyrolactone and β-valerolactone to poly(3-hydroxyalkanoates). *Journal of the American Chemical Society*, *124*(51), 15239–15248. https://doi.org/10.1021/ja020978r

Rivera-Briso, A. L., Aachmann, F. L., Moreno-Manzano, V., & Serrano-Aroca, Á. (2020). Graphene oxide nanosheets versus carbon nanofibers: Enhancement of physical and biological properties of poly(3-hydroxybutyrate-co-3-hydroxyvalerate) films for biomedical applications. *International Journal of Biological Macromolecules*, *143*, 1000–1008. https://doi.org/10.1016/j.ijbiomac.2019.10.034

Rodríguez-Contreras, A., Koller, M., Braunegg, G., & Marqués-Calvo, M. S. (2016). Poly[(R)-3-hydroxybutyrate] production under different salinity conditions by a novel Bacillus megaterium strain. *New Biotechnology*, *33*(1), 73–77. https://doi.org/10.1016/j.nbt.2015.08.006

Rodriguez-Perez, S., Serrano, A., Pantión, A. A., & Alonso-Fariñas, B. (2018). Challenges of scaling-up PHA production from waste streams. A review. In *Journal of Environmental Management* (Vol. 205, pp. 215–230). https://doi.org/10.1016/j.jenvman.2017.09.083

ROMANO, A. H., & PELOQUIN, J. P. (1963). Composition of the Sheath of Sphaerotilus Natans. *Journal of Bacteriology*, *86*, 252–258. https://doi.org/10.1128/jb.86.2.252-258.1963

Ruffino, B., Campo, G., Cerutti, A., Zanetti, M., Lorenzi, E., Scibilia, G., & Genon, G. (2016). Preliminary Technical and Economic Analysis of Alkali and Low Temperature Thermo-alkali Pretreatments for the Anaerobic Digestion of Waste Activated Sludge. *Waste and Biomass Valorization*, *7*(4), 667–675. https://doi.org/10.1007/s12649-016-9537-x

Russo, P., Carfagna, C., Cimino, F., Acierno, D., & Persico, P. (2013). Biodegradable composites reinforced with kenaf fibers: Thermal, mechanical, and morphological issues. *Advances in Polymer Technology*, *32*(SUPPL.1). https://doi.org/10.1002/adv.21282

Samorì, C., Abbondanzi, F., Galletti, P., Giorgini, L., Mazzocchetti, L., Torri, C., & Tagliavini, E. (2015). Extraction of polyhydroxyalkanoates from mixed microbial cultures: Impact on polymer quality and recovery. *Bioresource Technology*, *189*, 195–202. https://doi.org/10.1016/j.biortech.2015.03.062

Sanjay, M. R., Madhu, P., Jawaid, M., Senthamaraikannan, P., Senthil, S., & Pradeep, S. (2018). Characterization and properties of natural fiber polymer composites: A comprehensive review. *Journal of Cleaner Production*, *172*, 566–581. https://doi.org/10.1016/j.jclepro.2017.10.101

Sato, S., Kanazawa, H., & Tsuge, T. (2011). Expression and characterization of (R)-specific enoyl coenzyme A hydratases making a channeling route to polyhydroxyalkanoate biosynthesis in Pseudomonas putida. *Applied Microbiology and Biotechnology*, *90*(3), 951–959. https://doi.org/10.1007/s00253-011-3150-5

Scarfato, P., Di Maio, L., & Incarnato, L. (2015). Recent advances and migration issues in biodegradable polymers from renewable sources for food packaging. In *Journal of Applied Polymer Science* (Vol. 132, Issue 48). https://doi.org/10.1002/app.42597

Schaefer, A. K., Melnyk, J. E., He, Z., Del Rosario, F., & Grimes, C. L. (2017). Pathogen- and microbial- associated molecular patterns (PAMPs/MAMPs) and the innate immune response in crohn's disease. In *Immunity and Inflammation in Health and Disease: Emerging Roles of Nutraceuticals and Functional Foods in Immune Support* (pp. 175–187). https://doi.org/10.1016/B978-0-12-805417-8.00014-7

Schmidt, M., Ienczak, J. L., Quines, L. K., Zanfonato, K., Schmidell, W., & de Aragão, G. M. F. (2016). Poly(3-hydroxybutyrate-co-3-hydroxyvalerate) production in a system with external cell recycle and limited nitrogen feeding during the production phase. *Biochemical Engineering Journal*, *112*, 130–135. https://doi.org/10.1016/j.bej.2016.04.013

Schulz, H. (2008). Oxidation of fatty acids in eukaryotes. In *Biochemistry of Lipids, Lipoproteins and Membranes* (pp. 131–154). https://doi.org/10.1016/B978-044453219-0.50007-6

Schweitzer, D., Mullen, C. A., Boateng, A. A., & Snell, K. D. (2015). Biobased n-Butanol Prepared from Poly-3-hydroxybutyrate: Optimization of the Reduction of n-Butyl Crotonate to n-Butanol. *Organic Process Research and Development*, *19*(7), 710–714. https://doi.org/10.1021/op500156b

Seder-Colomina, M., Goubet, A., Lacroix, S., Morin, G., Ona-Nguema, G., Esposito, G., Van Hullebusch, E. D., & Pernelle, J. J. (2015). Moderate oxygen depletion as a factor favouring the filamentous growth of Sphaerotilus natans. *Antonie van Leeuwenhoek, International Journal of General and Molecular Microbiology*, *107*(5), 1135–1144. https://doi.org/10.1007/s10482-015-0405-7

Seder-Colomina, M., Morin, G., Benzerara, K., Ona-Nguema, G., Pernelle, J. J., Esposito, G., & Van Hullebusch, E. D. (2014). Sphaerotilus natans, a Neutrophilic Iron-Related Sheath-Forming Bacterium: Perspectives for Metal Remediation Strategies. *Geomicrobiology Journal*, *31*(1), 64–75. https://doi.org/10.1080/01490451.2013.806611

Seggiani, M., Cinelli, P., Mallegni, N., Balestri, E., Puccini, M., Vitolo, S., Lardicci, C., & Lazzeri, A. (2017). New Bio-Composites Based on Polyhydroxyalkanoates and Posidonia oceanica Fibres for Applications in a Marine Environment. *Materials*, *10*(4). https://doi.org/10.3390/ma10040326

Sehgal, R., & Gupta, R. (2020). Polyhydroxyalkanoate and its efficient production: an eco-friendly approach towards development. In *3 Biotech* (Vol. 10, Issue 12). https://doi.org/10.1007/s13205-020-02550-5

Selke, S. E., & Hernandez, R. J. (2001). Packaging: Polymers in Flexible Packaging. In *Encyclopedia of Materials: Science and Technology* (pp. 6652–6656). https://doi.org/10.1016/b0-08-043152-6/01176-1

Sepehri, A., & Sarrafzadeh, M. H. (2018). Effect of nitrifiers community on fouling mitigation and nitrification efficiency in a membrane bioreactor. *Chemical Engineering and Processing - Process Intensification*, *128*, 10–18. https://doi.org/10.1016/j.cep.2018.04.006

Serafim, L. S., Lemos, P. C., Albuquerque, M. G. E., & Reis, M. A. M. (2008). Strategies for PHA production by mixed cultures and renewable waste materials. In *Applied Microbiology and Biotechnology* (Vol. 81, Issue 4, pp. 615–628). https://doi.org/10.1007/s00253-008-1757-y

Sezgin, M., Jenkins, D., & Parker, D. S. (1978). A unified theory of filamentous activated sludge bulking. *Journal of the Water Pollution Control Federation*, *50*(2), 362–381.

Shah, T. V., & Vasava, D. V. (2019). A glimpse of biodegradable polymers and their biomedical applications. In *E-Polymers* (Vol. 19, Issue 1, pp. 385–410). https://doi.org/10.1515/epoly-2019-0041

Sharma, P. R., Zheng, B., Sharma, S. K., Zhan, C., Wang, R., Bhatia, S. R., & Hsiao, B. S. (2018). High Aspect Ratio Carboxycellulose Nanofibers Prepared by Nitro-Oxidation Method and Their Nanopaper Properties. *ACS Applied Nano Materials*, *1*(8), 3969–3980. https://doi.org/10.1021/acsanm.8b00744

Sharma, V., Sehgal, R., & Gupta, R. (2021). Polyhydroxyalkanoate (PHA): Properties and Modifications. *Polymer*, *212*(September), 123161. https://doi.org/10.1016/j.polymer.2020.123161

Shinde, N. G., & Patel, D. M. (2020). A Short Review on Automobile Dashboard Materials. *IOP Conference Series: Materials Science and Engineering*, *810*(1). https://doi.org/10.1088/1757-899X/810/1/012033

Shozui, F., Matsumoto, K., Nakai, T., Yamada, M., & Taguchi, S. (2010). Biosynthesis of novel terpolymers poly(lactate-co-3-hydroxybutyrate-co-3-hydroxyvalerate)s in lactate-overproducing mutant Escherichia coli JW0885 by feeding propionate as a precursor of 3-hydroxyvalerate. *Applied Microbiology and Biotechnology*, *85*(4), 949–954. https://doi.org/10.1007/s00253-009-2100-y

Singh, M., Kumar, P., Ray, S., & Kalia, V. C. (2015). Challenges and Opportunities for Customizing Polyhydroxyalkanoates. In *Indian Journal of Microbiology* (Vol. 55, Issue 3, pp. 235–249). https://doi.org/10.1007/s12088-015-0528-6

Singh, S., & Mohanty, A. K. (2007). Wood fiber reinforced bacterial bioplastic composites: Fabrication and performance evaluation. *Composites Science and Technology*, *67*(9), 1753–1763. https://doi.org/10.1016/j.compscitech.2006.11.009

Singh, S., Mohanty, A. K., Sugie, T., Takai, Y., & Hamada, H. (2008). Renewable resource based biocomposites from natural fiber and polyhydroxybutyrate-co-valerate (PHBV) bioplastic. *Composites Part A: Applied Science and Manufacturing*, *39*(5), 875–886. https://doi.org/10.1016/j.compositesa.2008.01.004

Smith, M. K. M., Paleri, D. M., Abdelwahab, M., Mielewski, D. F., Misra, M., & Mohanty, A. K. (2020). Sustainable composites from poly(3-hydroxybutyrate) (PHB) bioplastic and agave natural fibre. *Green Chemistry*, *22*(12), 3906–3916. https://doi.org/10.1039/d0gc00365d

Smolyakov, G., Pruvost, S., Cardoso, L., Alonso, B., Belamie, E., & Duchet-Rumeau, J. (2016). AFM PeakForce QNM mode: Evidencing nanometre-scale mechanical properties of chitin-silica hybrid nanocomposites. *Carbohydrate Polymers*, *151*, 373–380. https://doi.org/10.1016/j.carbpol.2016.05.042

Somleva, M. N., Peoples, O. P., & Snell, K. D. (2013). PHA Bioplastics, Biochemicals, and Energy from Crops. In *Plant Biotechnology Journal* (Vol. 11, Issue 2, pp. 233–252). https://doi.org/10.1111/pbi.12039

Song, M., Luo, C., Jiang, L., Peng, K., Zhang, D., Zhang, R., Li, Y., & Zhang, G. (2019). The presence of in situ sulphamethoxazole degraders and their interactions with other microbes in activated sludge as revealed by DNA stable isotope probing and molecular ecological network analysis. *Environment International*, *124*, 121–129. https://doi.org/10.1016/j.envint.2018.12.039

Srubar, W. V., Pilla, S., Wright, Z. C., Ryan, C. A., Greene, J. P., Frank, C. W., & Billington, S. L. (2012). Mechanisms and impact of fiber-matrix compatibilization techniques on the material characterization of PHBV/oak wood flour engineered biobased composites. *Composites Science and Technology*, *72*(6), 708–715. https://doi.org/10.1016/j.compscitech.2012.01.021

STOKES, J. L. (1954). Studies on the filamentous sheathed iron bacterium Sphaerotilus natans. *Journal of Bacteriology*, *67*(3), 278–291. https://doi.org/10.1128/jb.67.3.278-291.1954

Sudesh, K., Abe, H., & Doi, Y. (2000). Synthesis, structure and properties of polyhydroxyalkanoates: Biological polyesters. In *Progress in Polymer Science (Oxford)* (Vol. 25, Issue 10, pp. 1503–1555). https://doi.org/10.1016/S0079-6700(00)00035-6

Sullivan, K. P., Werner, A. Z., Ramirez, K. J., Ellis, L. D., Bussard, J. R., Black, B. A., Brandner, D. G., Bratti, F., Buss, B. L., Dong, X., Haugen, S. J., Ingraham, M. A., Konev, M. O., Michener, W. E., Miscall, J., Pardo, I., Woodworth, S. P., Guss, A. M., Román-Leshkov, Y., … Beckham, G. T. (2022). Mixed plastics waste valorization through tandem chemical oxidation and biological funneling. *Science*, *378*(6616), 207–211. https://doi.org/10.1126/science.abo4626

Sumanth Kumar, D., Jai Kumar, B., & Mahesh, H. M. (2018). Quantum Nanostructures (QDs): An Overview. In *Synthesis of Inorganic Nanomaterials: Advances and Key Technologies* (pp. 59–88). https://doi.org/10.1016/B978-0-08-101975-7.00003-8

Sun, S., Liu, P., Ji, N., Hou, H., & Dong, H. (2017). Effects of low polyhydroxyalkanoate content on the properties of films based on modified starch acquired by extrusion blowing. *Food Hydrocolloids*, *72*, 81–89. https://doi.org/10.1016/j.foodhyd.2017.05.030

Surmenev, R. A., Chernozem, R. V., Syromotina, D. S., Oehr, C., Baumbach, T., Krause, B., Boyandin, A. N., Dvoinina, L. M., Volova, T. G., & Surmeneva, M. A. (2019). Low-temperature argon and ammonia plasma treatment of poly-3-hydroxybutyrate films: Surface topography and chemistry changes affect fibroblast cells in vitro. *European Polymer Journal*, *112*, 137–145. https://doi.org/10.1016/j.eurpolymj.2018.12.040

Tajima, K., Igari, T., Nishimura, D., Nakamura, M., Satoh, Y., & Munekata, M. (2003). Isolation and characterization of Bacillus sp. INT005 accumulating polyhydroxyalkanoate (PHA) from gas field soil. *Journal of Bioscience and Bioengineering*, *95*(1), 77–81. https://doi.org/10.1263/jbb.95.77

Takeda, M., Nakano, F., Nagase, T., Iohara, K., & Koizumi, J. I. (1998). Isolation and Chemical Composition of the Sheath of Sphaerotilu. *Bioscience, Biotechnology and Biochemistry*, *62*(6), 1138–1143. https://doi.org/10.1271/bbb.62.1138

Tamang, P., Banerjee, R., Köster, S., & Nogueira, R. (2019). Comparative study of polyhydroxyalkanoates production from acidified and anaerobically treated brewery wastewater using enriched mixed microbial culture. *Journal of Environmental Sciences (China)*, *78*, 137–146. https://doi.org/10.1016/j.jes.2018.09.001

Tan, G. Y. A., Chen, C. L., Li, L., Ge, L., Wang, L., Razaad, I. M. N., Li, Y., Zhao, L., Mo, Y., & Wang, J. Y. (2014). Start a research on biopolymer polyhydroxyalkanoate (PHA): A review. *Polymers*, *6*(3), 706–754. https://doi.org/10.3390/polym6030706

Tanadchangsaeng, N., Kitagawa, A., Yamamoto, T., Abe, H., & Tsuge, T. (2009). Identification, biosynthesis, and characterization of polyhydroxyalkanoate copolymer consisting of 3-hydroxybutyrate and 3-hydroxy-4-methylvalerate. *Biomacromolecules*, *10*(10), 2866–2874. https://doi.org/10.1021/bm900696c

Tang, L., Yu, J., Pang, Y., Zeng, G., Deng, Y., Wang, J., Ren, X., Ye, S., Peng, B., & Feng, H. (2018). Sustainable efficient adsorbent: Alkali-acid modified magnetic biochar derived from sewage sludge for aqueous organic contaminant removal. *Chemical Engineering Journal*, *336*, 160–169. https://doi.org/10.1016/j.cej.2017.11.048

Thellen, C., Coyne, M., Froio, D., Auerbach, M., Wirsen, C., & Ratto, J. A. (2008). A processing, characterization and marine biodegradation study of melt-extruded polyhydroxyalkanoate (PHA) films. *Journal of Polymers and the Environment*, *16*(1), 1–11. https://doi.org/10.1007/s10924-008-0079-6

Tian, H., Tang, Z., Zhuang, X., Chen, X., & Jing, X. (2012). Biodegradable synthetic polymers: Preparation, functionalization and biomedical application. In *Progress in Polymer Science (Oxford)* (Vol. 37, Issue 2, pp. 237–280). https://doi.org/10.1016/j.progpolymsci.2011.06.004

Tian, J., Zhang, R., Wu, Y., & Xue, P. (2021). Additive manufacturing of wood flour/polyhydroxyalkanoates (PHA) fully bio-based composites based on micro-screw extrusion system. *Materials and Design*, *199*, 109418. https://doi.org/10.1016/j.matdes.2020.109418

Tiehm, A., Nickel, K., Zellhorn, M., Neis, U., & Tiehm, A. (2001). Ultrasonic waste activated sludge disintegration for improving anaerobic stabilization. *Water Research*, *35*(8), 2003–2009. https://doi.org/10.1016/S0043-1354(00)00468-1

Titow, W. V. (1984). PVC Technology. In *PVC Technology*. https://doi.org/10.1007/978-94-009-5614-8

Tjaden, D. H., & Goss, R. C. (1969). Sheath and Cellular Irregularities of Sphaerotilus natans Caused by Ferric Ammonium Citrate and Glucose. *Proceedings of the Iowa Academy of Science*, *76*(1), 38–44.

Tomano, N., Boondamnoen, O., Aumnate, C., & Potiyaraj, P. (2022). Enhancing impact resistance and biodegradability of PHBV by melt blending with ENR. *Scientific Reports*, *12*(1), 1–14. https://doi.org/10.1038/s41598-022-27246-z

Torres-Giner, S., Montanes, N., Fombuena, V., Boronat, T., & Sanchez-Nacher, L. (2018). Preparation and characterization of compression-molded green composite sheets made of poly(3-hydroxybutyrate) reinforced with long pita fibers. *Advances in Polymer Technology*, *37*(5), 1305–1315. https://doi.org/10.1002/adv.21789

Torres-Tello, E. V., Robledo-Ortíz, J. R., González-García, Y., Pérez-Fonseca, A. A., Jasso-Gastinel, C. F., & Mendizábal, E. (2017). Effect of agave fiber content in the thermal and mechanical properties of green composites based on polyhydroxybutyrate or poly(hydroxybutyrate-co-hydroxyvalerate). *Industrial Crops and Products*, *99*, 117–125. https://doi.org/10.1016/j.indcrop.2017.01.035

Tsai, S. W., & Pagano, N. J. (1968). Invariant properties of composite materials. *Composite Materials Workshop*, *March*, 233–253.

Tsuge, T. (2002). Metabolic improvements and use of inexpensive carbon sources in microbial production of polyhydroxyalkanoates. In *Journal of Bioscience and Bioengineering* (Vol. 94, Issue 6, pp. 579–584). https://doi.org/10.1016/S1389-1723(02)80198-0

Tsuge, T., Kikkawa, Y., & Doi, Y. (2004). Microbial synthesis and enzymatic degradation of renewable poly[(R)-3-hydroxybutyrate-co-(R)-3-hydroxyhexanoate]. *Science and Technology of Advanced Materials*, *5*(4), 449–453. https://doi.org/10.1016/j.stam.2004.01.013

United States Environmental Protection Agency. (2021). *Basic Information about NO2 | US EPA*. Nitrogen Dioxide (NO2) Pollution. https://www.epa.gov/no2-pollution/basic-information-about-no2#What is NO2

Urbina, L., Eceiza, A., Gabilondo, N., Corcuera, M. Á., & Retegi, A. (2019). Valorization of apple waste for active packaging: multicomponent polyhydroxyalkanoate coated nanopapers with improved hydrophobicity and antioxidant capacity. *Food Packaging and Shelf Life*, *21*. https://doi.org/10.1016/j.fpsl.2019.100356

Vahabi, H., Michely, L., Moradkhani, G., Akbari, V., Cochez, M., Vagner, C., Renard, E., Saeb, M. R., & Langlois, V. (2019). Thermal stability and flammability behavior of poly(3-hydroxybutyrate) (PHB) based composites. *Materials*, *12*(14). https://doi.org/10.3390/ma12142239

Valentini, F., Dorigato, A., Rigotti, D., & Pegoretti, A. (2019). Polyhydroxyalkanoates/Fibrillated Nanocellulose Composites for Additive Manufacturing. *Journal of Polymers and the Environment*. https://doi.org/10.1007/s10924-019-01429-8

Van Niekerk, A. M., Jenkins, D., & Richard, M. G. (1987). The competitive growth of Zoogloea ramigera and type 021N in activated sludge and pure culture - A model for low F:M bulking. *Journal of the Water Pollution Control Federation*, *59*(5), 262–273.

Vandi, L. J., Chan, C. M., Werker, A., Richardson, D., Laycock, B., & Pratt, S. (2019). Extrusion of wood fibre reinforced poly(hydroxybutyrate-co-hydroxyvalerate) (PHBV) biocomposites: Statistical analysis of the effect of processing conditions on mechanical performance. *Polymer Degradation and Stability*, *159*, 1–14. https://doi.org/10.1016/j.polymdegradstab.2018.10.015

Varghese, S. A., Pulikkalparambil, H., Rangappa, S. M., Siengchin, S., & Parameswaranpillai, J. (2020). Novel biodegradable polymer films based on poly(3-hydroxybutyrate-co-3-hydroxyvalerate) and Ceiba pentandra natural fibers for packaging applications. *Food Packaging and Shelf Life*, *25*(January), 100538. https://doi.org/10.1016/j.fpsl.2020.100538

Ventolini. (2014). Vaginal Lactobacillosis. *Journal of Clinical Gynecology and Obstetrics*. https://doi.org/10.14740/jcgo278e

Ventura, H., Claramunt, J., Rodríguez-Pérez, M. A., & Ardanuy, M. (2017). Effects of hydrothermal aging on the water uptake and tensile properties of PHB/flax fabric biocomposites. *Polymer Degradation and Stability*, *142*, 129–138. https://doi.org/10.1016/j.polymdegradstab.2017.06.003

Verlinden, R. A. J., Hill, D. J., Kenward, M. A., Williams, C. D., & Radecka, I. (2007). Bacterial synthesis of biodegradable polyhydroxyalkanoates. In *Journal of Applied Microbiology* (Vol. 102, Issue 6, pp. 1437–1449). https://doi.org/10.1111/j.1365-2672.2007.03335.x

Vijay, R., & Tarika, K. (2019). Microbial Production of Polyhydroxy alkanoates (PHAs) using Kitchen Waste as an Inexpensive Carbon Source. *Biosciences, Biotechnology Research Asia*, *16*(1), 155–166. https://doi.org/10.13005/bbra/2733

Vilos, C., Morales, F. A., Solar, P. A., Herrera, N. S., Gonzalez-Nilo, F. D., Aguayo, D. A., Mendoza, H. L., Comer, J., Bravo, M. L., Gonzalez, P. A., Kato, S., Cuello, M. A., Alonso, C., Bravo, E. J., Bustamante, E. I., Owen, G. I., & Velasquez, L. A. (2013). Paclitaxel-PHBV nanoparticles and their toxicity to endometrial and primary ovarian cancer cells. *Biomaterials*, *34*(16), 4098–4108. https://doi.org/10.1016/j.biomaterials.2013.02.034

Vinet, L., & Zhedanov, A. (2011). A "missing" family of classical orthogonal polynomials. *Journal of Physics A: Mathematical and Theoretical*, *44*(8). https://doi.org/10.1088/1751-8113/44/8/085201

Viretto, A., Gontard, N., & Angellier-Coussy, H. (2021). Urban parks and gardens green waste: A valuable resource for the production of fillers for biocomposites applications. *Waste Management*, *120*, 538–548. https://doi.org/10.1016/j.wasman.2020.10.018

Vishnuvardhan Reddy, S., Thirumala, M., & Mahmood, S. K. (2009). Production of PHB and P (3HB-co-3HV) biopolymers by Bacillus megaterium strain OU303A isolated from municipal sewage sludge. *World Journal of Microbiology and Biotechnology*, *25*(3), 391–397. https://doi.org/10.1007/s11274-008-9903-3

Volova, T. G., Prudnikova, S. V., Zhila, N. O., Menzyanova, N. G., Kiselev, E. G., Shishatskaaya, E. I., & Thomas, S. (2020). Natural Degradable Polyhydroxyalkanoates as the Basis for Creation of Prolonged and Targeted Pesticides to Protect Cultivated Plants from Weeds and Pathogens. In *Nanopesticides* (pp. 1–22). https://doi.org/10.1007/978-3-030-44873-8_1

Vu, D. H., Åkesson, D., Taherzadeh, M. J., & Ferreira, J. A. (2020). Recycling strategies for polyhydroxyalkanoate-based waste materials: An overview. In *Bioresource Technology* (Vol. 298). https://doi.org/10.1016/j.biortech.2019.122393

Walton, T. J. (1991). Microbial polyesters: In *Phytochemistry* (1st Editio, Vol. 30, Issue 7). Wiley-VCH. https://doi.org/10.1016/0031-9422(91)83684-d

Wambua, P., Ivens, J., & Verpoest, I. (2003). Natural fibres: Can they replace glass in fibre reinforced plastics? *Composites Science and Technology*, *63*(9), 1259–1264. https://doi.org/10.1016/S0266-3538(03)00096-4

Wang, B., & Li, Y. (2021). Plastic bag usage and the policies: A case study of China. *Waste Management*, *126*, 163–169. https://doi.org/10.1016/j.wasman.2021.03.010

Wang, H. hui, Li, X. tao, & Chen, G. Q. (2009). Production and characterization of homopolymer polyhydroxyheptanoate (P3HHp) by a fadBA knockout mutant Pseudomonas putida KTOY06 derived from P. putida KT2442. *Process Biochemistry*, *44*(1), 106–111. https://doi.org/10.1016/j.procbio.2008.09.014

Wang, Q., Garrity, G. M., Tiedje, J. M., & Cole, J. R. (2007). Naïve Bayesian classifier for rapid assignment of rRNA sequences into the new bacterial taxonomy. *Applied and Environmental Microbiology*, *73*(16), 5261–5267. https://doi.org/10.1128/AEM.00062-07

Wang, Shichao, Chen, W., Xiang, H., Yang, J., Zhou, Z., & Zhu, M. (2016). Modification and potential application of short-chain-length polyhydroxyalkanoate (SCL-PHA). In *Polymers* (Vol. 8, Issue 8). https://doi.org/10.3390/polym8080273

Wang, Shutian, Zhao, Q., Jiang, J., Wei, L., Wang, K., Ding, J., & Meng, F. (2021). Performance of sludge degradation, mineralization and electro-energy harvesting in a sludge treatment electro-wetland: Insight into the sludge loading rate. *Journal of Water Process Engineering*, *40*(July), 101779. https://doi.org/10.1016/j.jwpe.2020.101779

Wang, Tao, Shi, F., Zhang, Q., Qian, X., & Hashimoto, S. (2018). Exploring material stock efficiency of municipal water and sewage infrastructures in China. *Journal of Cleaner Production*, *181*, 498–507. https://doi.org/10.1016/j.jclepro.2018.01.253

Wang, Tianqi, Ran, M., Li, X., Liu, Y., Xin, Y., Liu, H., Liu, H., Xia, Y., & Xun, L. (2022). The Pathway of Sulfide Oxidation to Octasulfur Globules in the Cytoplasm of Aerobic Bacteria. *Applied and Environmental Microbiology*, *88*(3). https://doi.org/10.1128/aem.01941-21

Wang, Xianbao, Gao, C., Qi, X., Zhang, Y., Chen, T., Xie, Y., Zhang, A., & Gao, J. (2021). Enhancing sludge fermentation and anaerobic digestion by mechanical cutting pretreatment. *Journal of Water Process Engineering*, *40*(November), 101812. https://doi.org/10.1016/j.jwpe.2020.101812

Wang, Xiaofei, Bengtsson, S., Oehmen, A., Carvalho, G., Werker, A., & Reis, M. A. M. (2019). Application of dissolved oxygen (DO) level control for polyhydroxyalkanoate (PHA) accumulation with concurrent nitrification in surplus municipal activated sludge. *New Biotechnology*, *50*, 37–43. https://doi.org/10.1016/j.nbt.2019.01.003

Wang, Xin, Chen, T., Ge, Y., & Jia, Y. (2008). Studies on land application of sewage sludge and its limiting factors. *Journal of Hazardous Materials*, *160*(2–3), 554–558. https://doi.org/10.1016/j.jhazmat.2008.03.046

Wang, Yang, Jiang, X. L., Peng, S. W., Guo, X. Y., Shang, G. G., Chen, J. C., Wu, Q., & Chen, G. Q. (2013). Induced apoptosis of osteoblasts proliferating on polyhydroxyalkanoates. *Biomaterials*, *34*(15), 3737–3746. https://doi.org/10.1016/j.biomaterials.2013.01.088

Wang, Yuanpeng, Chen, R., Cai, J. Y., Liu, Z., Zheng, Y., Wang, H., Li, Q., & He, N. (2013). Biosynthesis and Thermal Properties of PHBV Produced from Levulinic Acid by Ralstonia eutropha. *PLoS ONE*, *8*(4). https://doi.org/10.1371/journal.pone.0060318

Wanner, J., & Grau, P. (1989). Identification of filamentous microorganisms from activated sludge: A compromise between wishes, needs and possibilities. *Water Research*, *23*(7), 883–891. https://doi.org/10.1016/0043-1354(89)90013-4

Wei, L., Zhu, F., Li, Q., Xue, C., Xia, X., Yu, H., Zhao, Q., Jiang, J., & Bai, S. (2020). Development, current state and future trends of sludge management in China: Based on exploratory data and CO2-equivaient emissions analysis. *Environment International*, *144*(August), 106093. https://doi.org/10.1016/j.envint.2020.106093

Wei, Y., Van Houten, R. T., Borger, A. R., Eikelboom, D. H., & Fan, Y. (2003). Minimization of excess sludge production for biological wastewater treatment. *Water Research*, *37*(18), 4453–4467. https://doi.org/10.1016/S0043-1354(03)00441-X

Weiss, I. M., Muth, C., Drumm, R., & Kirchner, H. O. K. (2018). Thermal decomposition of the amino acids glycine, cysteine, aspartic acid, asparagine, glutamic acid, glutamine, arginine and histidine. *BMC Biophysics*, *11*(1). https://doi.org/10.1186/s13628-018-0042-4

Wijeyekoon, S., Carere, C. R., West, M., Nath, S., & Gapes, D. (2018). Mixed culture polyhydroxyalkanoate (PHA) synthesis from nutrient rich wet oxidation liquors. *Water Research*, *140*, 1–11. https://doi.org/10.1016/j.watres.2018.04.017

Wilkes, C., Summers, J., Daniels, C., & Berard, M. (2005). PVC Handbook, Hanser,". In *PVC Handbook*.

Willemsen, O. H., Snel, M. M. E., Cambi, A., Greve, J., De Grooth, B. G., & Figdor, C. G. (2000). Biomolecular interactions measured by atomic force microscopy. *Biophysical Journal*, *79*(6), 3267–3281. https://doi.org/10.1016/S0006-3495(00)76559-3

Williams, S. F., Rizk, S., & Martin, D. P. (2013). Poly-4-hydroxybutyrate (P4HB): A new generation of resorbable medical devices for tissue repair and regeneration. In *Biomedizinische Technik* (Vol. 58, Issue 5, pp. 439–452). https://doi.org/10.1515/bmt-2013-0009

Wong, S., Shanks, R., & Hodzic, A. (2002). Properties of poly(3-hydroxybutyric acid) composites with flax fibres modified by plasticiser absorption. *Macromolecular Materials and Engineering*, *287*(10), 647–655. https://doi.org/10.1002/1439-2054(200210)287:10<647::AID-MAME647>3.0.CO;2-7

Woolnough, C. A., Yee, L. H., Charlton, T. S., & Foster, L. J. R. (2013). A Tuneable Switch for Controlling Environmental Degradation of Bioplastics: Addition of Isothiazolinone to Polyhydroxyalkanoates. *PLoS ONE*, *8*(10). https://doi.org/10.1371/journal.pone.0075817

Wortman, J. J., & Evans, R. A. (1965). Young's modulus, shear modulus, and poisson's ratio in silicon and germanium. *Journal of Applied Physics*, *36*(1), 153–156. https://doi.org/10.1063/1.1713863

Wu, C. S., Liao, H. T., & Cai, Y. X. (2017). Characterisation, biodegradability and application of palm fibre-reinforced polyhydroxyalkanoate composites. *Polymer Degradation and Stability*, *140*, 55–63. https://doi.org/10.1016/j.polymdegradstab.2017.04.016

Wu, M. H., Lin, C. L., Huang, W. C., & Chen, J. W. (2016). Characteristics of pervious concrete using incineration bottom ash in place of sandstone graded material. *Construction and Building Materials*, *111*, 618–624. https://doi.org/10.1016/j.conbuildmat.2016.02.146

Wu, X., Huang, J., Lu, Z., Chen, G., Wang, J., & Liu, G. (2019). Thiothrix eikelboomii interferes oxygen transfer in activated sludge. *Water Research*, *151*, 134–143. https://doi.org/10.1016/j.watres.2018.12.019

Xia, Y., Duan, P., & Chen, J. (2018). Modelling the nanomechanical responses of biofilms grown on the indenter probe. *Processes*, *6*(7). https://doi.org/10.3390/pr6070084

Xiang, H., Wen, X., Miu, X., Li, Y., Zhou, Z., & Zhu, M. (2016). Thermal depolymerization mechanisms of poly(3-hydroxybutyrate-co-3-hydroxyvalerate). *Progress in Natural Science: Materials International*, *26*(1), 58–64. https://doi.org/10.1016/j.pnsc.2016.01.007

Xiao, K., Abbt-Braun, G., & Horn, H. (2020). Changes in the characteristics of dissolved organic matter during sludge treatment: A critical review. In *Water Research* (Vol. 187). https://doi.org/10.1016/j.watres.2020.116441

Xu, S., Sun, M., Zhang, C., Surampalli, R., & Hu, Z. (2014). Filamentous sludge bulking control by nano zero-valent iron in activated sludge treatment systems. *Environmental Science: Processes and Impacts*, *16*(12), 2721–2728. https://doi.org/10.1039/c4em00333k

Xu, Z., Pan, C., Li, X., Hao, N., Zhang, T., Gaffrey, M. J., Pu, Y., Cort, J. R., Ragauskas, A. J., Qian, W. J., & Yang, B. (2021). Enhancement of polyhydroxyalkanoate production by co-feeding lignin derivatives with glycerol in Pseudomonas putida KT2440. *Biotechnology for Biofuels*, *14*(1), 1–38. https://doi.org/10.1186/s13068-020-01861-2

Yang, G., Zhang, G., & Wang, H. (2015). Current state of sludge production, management, treatment and disposal in China. *Water Research*, *78*, 60–73. https://doi.org/10.1016/j.watres.2015.04.002

Yang, J., Liu, X., Wang, D., Xu, Q., Yang, Q., Zeng, G., Li, X., Liu, Y., Gong, J., Ye, J., & Li, H. (2019). Mechanisms of peroxymonosulfate pretreatment enhancing production of short-chain fatty acids from waste activated sludge. *Water Research*, *148*, 239–249. https://doi.org/10.1016/j.watres.2018.10.060

Ye, L., & Zhang, T. (2013). Bacterial communities in different sections of a municipal wastewater treatment plant revealed by 16S rDNA 454 pyrosequencing. *Applied Microbiology and Biotechnology*, *97*(6), 2681–2690. https://doi.org/10.1007/s00253-012-4082-4

Yogesh, C., Pathak, B., & Fulekar, M. H. (2012). PHA - Production Application and its Bioremediation in Environment. *International Research Journal of Environment Sciences*, *1*(2), 46–52. www.isca.in/IJENS/Archive/v1/i2/9.ISCA-JEvsS-2012-009.pdf

Zampino, D., Mancuso, M., Zaccone, R., Ferreri, T., Borzacchiello, A., Zeppetelli, S., Dattilo, S., Ussia, M., Ferreri, L., Carbone, D. C., Recca, G., & Puglisi, C. (2021). Thermo-mechanical, antimicrobial and biocompatible properties of PVC blends based on imidazolium ionic liquids. *Materials Science and Engineering C*, *122*. https://doi.org/10.1016/j.msec.2021.111920

Zhang, J., Cao, Q., Li, S., Lu, X., Zhao, Y., Guan, J. S., Chen, J. C., Wu, Q., & Chen, G. Q. (2013). 3-Hydroxybutyrate methyl ester as a potential drug against Alzheimer's disease via mitochondria protection mechanism. *Biomaterials*, *34*(30), 7552–7562. https://doi.org/10.1016/j.biomaterials.2013.06.043

Zhang, M., Wu, H., & Chen, H. (2014). Coupling of polyhydroxyalkanoate production with volatile fatty acid from food wastes and excess sludge. *Process Safety and Environmental Protection*, *92*(2), 171–178. https://doi.org/10.1016/j.psep.2012.12.002

Zhang, Q., Hu, J., Lee, D. J., Chang, Y., & Lee, Y. J. (2017). Sludge treatment: Current research trends. *Bioresource Technology*, *243*, 1159–1172. https://doi.org/10.1016/j.biortech.2017.07.070

Zhang, X., Lin, Y., Wu, Q., Wang, Y., & Chen, G. Q. (2020). Synthetic Biology and Genome-Editing Tools for Improving PHA Metabolic Engineering. In *Trends in Biotechnology* (Vol. 38, Issue 7, pp. 689–700). https://doi.org/10.1016/j.tibtech.2019.10.006

Zhang, Y., Zhao, T., Zhang, Z., Wan, J., Feng, X., Liang, X., & Zhou, A. (2017). Modeling and dynamic assessment on sustainable development of drainage enterprise: Application of a coupled system dynamics- comprehensive assessment model. *Journal of Cleaner Production*, *141*, 157–167. https://doi.org/10.1016/j.jclepro.2016.09.055

Zhao, Xiaoying; Storts Sam; Cornish, Katrina; Vodovotz, Y. (2019). Natural Rubber-Toughened PHBV/PLA Biodegradable Bioplastic Films for Quieter Packaging Applications. *Fall 196th Technical Meeting of Rubber Division, ACS*. https://cornishlab.cfaes.ohio-state.edu/sites/hcs-cornishlab/files/imce/Natural Rubber-Toughened PHBV-PLA Bioplastic Films for Quieter Packaging Applications.pdf

Zhao, C., Li, J., He, B., & Zhao, L. (2017). Fabrication of hydrophobic biocomposite by combining cellulosic fibers with polyhydroxyalkanoate. *Cellulose*, *24*(5), 2265–2274. https://doi.org/10.1007/s10570-017-1235-8

Zhao, L., Schaefer, D., Xu, H., Modi, S. J., LaCourse, W. R., & Marten, M. R. (2005). Elastic properties of the cell wall of Aspergillus nidulans studied with atomic force microscopy. *Biotechnology Progress*, *21*(1), 292–299. https://doi.org/10.1021/bp0497233

Zhao, X., Cornish, K., & Vodovotz, Y. (2019). Synergistic mechanisms underlie the peroxide and coagent improvement of natural-rubber-toughened poly(3-hydroxybutyrate-co-3-hydroxyvalerate) mechanical performance. *Polymers*, *11*(3). https://doi.org/10.3390/polym11030565

Zhao, X., Lawal, T., Rodrigues, M. M., Geib, T., & Vodovotz, Y. (2021). Value-added use of invasive plant-derived fibers as PHBV fillers for biocomposite development. *Polymers*, *13*(12). https://doi.org/10.3390/polym13121975

Zhen, G., Lu, X., Kato, H., Zhao, Y., & Li, Y. Y. (2017). Overview of pretreatment strategies for enhancing sewage sludge disintegration and subsequent anaerobic digestion: Current advances, full-scale application and future perspectives. In *Renewable and Sustainable Energy Reviews* (Vol. 69, pp. 559–577). https://doi.org/10.1016/j.rser.2016.11.187

Zheng, X., Liu, T., Guo, M., Li, D., Gou, N., Cao, X., Qiu, X., Li, X., Zhang, Y., Sheng, G., Pan, B., Gu, A. Z., & Li, Z. (2020). Impact of heavy metals on the formation and properties of solvable microbiological products released from activated sludge in biological wastewater treatment. *Water Research*, *179*. https://doi.org/10.1016/j.watres.2020.115895

Zhong, R., Wang, C., Zhang, Z., Liu, Q., & Cai, Z. (2020). PCDD/F levels and phase distributions in a full-scale municipal solid waste incinerator with co-incinerating sewage sludge. *Waste Management*, *106*, 110–119. https://doi.org/10.1016/j.wasman.2020.03.020

Zhou, X., & Li, Y. (2020). Atlas of Oral Microbiology: From Healthy Microflora to Disease. In *Atlas of Oral Microbiology: From Healthy Microflora to Disease*. https://doi.org/10.1007/978-981-15-7899-1

Zhou, Y., Fan, M., & Chen, L. (2016). Interface and bonding mechanisms of plant fibre composites: An overview. In *Composites Part B: Engineering* (Vol. 101, pp. 31–45). https://doi.org/10.1016/j.compositesb.2016.06.055

Zhuikov, V. A., Zhuikova, Y. V., Makhina, T. K., Myshkina, V. L., Rusakov, A., Useinov, A., Voinova, V. V., Bonartseva, G. A., Berlin, A. A., Bonartsev, A. P., & Iordanskii, A. L. (2020). Comparative structure-property characterization of poly(3-Hydroxybutyrate-Co-3-Hydroxyvalerate)s films under hydrolytic and enzymatic degradation: Finding a transition point in 3-hydroxyvalerate content. *Polymers*, *12*(3). https://doi.org/10.3390/polym12030728

Zinn, M., Witholt, B., & Egli, T. (2001). Occurrence, synthesis and medical application of bacterial polyhydroxyalkanoate. In *Advanced Drug Delivery Reviews* (Vol. 53, Issue 1, pp. 5–21). https://doi.org/10.1016/S0169-409X(01)00218-6